8-2014

Managing End-of-Life Lithium-ion Batteries: an Environmental and Economic Assessment

Xue Wang

Managing End-of-Life Lithium-ion Batteries: an Environmental and Economic Assessment

by

Xue Wang

A DISSERTATION

Submitted in partial fulfillment of the requirements
for the degree of Doctor of Philosophy in Sustainability

Department of Sustainability

Golisano Institute for Sustainability
Rochester Institute of Technology

August 2014

Author: _____
Sustainability Program

Certified by: _____
Dr. Gabrielle G. Gaustad
Assistant Professor of Sustainability Program

Approved by: _____
Paul H. Stiebitz
Associate Academic Director of Sustainability Program

Certified by: _____
Dr. Nabil Nasr
Assistant Provost and Director, Golisano Institute for Sustainability and CIMS

Managing End-of-Life Lithium-ion Batteries: an Environmental and Economic Assessment

By

Xue Wang

Submitted by Xue Wang in partial fulfillment of the requirements for the degree of Doctor of Philosophy in Sustainability and accepted on behalf of the Rochester Institute of Technology by the dissertation committee.

We, the undersigned members of the Faculty of the Rochester Institute of Technology, certify that we have advised and/or supervised the candidate on the work described in this dissertation. We further certify that we have reviewed the dissertation manuscript and approve it partial fulfillment of the requirements of the degree of Doctor of Philosophy in Sustainability.

Approved by:

Dr. Gabrielle G. Gaustad _____
(Committee Chair and Dissertation Advisor)

Dr. Callie W. Babbitt _____

Dr. Nenad Nenadic _____

Dr. Thomas Smith _____

SUSTAINABILITY PROGRAM
ROCHESTER INSTITUTE OF TECHNOLOGY
August 2014

ABSTRACT

Golisano Institute for Sustainability
Rochester Institute of Technology

Degree Doctor of Philosophy **Program** Sustainability

Name of Candidate Xue Wang

Title Managing End-of-Life Lithium-ion Batteries: an Environmental and Economic Assessment

The growing market for lithium-ion batteries raises concerns about sustainable management of those batteries at end of life. Launching relevant policies requires a comprehensive understanding of potential economic values as well as environmental performance of end-of-life lithium-ion batteries. However, both recyclers and policymakers are facing a number of unanswered questions, including 1) how battery technology trajectory would affect the incentives for recycling? 2) what strategies are available to improve material recovery efficiency? and 3) what is the potential for nanoparticle release during end-of-life processing, particularly for next-generation lithium-ion batteries who contain nano-scale cathode materials? This dissertation aims to fill these research gaps.

Multi-criteria optimization modeling and fundamental material characterization methods were used to quantify environmental and economic trade-offs for end-of-life lithium-ion batteries. Results show that potential material recovery values decrease as battery cathode chemistry transitions to low-cost cathode materials, as a majority of potentially recoverable value resides in the base metals contained in the cathode. Cathode changes over time will result in a heavily co-mingled waste stream, further complicating waste management and recycling processes.

An optimization model was developed to analyze the economic feasibility of

recycling facilities under possible scenarios of waste stream volume and composition. Sensitivity analysis shows that the profitability is highly dependent on the expected mix of cathode chemistries in the waste stream and resultant variability in material mass and value. Estimated current collection rate of end-of-life lithium-ion batteries turned out to be extremely low, indicating more opportunities and higher profitability for local recycling facilities if this rate can be improved.

Aiming to achieve segregation of high value metallic materials in lithium-ion batteries, a pre-recycling process, including mechanical shredding and size-based sorting steps, which can be easily scaled up to the industrial level, has been proposed. Sorting results show that contained metallic materials can be effectively segregated into size fractions at different levels. In addition, using this pre-recycling process as a case study, the nanoparticle exposure potential during mechanical processing has been proactively investigated by using both traditional and nano-enabled lithium-ion batteries. Results show that a substantial amount of nanoparticles released during the mechanical shredding but not the size-based sorting process. Additionally, shredding nano-scale $LiFePO_4$ cathode batteries may have a higher potential for nanoparticle exposure.

Facing the rapidly growing volume of spent lithium-ion batteries, the results suggest policy or other incentives may be necessary to promote a robust collection and recycling infrastructure as the economic incentives will likely decrease as the chemistry transitions away from cobalt-based cathodes. This dissertation also demonstrates the importance of implementing a battery labeling system as recyclers will likely face a co-mingled waste stream. Specifying recycling-relevant information would increase the effectiveness of the pre-recycling system.

ACKNOWLEDGEMENTS

First and foremost I would like express my special appreciation and thanks to my Ph.D. advisor, Dr. Gabrielle Gaustad for encouraging my research, giving me all the support, and challenging me throughout these years. I am extremely grateful for her motivation, knowledge, and advice on my research. She has been an excellent example as a strong, intelligent, successful woman scientist and professor.

Thank you to Dr. Callie Babbitt, who provided me invaluable support and guidance during my doctoral training and served as my committee member. I would also like to thank my other committee members, Dr. Nenad Nenadic and Dr. Thomas Smith for their helpful insights and suggestions. Thanks to other faculty and staff members in the GIS program, Dr. Nabil Nasr, Paul Stiebitz, Dr. Thomas Trabold, Dr. Eric Williams, Lisa Dammeyer, and Donna Podeszek.

I also would like to thank my friends in the US and China for being an amazing supporting system and sources of laughter. A special thanks to Chelsea Bailey: thank you for being such an amazing girlfriend and lab partner, and for always being there for me during my tough times as well as those happy days. Thanks to my sweetest girlfriend, Tess Garvey, for being a positive influence and always having faith in me.

Last, but by no means least, I thank my parents, Xianping Zhao and Kexu Wang, and all family members in China for their unconditional love and infinite support.

TABLE OF CONTENTS

LIST OF FIGURES

LIST OF TABLES

Chapter 1. Introduction

1.1 Applications of LIBs

Since first being introduced for the commercial use in the early 1990s by Sony, lithium-ion batteries (LIBs) have quickly become the most popular power source for a wide variety of consumer electronic devices (such as laptops computers, mobile phones, digital cameras and electronic readers) due to their higher power and energy densities [11, 13, 14]. Figure 1.1(a) and (b) illustrate this growing market share by comparing the chemistries of batteries in mobile phones produced in 1996 to those produced in 2005. While a range of battery technologies were used to power older mobile phones, lithium chemistry is almost exclusively used in mobile phones produced in 2005. This shift can be seen for batteries in laptop computers as well (Figure 1.1c and d), and a similar pattern holds true for camcorders, digital cameras, and other types of portable electronic applications [9]. In 2012, LIBs represent more than 30% of the total rechargeable battery market (which increased 10% compared to in 2008) and are almost exclusively used on the portable rechargeable battery market, which is the fastest growing segment of the rechargeable battery market [15].

Beyond consumer electronic products, LIBs are also being used in electric vehicles[1] (EVs) and military as well as aerospace equipment most recently. In particular, while nickel-metal hydride batteries have been used in hybrid EVs, LIB technology dominates the battery used in new plug-in and all-batteries EVs. The Tesla Roadster, an EV sports car containing 6800 cells, was the first production automobile using LIB cells (see Figure 1.2) [16]. Until now, a number of automobile manufacturers use LIBs in their

[1] Electric vehicles (EVs) include hybrid EVs, plug-in EVs, and all-battery EVs.

EVs, such as Chevy Volt, Coda Sedan, Tata Nano, Nissan Leaf, Tesla Model S, etc. [17-20].

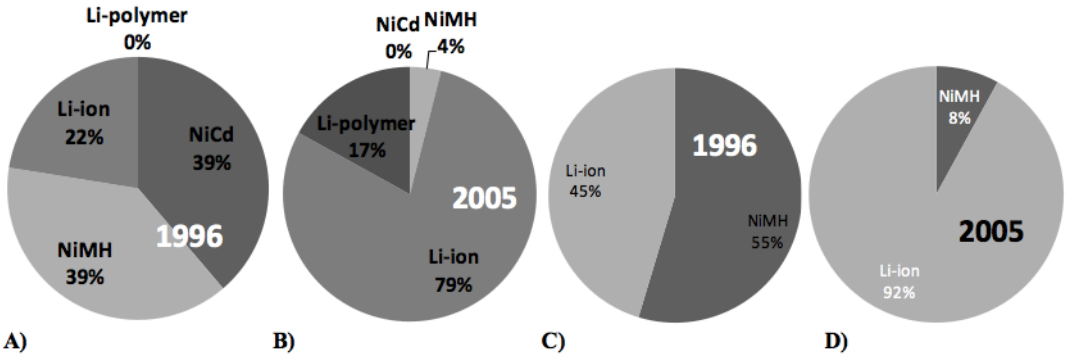

Figure 1.1 (a) Types of batteries in cell phones produced in 1996 where total production was 4.9 million units and (b) in 2005 where total production was 177 million units. (c) Types of batteries in laptops produced in 1996 where total production was 1.8 million units and (d) in 2005 where total production was 3.3 million units.

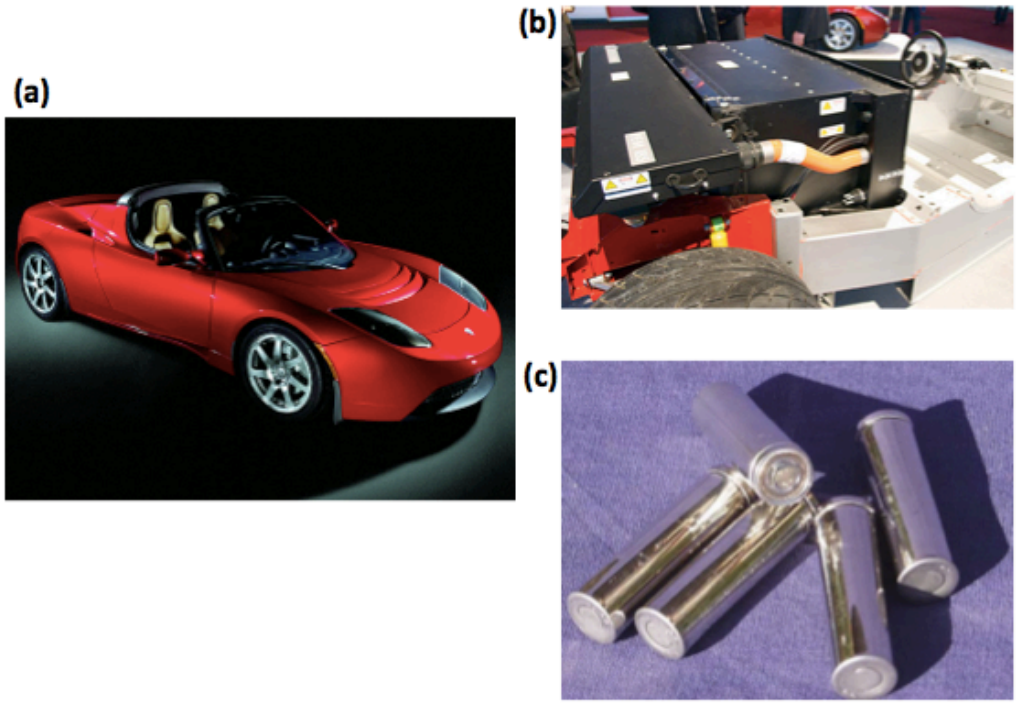

Figure 1.2 (a) Tesla Roadster, (b) Tesla Roadster battery pack, (c) LIB cells used in Tesla Roadster.

1.2 Motivation to promote LIB recycling

The consumption of all kinds of electronic devices has increased dramatically over recent decades (see Figure 1.3a and b as two examples). This increase is due to a variety of factors including both increasing population and electronic product ownership and decreasing lifespan of these products due to the faster replacement by newer generations. Meanwhile, although the current market share of EVs is relatively low (e.g., 3.81% in the US in 2013), this number is expected to increase along with the rising gas prices and increasing environmental concerns (see Figure 1.3c). A number of studies estimated that sales of EVs are likely to experience several jumps worldwide in the next few decades [21, 22]. LIB as the main power source for these portable products and EVs, its potential demand is expected to have a high growth rate and even big jumps in the near future. In 2006, $1.1 billion of LIBs were consumed globally, and this number is estimated to reach $25 billion by 2017 according to a research done by Research and Markets [15, 23].

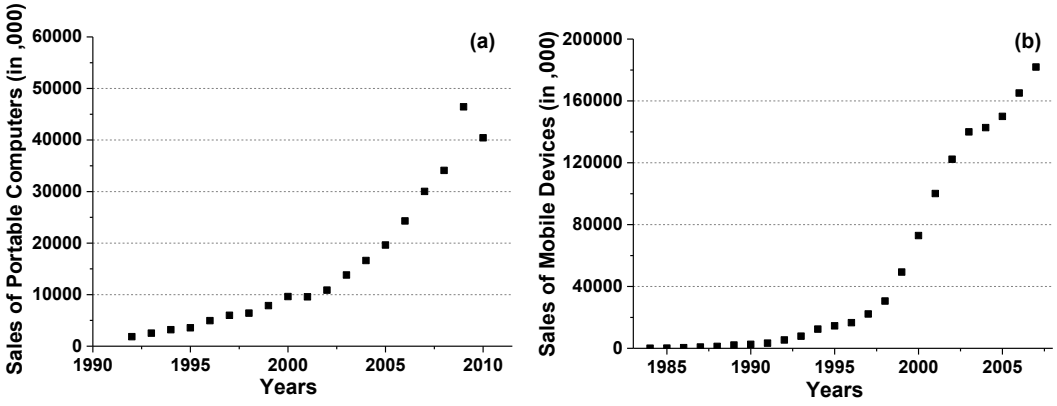

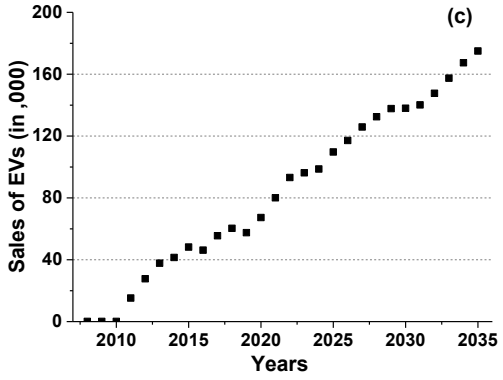

Figure 1.3 Sales of electronic products and EVs in the US over the years (a) historical data for portable computers, (b) historical data for mobile devices, and (c) historical and projected data for EVs (see Table B1 in Appendix B).

This rapidly growing demand for LIBs indicates a significant amount of LIBs will reach their end of life after a short period of time. Whilst LIBs are considered less toxic compared to lead acid and nickel-cadmium batteries, direct landfill disposal of huge amount of end-of-life (EOL) LIBs without any appropriate treatment has a high potential to cause a series of issues including resource depletion, energy waste, land and groundwater pollution, etc. Facing this evolving waste stream, our society is not ready yet. Currently, only a few companies process EOL LIBs (e.g., Toxco, and Umicore); recycled LIBs only account a very small percentage of the total number of EOL LIBs entering the waste stream every year. Moreover, advanced and sustainable recycling technologies need to be developed. Those existing recycling technologies usually process multiple products including several types of batteries and/or other metallic scraps at the same time with the target on a few high-value materials, such as cobalt; other contained materials end up into low-value byproducts or in landfills [24]. However, these currently non-targeted materials might also have environmental incentives to be recovered at a higher rate. For example, recovering aluminum, which is popularly being used in the

"can", has a significant energy saving potential due to significant less amount of energy required during the secondary production compared to the primary production (since the later one does not include the process of extracting raw materials from the earth). Figure 1.4 shows the difference in energy between primary and secondary production based on the data taken from life-cycle assessment (LCA) software database (ecoinvent v2.2 within SimaPro 7.2), and calculated according to the impact assessment methodology "cumulative energy demand v1.07"[25]. In the US, only California and New York state legislators have attempted to proactively address this waste challenge by issuing disposal bans on rechargeable batteries [26, 27]; the federal law regarding EOL LIB management is not in place yet. This dissertation aims to systematically examine the risks and opportunities for EOL LIBs with a focus on environmental and economic aspects, and to analyze the trade-offs between these two aspects. The results from this dissertation can assist policy-makers to make regulations or policies to promote better waste management of EOL LIBs for more sustainable and efficient use of resources.

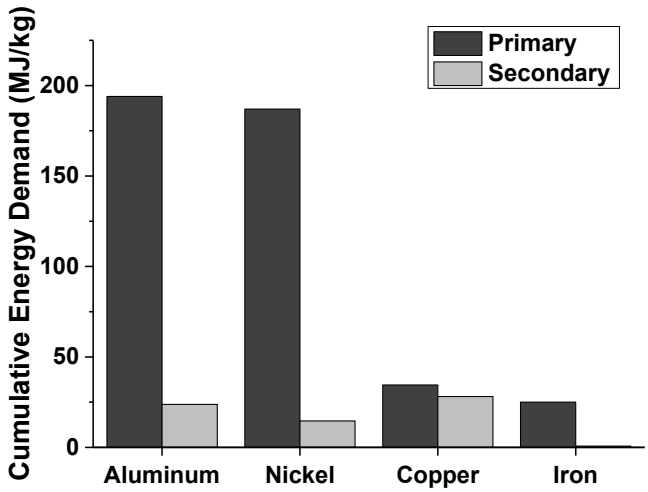

Figure 1.4 The comparison of cumulative energy demand for primary and secondary production of several types of metals.

1.3 Dissertation outline

LIBs are diverse and complex in terms of form factor, size, cathode chemistry, and morphology, indicating that recycling facilities are likely facing uncertain and ever-changing LIB waste streams. Chapter 2 explores the prioritization of material recovery from EOL products based on their material composition as well as several evaluating metrics. Metrics selected in this study include commodity values of recoverable materials representing the economic values, cumulative energy demand (CED), and eco-toxicity measuring the environmental impact. This proposed methodology is first applied to printed circuit boards (PCBs) as a case study (see Appendix A) and then to LIBs. Results show that besides commonly targeted high-value materials, many other contained materials also have incentives to be recovered at recycling facilities. Particularly, this chapter analyzes the impact of battery cathode technology trajectory (from lithium-cobalt based cathodes to less costly chemistry materials) on recycling incentives. As expected, the potential recoverable value decreases along with the initial value of the raw materials used; and more importantly, targeted materials would move away from cobalt. This chapter builds a foundation for this dissertation research and also sends a message to all stake-holders (i.e., recyclers, scientists, policymakers, and general public) that materials contained in EOL LIBs still have economic and environmental incentives to be recovered appropriately.

While the potential recoverable value of EOL LIBs has been demonstrated in Chapter 2, it cannot fully support that recycling LIBs at an industrial level is economically feasible. Particularly, since a diverse mix of cathode and anode materials have been developed and used in LIBs to improve the battery performance, the society

will be facing a highly uncertain and variable waste stream. Development of a robust EOL battery infrastructure requires a better understanding of how to maximize the economic opportunity of battery recycling while mitigating this uncertainty. Chapter 3 develops and applies an optimization model to analyze the profitability of recycling facilities given current estimates of LIB technologies, commodity prices of materials contained in batteries, and material composition for three common battery types (differentiated on the basis of cathode chemistry). According to the results, the profitability is highly dependent on the expected mix of cathode chemistries in the waste stream and the resultant variability in material mass and value. The initial results and a policy case study can help to promote end-of-life management and relative policymaking for spent LIBs. In addition, this chapter reveals the current low collection rate of spent LIBs from consumer electronics (i.e., less than 10%), and points out that improving this rate can make local recycling of LIBs possible.

Given the fact that current battery recycling processes as well as ongoing research only target on a few high-value materials (i.e., cobalt), recycling technology needs to be designed to have a broader target according to the results from the first two chapters. Mechanical pre-treatment can liberate the component materials, provide specific recycling technologies to different fractions, and therefore provide opportunities to improve the efficiency of subsequent recycling processes. Since a wide range of materials is contained in LIBs, the pre-recycling process is substantially important. Chapter 4 proposes a pre-recycling process, including a mechanical shredding and size-based sorting process. This process has a number of advantages over other designs, including automatic, low cost, easy-to-implement, and low environmental impacts. The results

show that this pre-recycling process can effectively free contained materials, achieve material segregation, and enrich metallic components in certain fractions; however, the effectiveness varies when applied to different cathode types. Another takeaway from this chapter is that pre-sorting by battery cathode type is also important as it can significantly reduce the input material uncertainty.

While several ongoing studies focus on evaluating environmental and economic impacts associated with LIBs, very little concerns have been given to nanoparticle exposure risk during battery end-of-life processing, particularly for next-generation LIBs, i.e., batteries contain nano-scale cathode materials. Chapter 5 aims to proactively fill this research gap using the mechanical treatment introduced in Chapter 4 as a case study. The analysis focuses on two potential sources: 1) nanoparticles formed from the mechanical pre-recycling process, 2) nanoparticles released from nano-enabled LIBs. Results show that a substantial amount of nanoparticles have been released during the mechanical shredding process but not the size-based sorting process; and shredding LIBs containing nano-scale materials may have a higher potential for nanoparticle exposure.

Chapter 2. Economic and environmental characterization of an evolving lithium-ion battery waste stream

2.1 Introduction

Facing the potentially looming waste problem of LIBs, California and New York state legislators have attempted to proactively address this waste challenge by issuing disposal bans on rechargeable batteries in their states [28, 29]; similar bans exist as part of the Battery Directive in the European Union [30]. However, eliminating landfill as a disposal option means that alternative end-of-life management strategies must be developed, particularly infrastructure for recycling valuable metals contained within the battery. Research on efficient extraction of specific materials contained in LIBs has increased dramatically over the last decade; excellent reviews of such work are provided in [31-33]. However, the potential recoverable values from spent LIBs are heavily dependent on the diversity in the waste steam, which is poorly characterized and continually evolving. A systematic review of potential value based on chemistry has not been conducted.

The wide variety of sizes, form factors, cathode chemistries, and morphologies indicate that the recycling infrastructure created will need to be responsive to a waste stream with diverse, uncertain, and continually changing materials. Introduction of large batteries for hybrid and all-electric vehicles will also complicate any forecasts in production volume by cathode, particularly given that each automotive company has chosen a different chemistry to pursue. For example, the Chevy Volt uses a Mn-spinel and mixed metal cathode [34], the Tesla Roadster and Model S use $LiCoO_2$ [35], the Coda Sedan and the Tata Nano use $LiFePO_4$ [36, 37], and the Nissan Leaf uses $LiMn_2O_4$

[36]. Existing battery waste processors are, by necessity, largely backwards-looking. That is, they typically plan for recovery of materials from battery technologies that are several years behind those currently under development by manufacturers, as these will not appear in the waste stream until the lifespan of the products they are contained in has ended [38, 39]. As a consequence, battery recycling facilities are focused on recovery of high value, high volume materials contained in LIBs (e.g. cobalt, nickel, copper) and many are unable to economically recover other materials (e.g., lithium, electrolyte, mixed metals). As a result, current battery recycling rates are comparatively low (not including lead-acid), despite the valuable materials currently found in batteries. Beyond the potential economic benefit from increasing battery recycling [40, 41], significant environmental gains could also be realized by recovering high embodied energy materials and offsetting future virgin material extraction demand [38].

This chapter provides necessary first steps towards evaluating battery recycling infrastructure by quantifying the dynamic linkage between evolving LIB cathode chemistries and potential end-of-life material value and environmental impacts. Specifically, LIB cathode chemistries representing recent shifts toward low-cost materials were characterized based on materials they contained and analyzed to project potential economic value recoverable from an evolving LIB waste stream. This value was also assessed for sensitivity to compositional variability of a co-mingled waste stream and the expected yields associated with common recycling technologies. The aim of this chapter is to highlight the economic and environmental opportunities and tradeoffs of LIB recycling as a catalyst for the following chapters and development of novel recovery

technologies as well as inform the development of proactive policies for LIB EOL management.

2.2 Methodology

2.2.1 Battery selection and scenario analysis

Battery compositions for a set of LIB cathode chemistries were determined using reported compositions from the literature, material safety data sheets (MSDS) for products containing LIBs, and bills of materials determined through physical disassembly. The base case analysis focuses on $LiCoO_2$ cathode chemistry as this is the prevalent chemistry found in most consumer electronics which make up the majority of the current LIB waste stream. The "18650" cylindrical form factor (18 mm diameter, 65 mm length) was chosen, as this is a common form factor for laptops and power tools. The compositions of this same cathode chemistry and form factor were compared for seven different manufacturers (see Table B2 in Appendix B).

In the cross-cathode comparison, the following chemistries were included: $LiCoO_2$, $LiFePO_4$, $LiMn_2O_4$-spinel, and a mixed metal cathode $Li(Ni_{1/3}Mn_{1/3}Co_{1/3})_2$. These four cathode chemistries encompass the most relevant Li-based technologies for current consumer electronics and current and near-term electric vehicles as detailed in Section 2.3.2. For all of the cases, the battery form factor was held constant for comparison purposes. While EVs will certainly make use of additional form factors (e.g. prismatic plate, pouch, etc.), the availability and quality of data with which to characterize the 18650 cells is much better, which provides a consistent basis to identify material-specific issues across chemistries. This analysis can then be expanded as other form factors become more prevalent.

Realistic recycling scenarios were also analyzed assuming a co-mingled stream and differing degrees of recycling rate and yield. For the current co-mingled case, it was assumed that the $LiCoO_2$ cathode chemistry would continue to dominate the waste stream (at 85 wt.%), with small amounts (5 wt.%) of the other three prevalent cathode chemistries part of the overall mix. For the future co-mingled scenario, it is assumed that development of high performance cathode materials coupled with further penetration of EVs will drive a weight percentage increase (to 10 wt.%) of non-cobalt based chemistries present in a mixed waste stream.

The base case, cross-cathode comparison, and co-mingled case assume that all of the materials within the battery can be successfully recovered implying a 100% yield rate. This provides policy-makers and waste management professionals with a 'best" case scenario for recycling; however, it is likely that yield will be significantly lower. Yield for recycling lithium-ion batteries at an industrial scale is currently unknown as the recycling infrastructure could take many forms: pyrometallurgical, hydrometallurgical, and a variety of mechanical/physical pre-sorting technologies are in development both at the lab-scale and industrially [42-45]. Three cases were analyzed to characterize changes in economic performance due to lower yields: a "medium" case of mid-value demonstrated yields from lab-scale pyrometallurical and hydrometallurgical recycling technologies, a "high" case of the highest demonstrated lab-scale yield, and a "low case" of the current municipal solid waste (MSW) recycling rate (Equation 2.1) for materials in the battery stream.

$$RR = \frac{\text{consumed old scrap} + \text{consumed new scrap}}{\text{apparent supply} + \text{imports} - \text{exports} + \text{adjustment}} \qquad (2.1)$$

For the demonstrated yields, values for cobalt, lithium, aluminum, copper, nickel, and manganese are shown in Table 2.1; other contained materials were assumed to be at their MSW recycling rate (Table 2.2) as further recovery has not been successfully demonstrated yet. Each of the scenarios investigated and their associated parameters are summarized in Table 2.3, including those used for analysis of economic and environmental impacts, with additional methods described in subsequent sections.

Table 2.1 Demonstrated lab-scale yields (both medium and high) for battery materials of interest.

Materials	Mid-Value		High-Value	
Cobalt	80%	[46]	99%	[47]
Lithium	55%	[48]	100%	[49]
Aluminum	55%	[46]	98%	[50]
Copper	10%	[51]	90%	[52]
Nickel	90%	[52]	99%	[53]
Manganese	92%	[47]	98%	[48]

Table 2.2 US 2010 recycling rates (low value) from USGS for battery materials of interest [7-9].

Recycling Rate (Equation 2.1)				
Aluminum	46%		Iron	41%
Cobalt	0%		Graphite	0%
Copper	30%		Carbon	0%
Lithium	0%		LiPF6	0%
Manganese	33%		PVDF	0%
Nickel	41%		Binders	0%
Steel	61%		Plastic	30%

Table 2.3 Summary of parameters for analyzed scenarios.

	Sec.	Cathode Chemistries (# Manufacturers)	Yield
Base Case	2.3.1	$LiCoO_2$ (7)	100%
Cross-Cathode Comparison	2.3.2	$LiCoO_2$ (7) $LiFePO_4$ (3) $LiMn_2O_4$-spinel (3) $Li(Ni_{1/3}Mn_{1/3}Co_{1/3})_2$ (4)	100%
Co-mingled Case	2.3.3	Current: 85% $LiCoO_2$, 5% $LiFePO_4$, 5% $LiMn_2O_4$-spinel, 5% $Li(Ni_{1/3}Mn_{1/3}Co_{1/3})_2$	100%
Variable recovery cases	2.3.4	$LiCoO_2$ (7) $LiFePO_4$ (3) $LiMn_2O_4$-spinel (3) $Li(Ni_{1/3}Mn_{1/3}Co_{1/3})_2$ (4)	US recycling rates High and average lab yields
Environmental impacts	2.3.5	$LiCoO_2$ (7) $LiFePO_4$ (3) $LiMn_2O_4$-spinel (3) $Li(Ni_{1/3}Mn_{1/3}Co_{1/3})_2$ (4)	100%

2.2.2 Battery compositions from disassembly

The total cell mass was recorded before disassembly, and any losses in the total mass before and after disassembly were assumed to be evaporated electrolyte. Three ½-inch diameter circular samples were punched from areas in each electrode with adhered coatings to the metal current collector and from the separator as well. Electrolyte contained in these samples was evaporated by drying in a vacuum oven at 100°C. The adhered coatings were removed from the dried electrode, leaving the metal current collector (Al for cathode and Cu for anode), the mass of which was directly measured. The coating mass was then calculated as the difference between the masses of the total dry electrode and the current collector. The mass percentages of electrode coating and current collector in the samples were then multiplied by the total electrode mass to scale up findings for the total electrode coatings and current collector masses in the cell. The electrode coating contains an active material, polymer binder, and carbon conductive

additive. The mass of the active material was calculated by dividing the cell capacity (mAh) by the specific active material capacity (mah/g). The carbon conductive additive and polymer binder (PVDF) were then assumed to be of equal percentage of the remaining electrode coating mass. This methodology follows the lab-scale disassembly of others [54, 55].

2.2.3 Potential value

For each material category identified through disassembly, representative commodity values were obtained to estimate the maximum economic value of an EOL LIB stream. This estimation assumes both primary commodity pricing for materials and no material losses due to recycling inefficiencies. This is referred to as the "theoretical maximum value" through-out the remainder of this chapter and represents the upper limit to the economic value associated with the waste stream, and would be reduced in reality once real secondary values and processing yields are taken into account. Although yield and secondary stream material values are unknown at this time, sensitivity analysis was performed in Section 2.3.4 to investigate how this might impact the economic return.

Current commodity prices have been significantly volatile, with large day-to-day swings. Regardless, to reflect current value, average spot prices for metals and plastics in March 2012 were collected from the London Metals Exchange (LME), American Metal Market (AMM), and a scrap trading website, GlobalScrap. These values were averaged both by geographic area and over the month time span and are available in Table 2.4. This variability is particularly relevant for lithium, as the United States Geological Survey (USGS) reports a significantly low value, while lithium spot prices have increased exponentially over the last year. Prices were taken from Alfa Aesar assuming

bulk discount for the electrolyte and binder materials that may be recoverable. The range of types of plastics used in LIBs make it challenging to select a specific value. Some high quality plastics have EOL value as high as $0.35/kg, however, plastics recovered from batteries will likely be co-mingled thermosets and therefore a lower, more typical, average value was used. As with the other materials, contamination and co-mingling may decrease this value significantly.

Table 2.4 Estimates for commodity value of materials contained in LIBs ($/kg).

	USGS '09	USGS '10	USGS '11	2012 Spot		USGS '09	USGS '10	USGS '11	2012 Spot
Lithium	$0.01	$0.01	$0.01	$62.20	Graphite/C	$0.67	$0.67	$0.67	$0.67
Cobalt	$39.34	$46.26	$39.68	$36.48	Steel	$0.20	$0.33	$0.67	$0.64
Nickel	$14.65	$21.70	$22.30	$24.23	Iron	$0.14	$0.23	$0.67	$0.64
Copper	$5.31	$7.53	$8.93	$9.56	Binders	$0.34	$0.34	$0.34	$0.34
Manganese	$0.01	$0.01	$9.10	$3.57	Plastics	$0.05	$0.05	$0.05	$0.05
Aluminum	$1.74	$2.25	$2.65	$2.64					

2.2.4 Environmental considerations

A variety of environmental metrics are available to evaluate EOL LIB impacts such as greenhouse gas emissions, eco-toxicity, and human health effects. However, comprehensive life-cycle inventory and impact assessment data for LIBs have yet to be quantified [56]. Therefore, CED was selected as a representative metric of the environmental impact of materials contained in the LIBs [57, 58]; these values are reported in Table 2.5. CED includes all direct and upstream energy inputs associated with mining, refining, and processing LIB materials from “cradle-to-gate”, but does not take into account the assembly and transportation of the LIBs once they have been fabricated from the supply materials. Refining has been included in this cumulative energy but should be considered a minimum and therefore conservative estimate for the CED as

inventory data does not exist for many of the extremely high purity materials included. There is a particularly high degree of uncertainty in the magnitude of CED for the advanced anode and electrolyte materials. However, a considerable amount of energy is required for mining, manufacturing, and transporting primary metals. Recycling provides an opportunity to recapture some of this energy albeit with its own set of environmental impacts. Energy data was taken from life-cycle assessment (LCA) software databases (ecoinvent v2.2 within SimaPro 7.2) and calculated according to the impact assessment methodology "cumulative energy demand v1.07" [25].

Table 2.5 Estimates for CED and eco-toxicity for materials contained in LIBs.

Materials	CED MJ/kg	Eco-toxicity CERCLA pts	Materials	CED MJ/kg	Eco-toxicity CERCLA pts
Lithium	399	415	Copper	35	805
Phosphorus	229	1145	Iron	25	NA
Aluminum	194	688	Steel	25	NA
Nickel	151	1005	Plastic	21	NA
Cobalt	128	1016	LiPF6	15	NA
Carbon	89	179	Carbonates	10	NA
Graphite	68	NA	PVDF	1.5	NA
Manganese	59	808			

Eco-toxicity is used as a representative metric of the environmental impact of releasing LIB materials into the environment, and measures the potential for pollutants (both natural and synthetic) to cause stress to ecosystems (including plants, animals, and humans). A variety of eco-toxicity metrics exist and have been widely used to identify chemical hazards [59]. For this study, the eco-toxicity metric used is based on the 2011 Priority List of Hazardous Substances from the Comprehensive Environmental Response, Compensation, and Liability Act (CERCLA) [60]; reported in Table 2.5. CERCLA provides comprehensive information about eco-toxicity of hazardous substances, taking

into account the frequency of occurrence of substances at national priorities list (NPL) hazardous waste sites and facilities, the Environmental Protection Agency's (EPA) reportable quantity ranking, EPA toxicity score, and the potential for human exposure; detailed information on how this score is calculated is available in the CERCLA support document [61]. This comprehensive metric avoids a narrow view of eco-toxicity that a single indicator metric such as LC50 (the median lethal concentration) or TD50 (the median toxic dose) may provide. While CERCLA eco-toxicity points are not normalized by a mass or volume metric, a points per kilogram extrapolation was performed in order to weight the compositional differences of materials within LIBs.

2.3 Results and discussion

2.3.1 Base case: $LiCoO_2$

The base case analysis uses the average compositional values from both literature and physical disassembly for sixteen different $LiCoO_2$ cathode LIBs representing seven different manufacturers. Even though this set of sixteen batteries shares the same cathode chemistry and form factor (18650), significant variability can be seen in Figure 2.1. Coefficient of variation (CV), the standard deviation normalized by the mean, ranges from 21% for binders to 126% for carbon black. The base metals have relatively lower variability ranging from 21% for steel to 37% for aluminum; however, this degree of variation is still a significant source of concern for recyclers. As cobalt is one of the key materials targeted for recycling and recovery, it is interesting to note that the standard deviation of +/- 1.8 grams Co could result in a range of secondary values between $0.15-$0.42 per 18650 cell (based on March 2012 spot prices). This difference is quite extreme when extrapolated to volumes of spent batteries that may be processed by a typical

recycler. For example, a current lead-acid battery recycling facility in the US processes between 132,000-176,000 metric tons per year [62]. Spot prices for commodity metals have significant volatility, however, even 2011 average USGS prices show an even larger range in value of \$0.18-\$0.50 per 18650 $LiCoO_2$ cell.

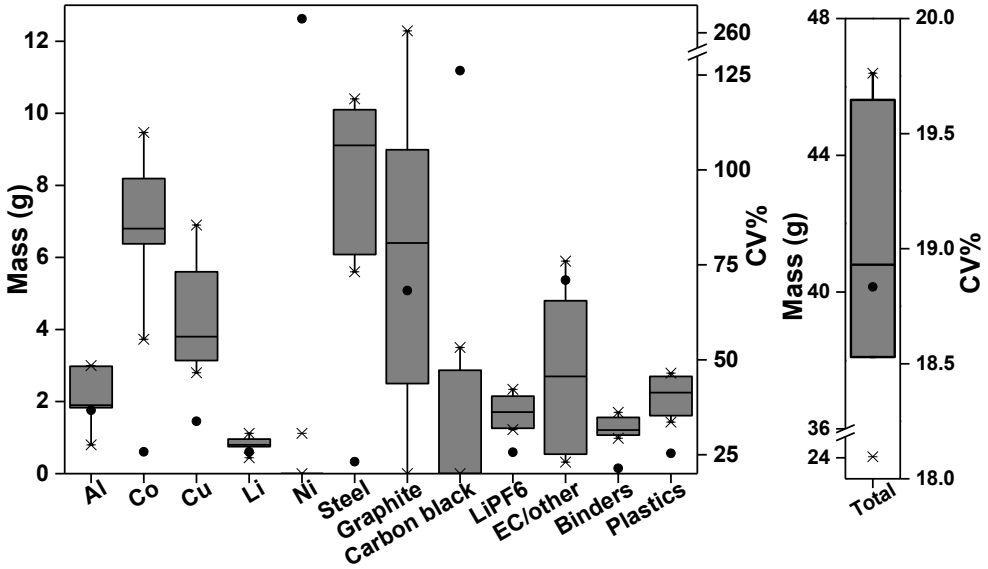

Figure 2.1 (a) Statistical analysis of sixteen $LiCoO_2$ LIBs for various material categories, (b) analysis for the total weight, the grey box represents the 25^{th}-75^{th} percentile with the line being the median, x's present the 1^{st}-99^{th} percentile, and the black dot is the coefficient of variation; see the description of the legend in Figure B1 in Appendix B.

It is again emphasized that this is the maximum theoretical value for recyclers, as the calculation assumes that high yield recovery of all materials from the LIB is possible. These results show that there is significant potential for valuable resource recovery; given an average weight of 40.5 grams per 18650 cell, one metric ton of this scrap could be worth \$4,400-\$10,400. The cost to collect and process these scraps would make the profit margin significantly less than this total, however, compared to other scrap materials this is still quite valuable. For example, mixed electronic scrap sells in the range of \$1,000 per metric ton and up to \$8,000 per metric ton for high grade sorted PCBs [63]. Ferrous scrap

from shredded automotive hulks averages around $525 per metric ton [10]. This strong economic incentive may be a likely driver for many electronic waste (e-waste) processors moving toward processing batteries as well.

The compositional uncertainty seen for the $LiCoO_2$ cathode chemistry LIBs is present for other cathode chemistries as well. Detailed results for six $LiFePO_4$ 18650 cells from three different manufacturers (two each from Tenergy, A123, and Sony) are shown in Figure 2.2.

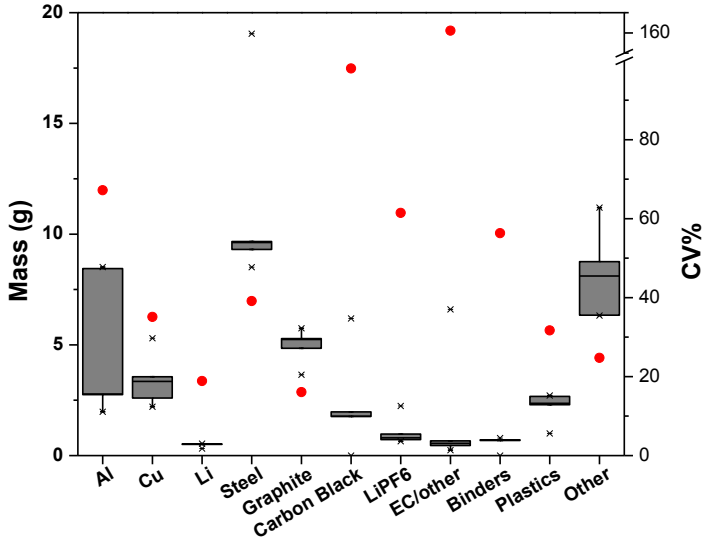

Figure 2.2 Mean and standard deviation of six 18650 $LiFePO_4$ cells from three manufacturers, the grey box represents the 25th-75th percentile with the line being the median, x's present the 1st-99th percentile, and the red dot is the coefficient of variation; see the description of the legend in Figure B1 in Appendix B.

2.3.2 Technology trajectory: cross-cathode comparison

While $LiCoO_2$ cathode chemistries dominate in terms of current manufactured volume, significant progress in the rechargeable battery field has been made through research and development of late. Increases in energy density and reduction in costs have been found through exploration of other cathode chemistries as well as changes in

anodes, cans, and processing routes. A variety of chemistries are currently being used commercially, with many more being actively developed for future high volume applications, namely transportation. Figure 2.3 shows an approximate chronological progression of explored cathode chemistries, illustrating a slight improving trend in energy density. While it is not clear which cathode types may be the next generation in high volume production, $LiFePO_4$, $LiMn_2O_4$-spinel, and mixed metal type cathodes have emerged as clear contenders, particularly for electric vehicles which may require a significant volume of batteries as their penetration increases. Examples of EVs with these battery types were detailed in the introduction. Regardless of which batteries dominate production, these changes in battery composition in all demand sectors will have significant impacts on the stability and profit of recycling infrastructure.

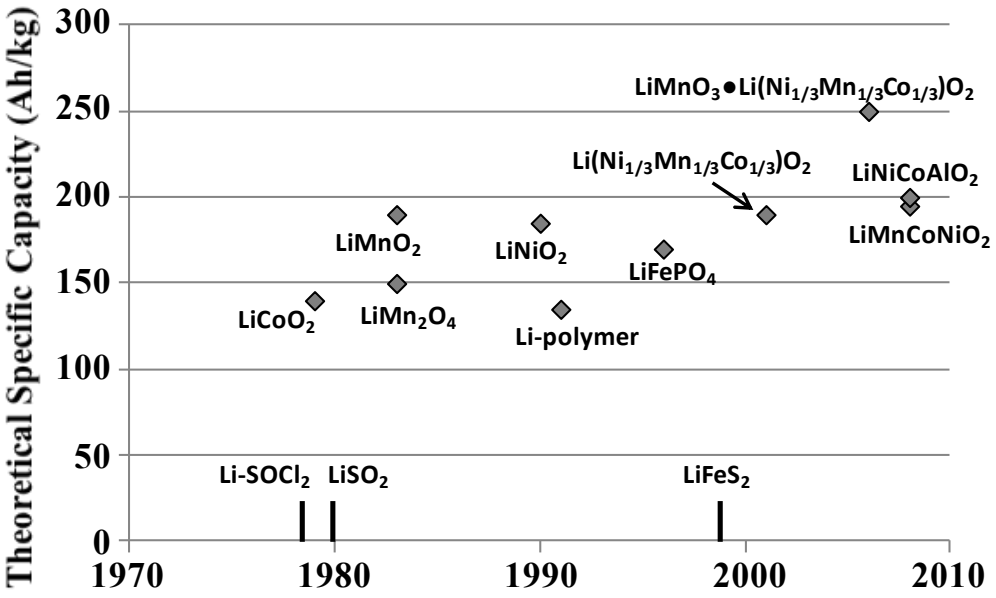

Figure 2.3 Approximately chronological set of cathode materials showing modest increases in specific capacity [1-5].

Not surprisingly, batteries with varying cathode chemistries have significantly different overall material compositions. Figure 2.4(a) shows the compositional breakdown by weight for three cathode chemistries chosen to represent batteries with high likelihood of gaining considerable market share compared to $LiCoO_2$. All four are taken from 18650 form factor cells with a minimum sample size of four per chemistry. While base metals as a whole make up the largest fraction of total mass, thus driving metrics of interest (value, embodied energy, eco-toxicity, etc.), there is little consistency in composition or amount of specific metals (Figure 2.4b). Steel makes up a significant portion of the base metal weight for most of the battery types due to its use in the "can", the outer packaging of the cell, however some cells use aluminum as the can such as the mixed $Li(Ni_{1/3}Mn_{1/3}Co_{1/3})_2$ cathode (labeled as $LiMO_2$). Regardless of the remainder of the composition, cobalt has the most impact on recoverable value. Figure 2.5 compares the values of these four cathode chemistry types given commodity market prices for different years. Mn-spinel and iron phosphate cathode batteries have potential material values 73% and 79% less than cobalt cathode batteries, respectively.

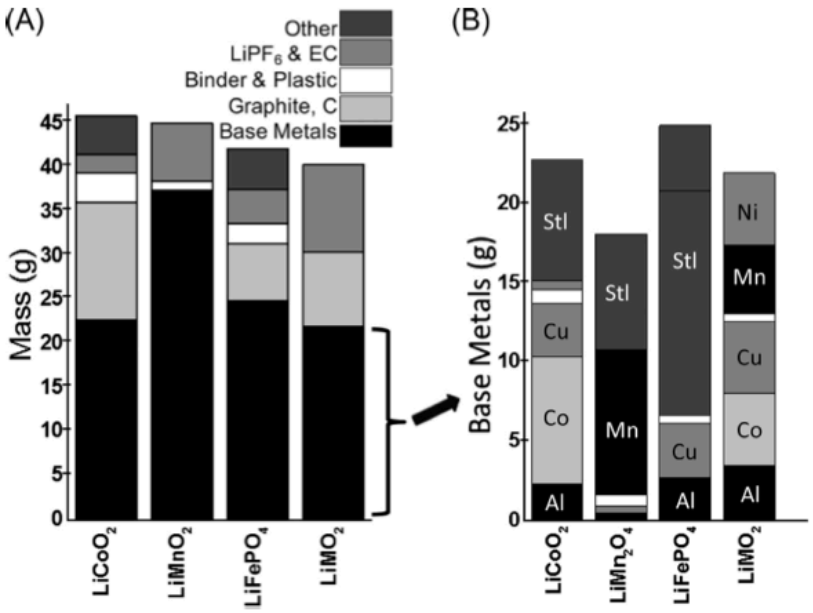

Figure 2.4 Compositional breakdown in total (a) and for base metals (b) for 18650 cells of varying cathode chemistry.

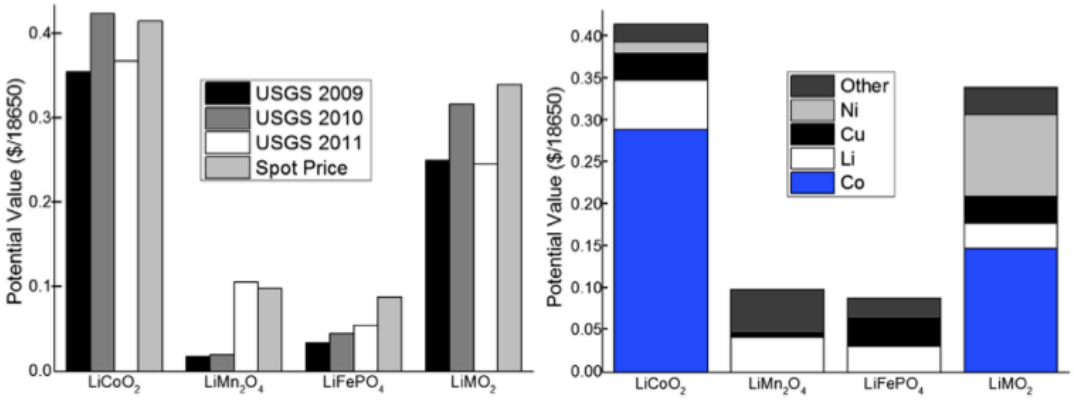

Figure 2.5 Cross cathode comparison of potential value per 18650 form factory battery.

This analysis assumes lithium can be economically extracted at scale, implying that the spot price of lithium would have to reach over 600% its present value before these two chemistries had EOL values comparable to cobalt based chemistries. Even for the mixed metal cathodes, which contain a large proportion of cobalt, reaching an EOL

value on par with wholly cobalt based chemistries would require high purity extraction of both copper and nickel; technology which has not been successfully developed or scaled-up yet. This emphasizes the need to develop a recycling infrastructure for LIBs that is robust enough to handle processing materials beyond cobalt in order to ensure profitability for waste managers. Figure 2.5 highlights the need to recover lithium for future cathode chemistries such as $LiMnO_2$ and $LiFePO_4$ as it makes up a significant portion of the total value. For these cathode chemistries, copper and steel (included in "other") also become significant portions of the total value which would incentivize prioritizing their recovery as well. As stated previously, these are also theoretical maximum values assuming a high degree of purity and consistency in the LIB waste stream; actual recycling rates as explored in Section 2.3.4 will lower the profitability as well. Waste managers may need further investment in sorting and separation technologies to achieve a higher purity stream as explored more fully in the following section.

2.3.3 Managing a mixed stream: co-mingled case

Compositional uncertainty that arises from having a co-mingled scrap stream can create a barrier to recycling by raising processing costs, increasing the likelihood for off-specification products, and complicating batching management [64, 65]. Two key mechanisms for co-mingling for LIBs at EOL are 1) being mixed in with other e-waste as they are often not removed from laptops, cell phones, etc. upon disposal, and 2) the wide variety of form factors and cathode chemistries mentioned previously. For most consumer electronic LIBs, the former is most likely as these scraps are often shredded; a pre-processing step performed by most studies researching hydrometallurgically based recovery technologies and being done by many industrial recyclers. For EVs, the later is

the most probable mechanism as H/EV batteries will likely have a dedicated collection and processing infrastructure. To illustrate the degree of uncertainty that one of these aspects, cathode chemistry, would contribute to overall composition of the mixed stream, a hypothetical mixture of different cathodes and manufacturers (all 18650 cells) was created. This mixed scenario was dominated by $LiCoO_2$ cells reflecting the product make-up of the current EOL stream, however, other cathode chemistries were present, thus contributing to higher overall uncertainty. Figure 2.6 shows that the CV for the base metals ranges from 70% (Li) to 175% (Al) with accompanying significant ranges in weight percent.k It is assumed that batteries mixed with other e-waste would have an even higher coefficient of variation.

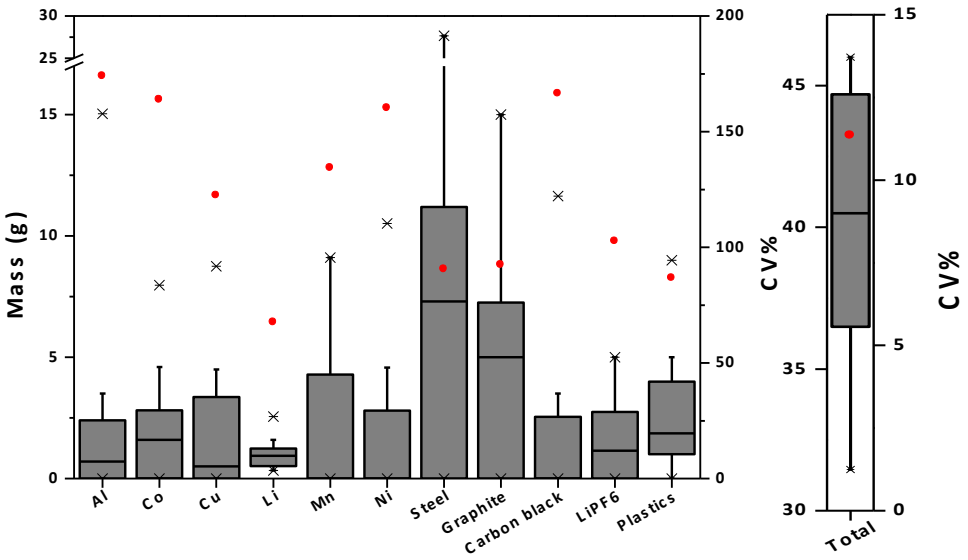

Figure 2.6 Average mass and standard deviation for a mixed stream of Li-based battery cells of the same form factor (18650), the grey box represents the 25th-75th percentile with the line being the median, x's present the 1st-99th percentile, and the red dot is the coefficient of variation. See the description of the legend in Figure B1 in Appendix B.

2.3.4 Variable recovery cases: yield, recycling rate, and disassembly effects

Up to this point, the discussion of economic attributes of a LIB waste stream has centered on the maximum economic content of the waste stream itself, rather than the actual recoverable value, once recycling process inefficiencies are accounted for. This consideration is treated separately here, due to the different end-of-life avenues potentially available to batteries. As highlighted in Table 2.1, a number of hydrometallurgical studies have demonstrated yields above 90% at the lab-scale for a variety of battery materials. However, many of these recycling technologies involve a multitude of steps, are still in development, and reported efficiencies at the lab scale may not be reproducible once the recycling infrastructure is scaled up and complicated by the compositional and co-mingling issues raised earlier in this paper. Some companies (e.g. Toxco, Umicore) have begun successfully scaling up battery recovery facilities, however the focus has been on high yield of cobalt with other materials being recovered at significantly lower rates.

Here, we examine how the potential recoverable economic value changes based on three scenarios of recycling efficiencies: highest known (lab scale) efficiency (high), average lab-scale efficiency (medium), and US cumulative recycling rate (low). Figure 2.7 shows that relying on current recycling rates results in significantly less recoverable value of the LIB scrap stream ranging from 23% for iron-phosphate cathodes to 5% for cobalt based cathodes. It should be noted that on an absolute basis, the value is still much higher for cobalt based cathodes even at 5% compared to others due to its overall higher value (cf. Figure 2.5). More surprising is that current demonstrated lab-scale maximums can achieve quite close to the maximum economic value ranging from 89% for Mn-spinel cathodes to 96% for both mixed metal and cobalt based cathodes. Each set of

technologies used to achieve these yields will have cost trade-offs as well, for example, it could be assumed that the low case would not incur much additional cost as the yield depends on the recycling infrastructure already in place for each of those materials. The medium and high yield cases would incur much higher costs and both capital investment as well as scale-up research and development would need to be implemented in order to achieve those higher yield rates. None of the studies cited in Table 2.1 have conducted cost or economic related analysis for their recovery technologies.

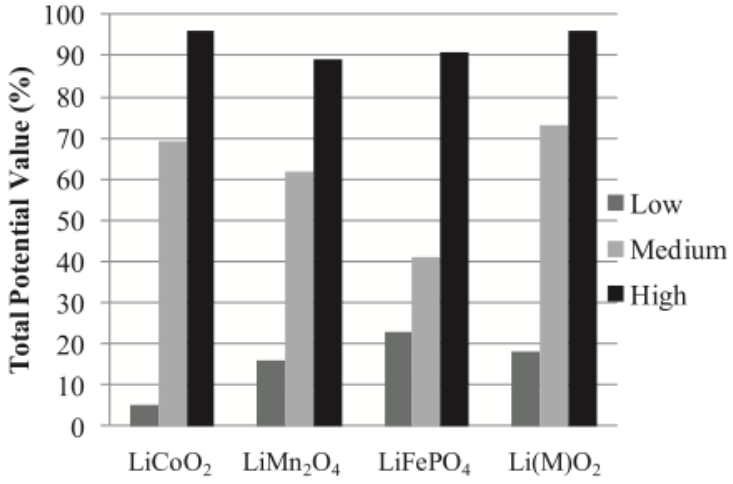

Figure 2.7 Percentage of the total recoverable value (spot price value in Figure 2.5) achieved with potential yield scenarios.

One other potential recycling avenue is the partial or full disassembly of LIBs for recycling given safety concerns of shredding and sorting processes [20, 66, 67]. While some of these studies performed such disassembly by hand for their work, a quantitative assessment based on resulting compositional yield and purity has not been conducted. Here, we compare the relative mass and economic value recoverable at each stage of the disassembly process, if a manual recovery system was employed. One can see that a

majority of the mass is contained in the anode and cathode active materials. If one were to extrapolate from the value results in Figure 2.5, it is clear that the majority of the value is in the cathode active materials which are accessed at the last stage of disassembly shown in Figure 2.8. This would indicate that partial or component-level disassembly would not be economically viable; however, the economics of disassembly compared to shredding combined with a hydrometallurgical or pyrometallurgical process have not been explored.

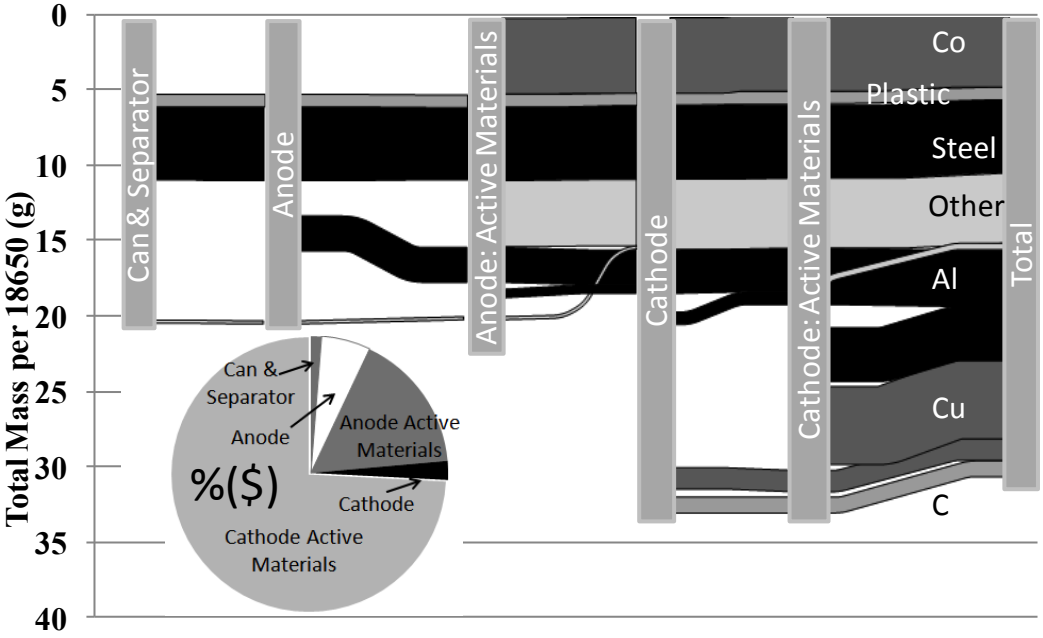

Figure 2.8 Sankey diagram of disassembly showing portion of total weight by component, in order to disassembly for a $LiCoO_2$ cathode chemistry 18650; inset pie shows the breakdown by percent value.

2.3.5 Environmental considerations

To assess environmental impacts, the cross-cathode comparison was revisited (Table 2.3) and average mass was used for each of the cathode chemistries. For this analysis, yield is not a relevant factor as the environmental impacts are assessed for the

total magnitude of materials contained within a battery. Similar to the economic results, the base metals dominate as major contributors to the life-cycle CED of all battery materials. While only making up a small portion of the weight percent (cf. Figure 2.4), aluminum makes up a large percentage of the total CED due to the energy intensity of Hall-Heroult process. Particularly, it accounts for 25% of the base case $LiCoO_2$ cathode, 45% of the $LiFePO_4$ cathode, and 25% of the mixed metal cathode (Figure 2.9a). Diverging from economic results, a key contributor for all four battery types is the carbon black and graphite contained in the cells, ranging from 19% for $LiFePO_4$ to 42% for the $LiMn_2O_4$ cathode (but less than 2% by value for these same chemistries). Battery grade carbon and graphite require additional purification steps that add to their overall energy impact. For the mixed metal cathode, the other category is dominated by manganese (6%), steel and lithium (5% each), and copper (3%). The steel casing dominates the other category for the $LiFePO_4$ cathode at 14%, followed by lithium (8%) and copper (5%). Not surprisingly, manganese is the main contributor in the other category for $LiMn_2O_4$ cathode battery at 22%, followed by lithium (11%) and the steel can (8%). For the cobalt base case, lithium is the largest of the other category at 10% of the total embodied energy with steel accounting for 5%.

The difference in CED between the four cathode chemistries is not as dramatic as the difference in potential economic value. The iron phosphate and manganese based cathode chemistries have roughly 35% less lifecycle CED compared to the cobalt based chemistry (compared to nearly 80% less economic value). For the most part, these results indicate an alignment of economic and energy incentives regarding prioritization of material recovery: the base metals are clear priorities. Thus, additional policy is likely

unnecessary to ensure optimization of recycling from an energy perspective for the profit based infrastructure in place currently. One key difference, however, is the importance of carbon black and graphite from an energy perspective, whereas these materials are low recycling priorities when considering value or potential recovery infrastructure.

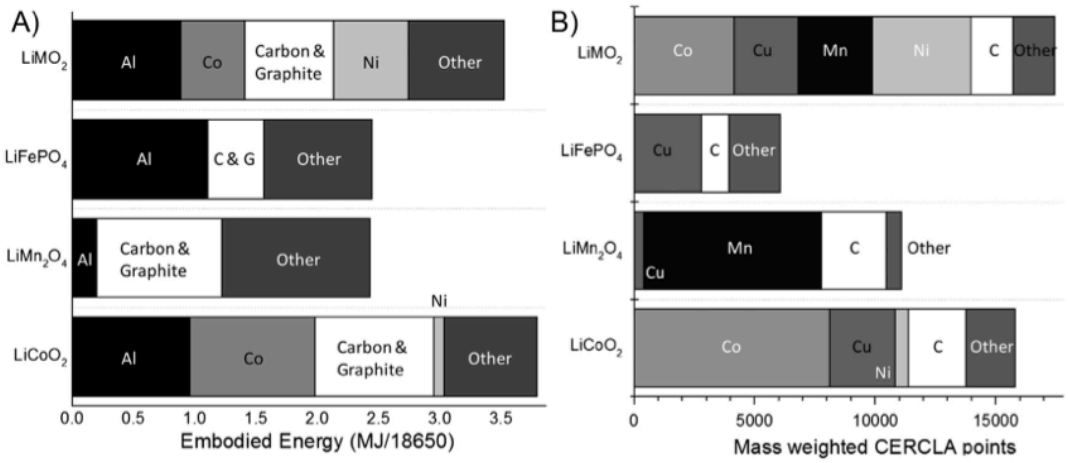

Figure 2.9 (a) Estimated embodied energy for four selected case study cathode chemistries showing key contributors, (b) EPA CERCLA points weighted by mass.

In considering eco-toxicity of materials contained in the battery, should they be released during recycling, the CERCLA point system was adapted by multiplying material-specific points by the mass of each material in the battery. Following the economic and energy results, the base metals are again the major contributors to potential eco-hazard. Nickel, cobalt, manganese, and copper have the highest potential according to CERCLA, and even though their weight percent is comparatively low, they become the key contributors to overall eco-toxicity risk. Not surprisingly, cobalt and manganese are respectively highest for chemistries in which they are dominant metals (Figure 2.9b). The mixed metal cathode has total potential risk roughly evenly divided among its mix of included metals and actually has a 10% higher potential risk compared to the cobalt base

case, mainly due to the inclusion of nickel. $LiMn_2O_4$ cathode batteries have 30% less potential risk compared to the cobalt base case and $LiFePO_4$ has a 62% reduction in potential eco-toxicity risk. While phosphorus has relatively high CERCLA points, its inclusion as an oxide poses little risk; however, it should be noted that certain acid-based hydrometallurgical recycling routes have the potential to reduce and therefore release contained phosphorus.

2.4 Conclusions and implications

Results shown in this chapter suggest that environmental and economic perspectives lead to generally consistent prioritization of materials to be recovered from a LIB waste stream. However, the actual recovery system will need to take into account geographically based regulations on emissions, disposal bans, and producer responsibility. The metrics presented here are somewhat narrowly scoped for a first approximation; but can be expanded into a more holistic life-cycle assessment as additional data on recycling processes and the upstream battery manufacturing processes become available.

Given a profit-based waste management system, results presented in this chapter help stakeholders comprehend what materials within LIBs should be prioritized for recovery. Particularly, results show which materials may require additional policy intervention to overcome economic limitations. As automotive batteries for hybrid and all-electric transportation applications shift towards different form factors, sizes, and configurations, the relative mass contributions to battery components will change. For example, prismatic cells will have a higher ratio of cathode and anode materials to packaging (can and plastics). The choices that automotive companies make in cathode

chemistry coupled with speed of adoption will greatly impact the value of the stream seen by recyclers. While it is clear that economics of recovery and recycling will be impacted by a transition away from cobalt based chemistries, the rapidity and magnitude of this shift are still unclear.

The preceding results suggest policy or other incentives may be necessary to promote a robust recycling infrastructure as the economic incentives will likely decrease as the battery stream changes. For example, widespread battery disposal bans will likely be needed to ensure collection and recovery of LIBs of many next-generation cathode chemistries that exclude high-value cobalt in their composition. Regulation concerning energy savings and eco-toxicity will also favor cathode chemistries without cobalt included. Large packs for hybrid and all-electric vehicles may still benefit from such proactive engineering design. It also appears that any collection or recycling infrastructure will likely need the capacity to process a co-mingled LIB scrap stream. While the results in this chapter can inform both incentives for build-out of collection infrastructure as well as economically efficient recycling strategies, the scale-up scenario also needs to be examined. In the next chapter, the profitability of recycling facilities based on current battery recycling technologies as well as possible co-mingled waste streams will be explored.

Chapter 3. Economies of scale for future lithium-ion battery recycling infrastructure

3.1 Introduction

LIBs in most consumer products have a lifespan of less than three years and those in hybrid and all-electric vehicles are projected to have a lifespan of roughly ten years [67, 68]. Given these low lifespans as well as increasing production, a rapidly growing co-mingled battery waste stream is likely; however, infrastructure required to recycle batteries diverted from the landfill is still lagging. Some companies have developed recycling processes (e.g. Toxco and Umicore) and some companies have sprung up to take on collection (e.g. Call2Recycle), however, a fully operational, broadly reaching recycling infrastructure for EOL LIBs is not well developed and the costs of such infrastructure have not been examined in depth.

From an environmental perspective, the ability to recover materials (e.g., cobalt and nickel) from spent LIBs and return them to new battery production has the potential to reduce the battery's life cycle impact by about 51%, when comparing natural resources consumption from using only primary materials [38]. In addition, increasing concerns about leaching potential of some hazardous materials contained in LIBs during landfill disposal also drive relevant research studies [69].

Economically, recycling has also traditionally offered an opportunity to recover valuable materials used in battery production, namely cobalt, which is widely used in LIBs due to its high energy density. However, manufacturers are moving towards low-cost cathode materials to reduce the cost of battery manufacturing. Cathode materials such as lithium iron phosphate and lithium manganese-spinel are projected to be the next

generation of LIB technology [3]. The previous chapter has demonstrated that the transition from expensive cathode materials to less expensive options reduces the economic incentives to recycle those batteries at their end of life. However, the technology trajectory of LIB cathode chemistries dominating future production volumes is unclear and not necessarily predictable; single recycling facilities will likely see a co-mingled stream. All these uncertainties bring difficulties to LIB recycling.

This highly variable battery waste stream is likely to find parallels in the challenges currently observed for managing the larger e-waste stream. Existing recycling programs for e-waste have been discussed extensively in the literature. Kang et al. and many others have pointed out the increasing volume of e-wastes and outlined the variety of existing recycling programs in the US and their related collection methods [70]. Their work provided a review of U.S. infrastructure for e-waste recycling at a broad level and pointed out domestic infrastructure is insufficient to manage this growing waste stream. However, their discussion did not go into detail for individual recycling facilities or raise issues specific to EOL LIBs. Kahhat et al. reviewed e-waste management systems outside the U.S., including the European Union, Japan, South Korea, and Taiwan, to evaluate the feasibility in the U.S.; and then based on those existing international e-waste management programs and the specific culture in the U.S., proposed an e-waste collection system named “e-Market for Returned Deposit” [71]. However, for LIBs specifically, this proposal would require adjustment because 1) direct reuse may not be an option due to their low-performance after regular life time [72], and 2) unlike other types of e-waste, LIBs are much smaller and they are usually being sold along with electronic products, not individually. Cueto et al. have studied the reverse logistics model, including collection

and recycling systems, for recovering mobile phones in Spain [73]. The requirement of high volume of mobile phones to ensure recycling plants being profitable has been discussed together with the reality of low collection rate of EOL mobile phones.

Considering the challenges and knowledge gaps identified in the broader e-waste literature, it is clear that a more proactive approach must be taken to develop a robust LIB recycling infrastructure. To date, an analysis of profitability and trade-offs of recycling have not been applied to EOL LIBs. From a recycling firm's perspective, it will be essential to forecast economic feasibility of LIB recycling, given uncertainty and variability in cost, volume, and profit. The goal of this chapter is to examine the economic feasibility of recycling spent LIBs under possible scenarios of waste stream volume and composition. An optimization model is used to assess these scenarios, which include compositional variability (i.e., by cathode chemistry type, or manufacturer) for different LIB types, and chemistry distribution of the overall battery waste stream.

3.2 Method

3.2.1 Optimization model

This chapter develops an optimization model, Equation (3.1)-(3.5), to identify the minimum amount of spent LIBs (T) for a recycling facility to be profitable based on the costs and revenue (R), assuming all metallic materials contained in LIBs can be recovered at an average recycling efficiency respectively (RE_j). The indices in Equation (3.3)-(3.5) are shown in Table 3.1.The costs includes the variable cost (VC) and the annual fixed cost (FC). LIBs come in many different sizes, form factors, pack configurations, and cathode chemistries; therefore the LIB scrap stream will likely be co-mingled. In this chapter, three types of cathode materials have been considered: $LiCoO_2$,

the most common, and $LiFePO_4$, and $LiMn_2O_4$, emerging cathode chemistries likely to be in EVs [18, 19]. To illustrate how the proportion of each cathode chemistry type (α_i) can affect our result, the break-even amount (T) has been analyzed for several possible chemistry-distributional scenarios of a co-mingled LIB scrap stream. The unit revenue (R) was determined using commodity values of recoverable materials from one metric ton of co-mingled spent LIBs. The potential value of each type of metal being recovered from one specific LIB cathode chemistry type was calculated based on the material composition of that kind of LIB ($Ava_{i,j}$), recycling efficiency (RE_j) for each type of metal, and primary commodity market price for each type of metal (P_j). The minimum amount of LIBs for a recycling facility being profitable was identified by calculating the break-even point, meaning annual revenue is equal to the sum of fixed and variable costs.

$$Min.T \tag{3.1}$$

$$St.T * R - (FC + VC * T) \geq 0 \tag{3.2}$$

$$R = \sum_{i=1}^{3} (\alpha_i * \sum_{j=1}^{7} (P_j * Ava_{i,j} * RE_j)) \tag{3.3}$$

$$\sum_{i=1}^{3} \alpha_i = 1 \tag{3.4}$$

$$0 \leq \alpha_1, \alpha_2, \alpha_3 \leq 1 \tag{3.5}$$

Table 3.1 Indices' information.

Variables	Indices	Notes		Variables	Indices	Notes
i	1	$LiCoO_2$		*j*	3	Lithium
	2	$LiFePO_4$			4	Manganese
	3	$LiMn_2O_4$			5	Iron/Steel
j	1	Cobalt			6	Aluminum
	2	Nickel			7	Copper

3.2.2 Base case: current battery waste stream

3.2.2.1 Composition

In the base case, only $LiCoO_2$ cathode batteries are considered since they currently dominate the battery market for consumer electronic products. Further, the base case only considered 18650 cylindrical cells, as these are the most commonly used in electronics like laptop computers, and they can provide a fair comparison between different manufacturers and, in later sections, the different cathode chemistries. Sensitivity analysis conducted in (Richa et al., 2013) demonstrated that the total volume and basic material breakdown of an EOL LIB waste stream will not change significantly if prismatic form factor is considered, particularly for LIBs in EVs [74].

It is expected that the material composition in LIBs would vary significantly between different cathode chemistry types; however, even considering the same cathode chemistry, batteries made by different manufacturers are likely to show variation in their bills of materials (BOMs). The BOM for $LiCoO_2$ cathode batteries from seven manufacturers, including Panasonic, Lishen, Sony, Moli, AT&T, Sanyo, and Matsushita, has been provided in Table B2 in Appendix B. The average material composition for all of the previously sampled $LiCoO_2$ cathode batteries was calculated and used in the base case (see Table 3.2). Variability in composition for $LiCoO_2$ cathode LIBs from different

manufacturers and its associated impacts on the breakeven point has been analyzed in section 3.3.3.1 by using the maximum and minimum value.

Table 3.2 Metals prices [10], BOMs[11], and recovery efficiency for LIBs.

Base Metals	Prices ($/kg material)	Composition (kg/ton spent LIBs)			Recycling Efficiency (RE)	
		$LiCoO_2$	$LiFePO_4$	$LiMn_2O_4$	RE (%)	References
Cobalt	46.30	173	0	0	89	[75]
Nickel	21.72	12	0	0	62	[76]
Lithium	62.26	20	12	15	80	[41, 77]
Manganese	0.01	0	0	204	53	[78]
Iron/Steel	0.05	165	432	164	52	[79]
Aluminum	2.25	52	65	11	42	[80]
Copper	7.54	73	82	11	90	[81]

3.2.2.2 Costs

The potential value of materials that can be recovered from spent LIBs was calculated using yearly average commodity metals prices from USGS for 2012. Recycling efficiency of each metal contained in LIBs was estimated from literature (Table 3.2). It should be noted that the recycling efficiencies (RE (%) in Table 3.2) represent an optimistic or best-case recycling processes, as these are typically demonstrated at the lab-scale and not industrially. The recycling efficiency or yield of metals will vary depending on numerous factors including the recycling process or technology employed (e.g. hydrometallurgical vs. pyrometallurgical), and the type and quality of the input scraps. When applying this model to a specific facility, the recycling efficiency can be adjusted based on the actual situation, which may scale the result linearly. Lower recycling efficiencies will require a higher volume of spent LIBs to cover the costs.

Besides the potential value of recovered materials from LIBs, economies of scale for battery processing are also a function of collection and recycling costs. The costs for most recycling facilities fall into two key categories: variable and fixed. Variable costs are expenses that scale proportionately with the volume of outputs [82]; these costs will change according to the battery scrap stream (cathode type, size, purity), recycling technology, geographic location, etc. Data on the variable costs of battery recycling, including collection, transportation, and processing cost, has been shown in Table 3.3. (Labouze and Monier, 2003) and (Moura Bernardes et al., 2003) provide recent estimates, but are based on European data [83, 84]; (Shapek, 1995) and (McMichael and Henderson, 1998) provide data that are specific to the U.S., but are too outdated to effectively represent the current situation [85, 86]. As can be seen for a specific area, e.g., Florida, the variable cost changed over the years. The mean value of listed variable costs in Table 3.3, $2,800/ton, was used as the base case. Standard deviation of data in Table 3.3 is $1,200/ton, indicating there is about a 70% chance that the variable cost would fall between $1,600 and $4,000. As it is difficult to find data on variable costs in recent years due to confidentiality, a time series analysis has been performed to address this data timeliness issue (see Appendix C). Assuming the average variable costs used in the base case ($2,800 per ton) is for the year 2001, the results show variable costs in the next 12 years (i.e., from 2002 to 2012) have not changed substantially. In particular, estimated variable costs for the year 2012 is only about 5% lower compared to the variable costs assumed in the base case. Therefore, the calculation in the base case stays with collected data points for the variable costs for simplicity.

Table 3.3 Information about variable costs (in $/ton).

Regions	Products	Variable Costs	References
Austria	Portable batteries	1,258	[83]
Belgium	Portable batteries	4,218	
France	Portable batteries	2,712	
Germany	Portable batteries	1,260	
Netherlands	Portable batteries	3,975	
Denmark	NiCd	3,198	
Florida (in 1993)	Dry cell household batteries	2,260	[85]
Florida (in 1994)	Dry cell household batteries	2,615	
Florida (in 1995)	Dry cell household batteries	2,375	
Florida (in 1996)	Dry cell household batteries	2,441	
Florida (in 1997)	Dry cell household batteries	2,514	
Belgium	Portable batteries	5,650	[84]
Netherlands	Portable batteries	4,181	
Austria/Germany	Portable batteries	1,469	
US	NiCd	2,200	[86]

Fixed costs are costs that are not dependent on the volume of batteries being recycled, including management salaries, rents of office, and processing areas, etc. [87]. Generally, fixed costs for a recycling facility do not change during the fiscal year; or in other words, fixed costs will not be affected by changes in actual volume of collected spent LIBs and variable costs. Typically, the maximum recycling capacity of a facility is a key parameter in determining overall fixed costs [88]. Given a certain size of recycling plant, available equipment, and people in place, the fixed costs will not rise in proportion to the actual recycling quantity. However, the relationship between the fixed costs and maximum recycling capacity is difficult to analyze due to the many factors involved. For example, geographical location is a key factor in determining overhead labor costs and energy costs associated with the local grid. A recycling facility located in Europe usually has higher fixed costs compared to the one having the same recycling capacity in Mexico, due to higher rents, machinery, and management salaries in European countries.

Intuitively, the higher the maximum capacity, the higher the fixed costs; however, this relationship is likely not linear, usually being shown by Equation (3.6).

$$\frac{I_2}{I_1} = (\frac{Q_2}{Q_1})^x \tag{3.6}$$

where I_1 refers to the known investment for capacity Q_1; I_2 refers to the investment desired for capacity Q_2; and x is the investment-capacity factor.

The value of this investment-capacity factor is empirically derived, usually falls between 0 and 1, and varies depending on the type of industry or products [89]. Since LIB recycling is still in its infancy, there is not enough data to make a meaningful estimation of this factor from a statistical perspective. Therefore, the six-tenths factor rule ("0.6 rule") has been assumed. The "0.6 rule," which says the capital investment typically increases along with production capacity to the power of 0.6, was adduced initially based on the relationship between individual equipment and their capacities and has been extended to complete e-waste recycling plants [89, 90]. Information about several cases, including in the US, Canada, Italy, and Mexico, are detailed in Table 3.4. Annual fixed costs for those published cases were calculated based on the assumption of a 30 year payback period and plotted in Figure 3.1 with corresponding maximum recycling capacities. Also, geographic location can be an important factor; even having similar fixed costs, the facility in Mexico would be able to recycle more e-waste compared to the one located in South Carolina. According to current annual fixed cost for a battery recycling facility (ranging from 0.8 to 5 million dollars per year), 1 million dollars per year has been selected as the starting point in the base case. The reason why a low fixed cost has been chosen in the base case is because unlike existing recycling facilities, which

handle multiple types of e-waste, this chapter only focuses on LIB recycling. Therefore, the Italian facility, which has the similar size and processing condition, is used as the reference. The corresponding maximum recycling capacity for the base case is 34,000 tons per year, calculated based on Equation (3.6).

Table 3.4 Fixed costs and capacities for existing battery recycling facilities.

Total Investment ($)	Capacity (t/yr)	Fixed Costs[a] ($/yr)	Region	References
25,000,000	25,000	833,333	Italy	[91]
16,800,000	22,000	560,000	US	[92]
100,000,000	200,000	3,333,333	Edmonton	
150,000,000	132,000	5,000,000	South Carolina	[93]
150,000,000	176,000	5,000,000	Mexico	[62]

[a] Assuming payback period for existing facilities is 30 years.

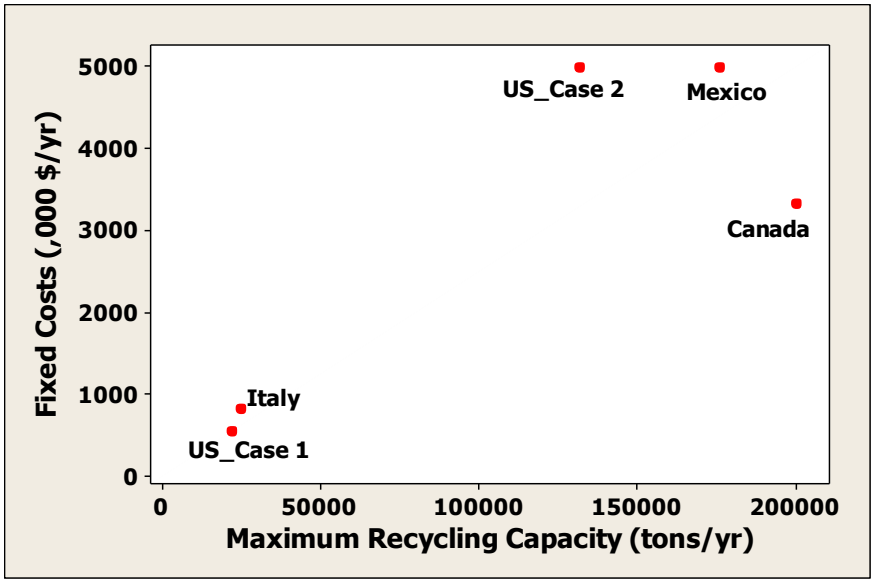

Figure 3.1 Fixed costs and maximum recycling capacities for facilities in different locations.

To understand how fixed costs and variable costs would affect the minimum amount of LIB feedstock for a recycling facility to cover all expenses, a sensitivity

analysis was performed on those two cost categories in section 3.3.2. In the base case, the mean value of variable costs collected from literature ($2,800) has been used, however, this number may fall in the future due to the increasing volume of collected EOL LIBs as well as advancements and improvements in recycling technologies. Also, it is possible that for some recycling facilities, variable costs maybe higher than the average, such as the facility in Belgium (Table 3.3). Therefore, we set up $1,100 and $4,500 per ton as the lower bound and upper bound of variable costs respectively.

Fixed costs including rent, insurance fees, and loan payments on equipment might go up or down depending on a variety of factors. We centered the maximum recycling capacity in the base case (34,000 tons per year), and assume it might go down or up by 50%. According to available data collected (see Table 3.4), this range should represent the possible fixed costs for battery recycling facilities.

3.2.3 Extended case: co-mingled LIB chemistries

Currently, lithium cobalt oxide is the most common cathode chemistry being used in LIBs; this cathode chemistry is present in nearly all mobile phones and laptop batteries as well as some power tools and EVs, e.g. the Tesla Roadster [20]. However, to improve safety, performance and cost in vehicle applications, research and development has led to higher energy density and less expensive cathode materials, including $LiNiO_2$, $LiFePO_4$, $LiMnO_2$, $LiMn_2O_4$, $Li(Ni_{1/3}Mn_{1/3}Co_{1/3})O_2$, and $LiNiCoAlO_2$. In the near future, it is highly unlikely that a single type of LIBs will be collected as the feedstock for a recycling facility, but all types of LIBs will be contained in the waste stream. However, there will be a high uncertainty in the composition of the co-mingled LIB scrap stream in terms of the distribution of cathode chemistry types. As discussed in section 3.2.2.2, the

base case assumed a single scrap stream having 100% $LiCoO_2$ cathode batteries by weight, which is likely representative of the current and near-term LIB waste stream, comprised largely of batteries from portable electronics. To encompass the broad uncertainty in longer term waste stream composition, this extended case has analyzed all possible scenarios of a co-mingled LIB waste stream in section 3.3.3.2. Any one of the three most common types of LIBs (i.e., $LiCoO_2$, $LiFePO_4$, and $LiMn_2O_4$) can make up between 0% to 100% of the scrap stream.

3.3 Results and discussion

3.3.1 Base case

According to the parameters detailed above, an input stream of at least 170 tons per year of spent LIBs is required for the base case facility to cover all associated costs (Table 3.5). This break-even amount is the minimum steady-state supply required; higher volumes would result in a net profit. Achieving this target will be determined by a number of factors, including service area, population density, usage patterns, available transportation infrastructure, potential capacity, and collection rate.

Table 3.5 Assumptions and results for the base case.

	Variables	Values	Units	Notes
Assumptions	Variable Costs	2,800	$/ton	Average variable costs
	Fixed Costs	1,000,000	$/yr	Assumption based on literatures
	Maximum Capacity	33,900	tons/yr	Calculated based on "0.6 factor rule"
	% $LiCoO_2$	100	%	Proportion in the waste stream
Results	Min. Amount	170	tons/yr	Minimum volume to cover total costs
	Unit revenue	8,900	$/ton	Unit value of recovered materials
	Total Costs	1,462,000	$/yr	Total costs equals total revenue at the breakeven point
	Total Revenue	1,462,000	$/yr	
	Profit	0	$/yr	No profit

While the volume of LIBs being discarded currently is not well known on national or state levels, some estimation based on relevant statistics can be made. Call2Recycle® is one of the few battery collection programs in North America with over 60,000 public and private collection sites throughout the US and Canada [94]. According to the statistics in their annual report, approximately 10 million pounds (4,500 tons) of rechargeable batteries were collected in 2012. Assuming 20% of this stream is made up of LIBs [95], approximately 2 million pounds (910 tons) of spent LIBs were collected by Call2Recycle® in 2012. The calculated economic breakeven point in the base case (170 tons per year) is about one quarter of the total spent LIBs collected by Call2Recycle; this equates to four LIB recycling facilities like the one assumed in the base case in viable operation.

While Call2Recycle and other existing programs have made contributions to battery recycling, current collection rates are still low. The true amount of spent LIBs is much higher than 910 tons; many LIBs are currently thrown into municipal solid waste, are in storage, or are otherwise uncollected. Hypothetically, assuming all 910 tons of collected LIBs in 2012 by Call2Recycle were removed from EOL laptops, which contained six 18650 form factor cells each weighing 45 grams on average, then an estimated 3.3 million[2] laptops' batteries were collected, which is only approximately 10% of the roughly 33 million laptops reaching their end-of-life in the U.S. in the year 2012 (see Table 3.6). In reality, the collection rate may be even lower than 10%, since LIBs would enter the waste stream in other types of electronic devices beyond laptops. True tonnage of spent LIBs generated in 2012 should be able to satisfy more than four recycling facilities. Using a similar thought process, a minimum collection rate can also

[2] (910 tons)*(1,000,000 grams/ton)/(45 grams)/6=3.3 million

be estimated. Considering New York State alone, to achieve 170 tons of spent LIBs would require a collection rate of at least 32% [3]. Therefore, before planning a network for EOL LIB collection and transportation or building recycling infrastructure, it will be imperative to increase the collection rate to enable an economically efficient system.

[3] The population of New York State is 6% of the U.S.'s population. Assuming this percentage can represent the distribution of laptop ownership across the U.S., approximately 2 million laptops, containing 530 tons of spent LIBs, reached their end-of-life in New York State in 2012. This indicates in order to satisfy the minimum feedstock of one local LIB recycling facility (170 tons per year) in New York State, the collection rate should reach at least 32%.

Table 3.6 The estimation of end-of-life laptops generated in the United States in 2012 by using material flow analysis (MFA). This MFA study is based on sales data from [12], assuming laptops' lifespans follow a normal distribution with mean equal to 4 and standard deviation equal to 1.

		Units of laptops reaching their end-of-life in each year									
Year	Sales	2003	2004	2005	2006	2007	2008	2009	2010	2011	2012
2002	10,880,000	14,687	232,835	1,478,648	3,713,831	3,713,831	1,478,648	232,835	14,342	341	3
2003	13,810,000		18,642	295,537	1,876,850	4,713,971	4,713,971	1,876,850	295,537	18,205	433
2004	16,620,000			22,435	355,672	2,258,743	5,673,150	5,673,150	2,258,743	355,672	21,909
2005	19,620,000				26,485	419,873	2,666,458	6,697,184	6,697,184	2,666,458	419,873
2006	24,300,000					32,803	520,026	3,302,494	8,294,677	8,294,677	3,302,494
2007	30,020,000						40,524	642,435	4,079,872	10,247,169	10,247,169
2008	34,110,000							46,045	729,962	4,635,724	11,643,269
2009	46,440,000								62,689	993,827	6,311,434
2010	40,420,000									54,563	864,997
2011	55,349,000										74,717
2012										Total	32,886,299

Many factors can affect the break-even point calculated in the base case, including variable and fixed costs, and the cathode chemistry distribution of LIB scrap streams. To quantify and compare the extent to which these factors contribute to the break-even point, sensitivity analyses are performed in the following sections by varying each parameter independently.

3.3.2 Sensitivity analysis on fixed and variable costs

Both fixed costs and variable costs will significantly affect the break-even amount for a LIB recycling facility. Usually, given a certain unit variable cost, the volume of spent LIBs needed to turn a profit decreases as the annual fixed costs are reduced, and vice versa.

Figure 3.2 is a contour plot showing the relationship among three variables: variable costs (X axis), fixed costs (left-Y axis) and the break-even amount (isolines). In addition, maximum recycling capacities as a function of fixed costs are shown on right-Y axis. Representative isolines (i.e., 100, 150, 200 …) were interpolated between color-coded contour levels: darker color refers to lower break-even levels; lighter color refers to higher levels. Since the interaction of variable costs and fixed costs does not affect the break-even amount, contour levels in Figure 3.2 are linear. The break-even amount ranges from 60 tons (at the lowest fixed and variable costs) to 350 tons (at the highest fixed and variable costs).

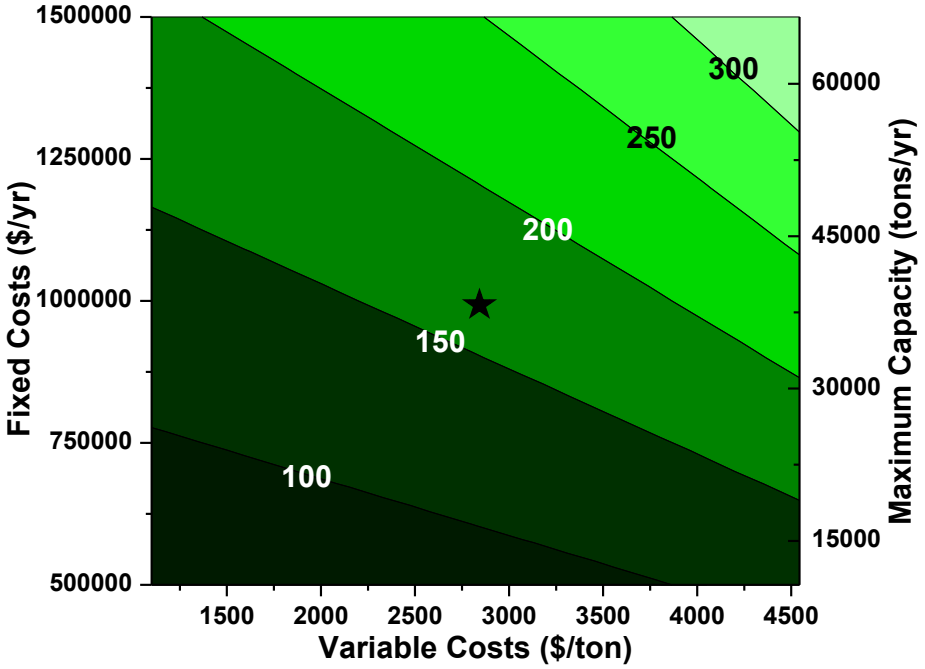

Figure 3.2 Minimum volumes of spent LIBs for a recycling facility to cover all expenses for different fixed and variable costs. Star refers to the base case. Darker color refers to lower break-even levels; lighter color refers to higher levels.

Isolines are unevenly distributed across the plot: there is a greater difference in values across each unit of distance at higher costs compared to at lower costs. This indicates if recycling spent LIBs is an expensive process, i.e. requiring a large investment and/or high processing costs, reducing the overall costs has a strong influence on lowering the break-even amount; however, this influence gets weaker as the total cost decreases. The star indicates the base case scenario: variable cost ($2,800 per ton) is assumed based on the current average variable cost, maximum recycling capacity (34,000 tons per year) is estimated based on the assumed fixed cost ($1 million per year), and the break-even amount (170 tons per year) is calculated using Equation (3.1)-(3.5). Reducing both fixed and variable costs can lower the required volume of LIB feedstock to such a recycling facility, which can in turn bring more profit. For example, if the recycling

facility assumed in the base case could reduce its variable cost by $500, its break-even point would drop below 150 tons per year, indicating the profitability of such a recycling facility can be largely improved and an additional recycling facility would become feasible. Adding one more facility means a smaller service region for each facility, indicating lower costs on transportation (variable costs). Figure 3.2 can be used as a rough planning tool: in the current scenario, if the available recycling technologies are settled, then these data can be used by a recycling facility or municipality to inform decisions about plant size and maximum desired recycling capacity based on the available volume of LIBs in a given area. In most areas, the current LIB collection rate is low due to lack of recycling infrastructure; volumes beyond the break-even point would bring higher profits to recycling facilities.

The break-even point in the base case will most likely move left as variable costs of recycling LIBs decrease due to technological progress, such as processing efficiency improvements. Table 3.7 illustrates the change in unit revenue through improving recycling efficiency (increased by 10%) for each type of metal and for different cathode chemistry types, respectively. Improving recycling efficiency for cobalt can increase the revenue by up to 9% when processing cobalt based LIBs, but would make no difference when recycling other LIB types that do not contain cobalt-based cathodes. On the other hand, improving recycling efficiency for lithium shows an improvement, albeit to different degrees, across all battery types. Improving efficiency of recycling copper is also promising, since an increase of 10% can raise the total unit revenue by 5% for $LiFePO_4$ cathode LIBs, and 1% for both $LiCoO_2$ and $LiMn_2O_4$ cathode LIBs. The other materials have relatively low priorities in terms of recycling technology development.

Table 3.7 Increase in unit revenue through improving recycling efficiency for each type of metal.

		Co	Ni	Li	Mn	Fe/Steel	Al	Cu
RE (%)[a]		89	62	80	53	52	42	90
Improved RE (%) =RE(%) +10%		99	72	90	63	62	52	100
$LiCoO_2$	Δ Unit revenue ($/ton)	$800	$30	$130	$0	~$0	$10	$50
	Increased%, compared to $8,870	9%	<1%	1%	0%	<<1%	<1%	<1%
$LiFePO_4$	Δ Unit revenue ($/ton)	$0	$0	$70	$0	~$0	$10	$60
	Increased%, compared to $1,230	0%	0%	6%	0%	<<1%	1%	5%
$LiMn_2O_4$	Δ Unit revenue ($/ton)	$0	$0	$100	~$0	~$0	~$0	$10
	Increased%, compared to $860	0%	0%	12%	<<1%	<<1%	<<1%	1%

[a] see Table 3.2.

Moreover, operating spent LIB recycling in lower-labor-cost areas could also bring more profits to the facilities. However, this improvement will not be significant because the collection and recycling cost represents roughly 40% and 60% of the total variable cost, respectively [83]. While the collection process is labor intensive (labor costs account for about 50% of the collection cost [85]), this work cannot be shipped overseas. In addition, the labor cost only represents a small proportion of the recycling cost. Assuming labor-related costs account for 30% of the recycling cost, shifting this part of work to a place with cheaper labor (20% of the assumed labor cost) would only save 14% of the total variable cost assumed in the base case. However, this calculation has not considered the associated increase in transportation cost, which will diminish or possibly even exceed the savings on labor.

3.3.3 Sensitivity analysis on feedstock LIB compositional variability

Besides variable costs and fixed costs, uncertainties associated with LIB feedstock themselves also need to be taken into account when calculating the break-even amount. Two dimensions of compositional uncertainty were considered here: variability

due to multiple cathode chemistries and variability within each chemistry due to differences among manufacturers. This co-mingled stream would bring a compositionally uncertain feedstock to recyclers. An example hierarchy of variability in the LIB scrap stream is shown in Figure 3.3(a): when all collected spent LIBs have the same cathode chemistry and are from the same manufacturer, less uncertainty exists as to the composition of the stream; this scenario is highly unlikely. Even with the same cathode chemistry and form factor, LIBs from different manufacturers (assumed in the base case) would add compositional uncertainty. In the future, LIBs having different cathode chemistries, form factors, and manufacturers are likely to be found in co-mingled scrap stream, which will significantly impact the economics of recycling.

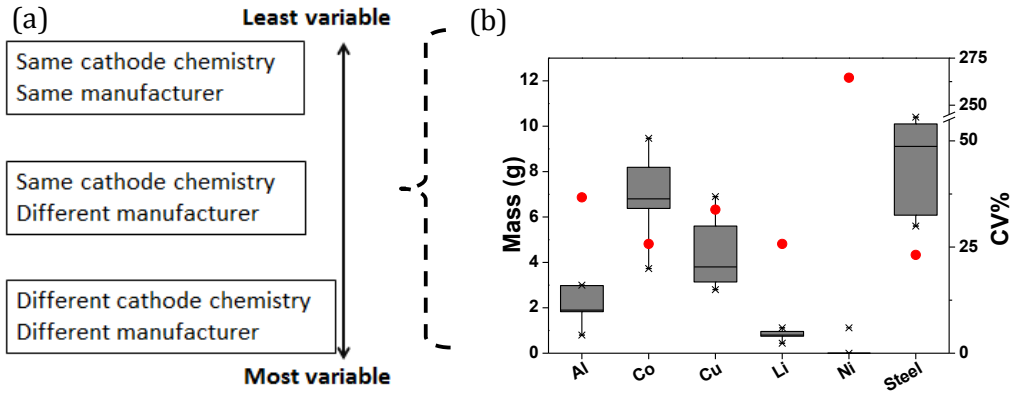

Figure 3.3 (a) Hierarchy of variability in LIB scrap stream, (b) compositional variation for metals in $LiCoO_2$ cathode LIBs; key values from summary statistics are shown in Figure B1 in Appendix B.

3.3.3.1 Batteries from different manufacturers

Even LIBs sharing the same cathode chemistry (e.g. $LiCoO_2$) and form factor (18650 cells) have compositional variability in the batteries due to different manufacturers (Figure 3.3b; key values from summary statistics represented in Figure

3.3b are shown in Figure B1 in Appendix B). The greatest variability observed is for nickel, which has the highest CV (265%), as it was only observed to be present in one manufacturer's cobalt based LIBs. Variability is also present due to differences in battery packaging materials. CVs of 21% for steel to 37% for aluminum are due largely to the use of one or the other of these materials for the battery casing. To what extent this compositional variability can affect the break-even amount is a great concern to a recycling facility.

In our base case, we used the *average* value of material composition for $LiCoO_2$ cathode chemistry type to estimate the minimum requirement of spent LIBs to cover all recycling expenses. Since cobalt is the main economic driver for recycling, the variability of cobalt-content in LIBs is expected to have the greatest impact on break-even point. In this section, the *maximum* and *minimum* cobalt-content for $LiCoO_2$ cathode LIBs was used to estimate a wider range of break-even points (Figure 3.4a and b). The color-coding of contour levels in Figure 3.4(a) and (b) are consistent with Figure 3.2. Since the processing cost of spent LIBs is expected to be reduced in the future, variable costs ranging from $1,100 to $3,300 per ton were assumed.

The value of materials potentially recovered from one ton of LIBs with high cobalt-content LIBs instead of the average composition would increase 20% compared to the base case. Because of this increased value, only 130 tons of LIBs will be needed annually to cover the total costs, a reduction of about 23% from the base case (Figure 3.4a). In addition, both fixed and variable costs have less effect on break-even amount when recycling higher cobalt-content LIBs.

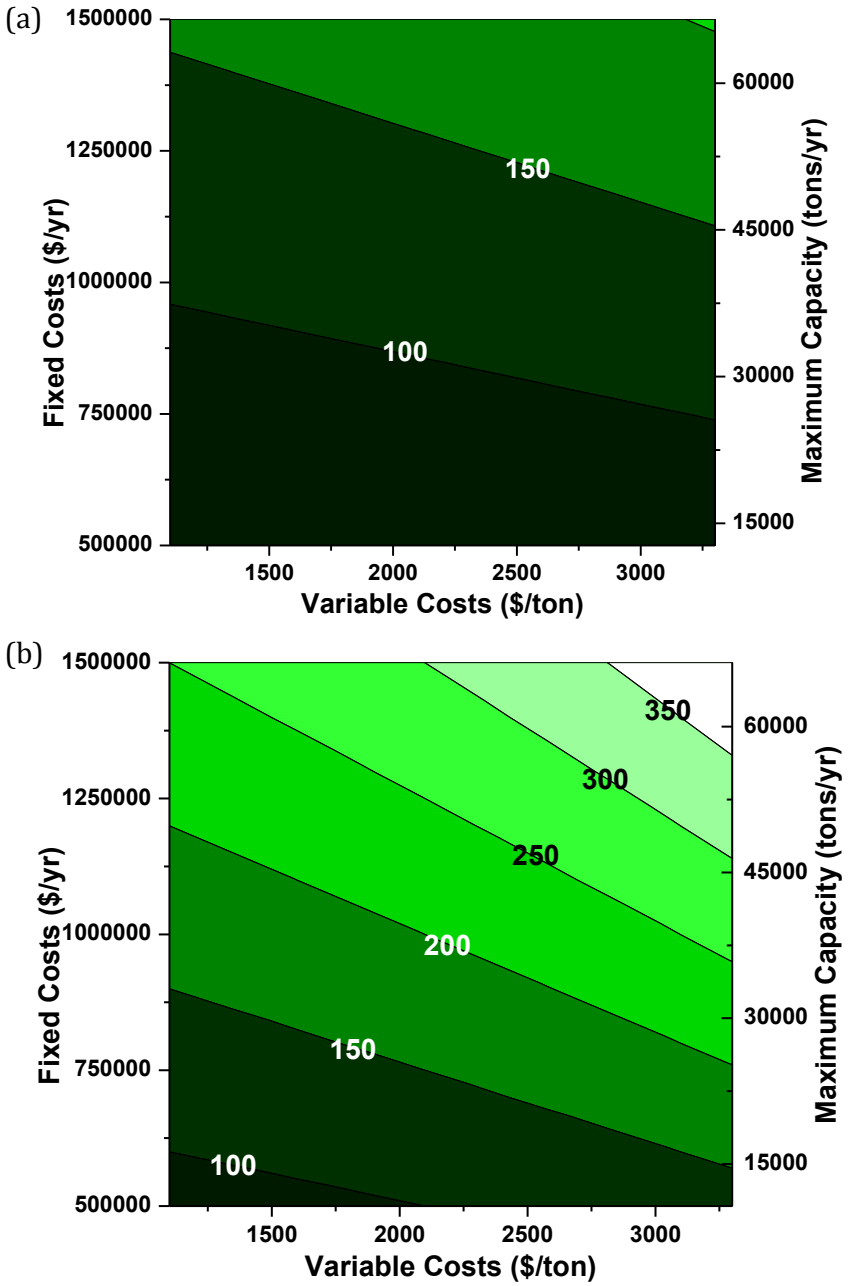

Figure 3.4 Minimum amount of spent LIBs for a recycling facility to cover all expenses for different fixed and variable costs, (a) considering high cobalt-content LIBs, (b) considering low cobalt-content LIBs. Darker color refers to lower break-even levels; lighter color refers to higher levels.

However, there is no guarantee that a recycling facility will get high cobalt-content LIBs for every single batch. Low cobalt content results in a much lower value of recovered materials as expected: $7,100 per ton, or 20% less than the base case, indicating more batteries would be needed to cover the recycling expenses. In this case, the break-even point would increase 42% compared to the base case scenario (Figure 3.4b). Both fixed and variable costs have a stronger influence on the break-even volume because lower unit profits make facilities less flexible on the minimum requirement of recycling quantity.

3.3.3.2 Batteries of multiple chemistries

The previous results show that the economics of the recycling system depend strongly on the material composition of spent LIBs even under a fixed scrap stream with a single battery cathode chemistry type. Therefore, the probable shifts in cathode chemistries will also be a significant factor. Since it is difficult to predict individual feedstock for a particular recycling facility, potential economic values for several possible co-mingled scenarios were evaluated. Material composition for each LIB cathode type uses the average value from multiple battery manufacturers as in the base case. Potential revenues from recycling one ton of co-mingled LIBs are shown in Figure 3.5. Each side of triangle (or axis) represents the proportion of one of the three considered LIB types in one ton of co-mingled scrap stream: zero means this LIB type is void, and one means only this LIB type is present. The coordinate of every point on this ternary plot is a composition of three proportions, with the summation equal to one.

The darker color indicates that materials reclaimed from those sets of co-mingled LIB feedstock have high economic values; the light color means any scrap streams

showing those chemistry distributions bring the facility less value. If the unit revenue cannot cover the unit variable cost, the facility would never be profitable no matter how many tons of LIBs being processed. The threshold of profitability is represented by points lying on the thicker dashed line, showing unit revenue equals to 2,800 dollars per ton (the assumed variable costs for the base case). Scenarios to the right of this line suggest that such a recycling facility (parameters specified in the base case) has the potential to make profits; any scenarios on or to the left of this line result in the facility losing money by recycling LIBs. In addition, it should be noted that high recovery efficiency for recycling processes were assumed, implying the values showed in Figure 3.5 are optimistic for recyclers. However, because of scientific and technological progress, the recycling efficiency of materials is expected to improve.

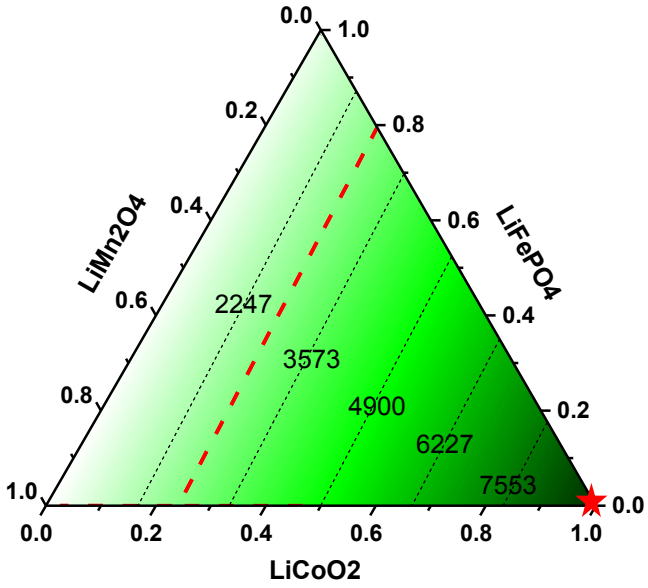

Figure 3.5 Unit revenues ($/ton) from recycling LIBs for all possible scenarios of chemistry distribution. Representative isolines are plotted in thinner dash lines with labeled values; the thicker dash line represents the assumed variable costs in the base case; the star refers to the base case.

Unit revenues are strongly and proportionately linked with increasing amounts of $LiCoO_2$ cathode batteries in the waste stream. The revenue generated from recycling one ton of $LiCoO_2$ cathode LIBs is seven times higher than $LiFePO_4$ cathode LIBs, and ten times higher than $LiMn_2O_4$ cathode LIBs. In this scenario, $LiCoO_2$ cathode batteries have to make up to at least 21% of the co-mingled scrap stream to cover the processing expenses. While this proportion is likely satisfied at present due to widely used cobalt-based LIBs in consumer electronics, it might be difficult to meet in the future, particularly when higher volumes of EV LIBs with less expensive cathode materials enter the waste stream. However, this proportion only shows the possibility; getting such co-mingled LIB collections alone cannot guarantee the facility can be profitable, because 1) fixed costs also need to be considered in this calculation and 2) the maximum recycling capacity limits facilities' processing volume.

Since the composition of the scrap stream will have large variance, including a material sorting process becomes valuable. For example, a system to pre-sort LIBs by chemistry could enable recyclers to maximize operational efficiency by selecting an appropriate technology for a specific batch. For example, when $LiCoO_2$ cathode LIBs dominate the collected batteries, hydrometallurgical recycling technologies may be most effective to recover cobalt [75, 96]; if the scrap scream contains a high proportion of other types of LIBs, pyrometallurgical processes might be more appropriate from an economic perspective. Such a system would be enhanced if manufacturers were to add labels containing chemistry information to LIB packs to aid in the sorting process. Because a well-established battery distribution system on the EOL side does not yet exist, strategies like labeling and sorting should be considered proactively in its development.

3.4 Policy and incentive analysis

In many European countries, rechargeable battery take-back laws have been passed to ensure the growing volume of discarded batteries will be managed in an environmentally friendly manner [97, 98]. However, in the U.S., a standard collection and recycling infrastructure for LIBs is not available at the national level. Relevant laws and regulations, particularly those with compliance strategies such as financial penalties, may create incentives for people to recycle spent LIBs. According to New York State Rechargeable Battery Law, non-compliance with the law is subject to civil penalties of up to $200 for the consumer, $500 for retailers, and $5,000 for manufacturers [29]; financial penalties are not based on the volume or unit, but the times of violation.

For smaller recycling facilities including typical electronic waste processors, it may be difficult to achieve economies of scale due to their limited resources and recycling capacity. Achieving a target spent battery input stream may require businesses to expand their service area, which carries additional costs of transportation and collection logistics. In many European countries, extended producer responsibility (EPR) has been adopted to hold manufacturers responsible for managing their products at end-of-life to deal with the growing volume of e-waste [99]. Producers might not do the collection themselves; in many cases, they contract with third parties (e.g. small collection companies or recyclers) who handle the wastes. EPR legislation has not been adopted at the federal level in the U.S.; however, it may be reasonable for U.S. lawmakers to consider it, particularly as adoption of EVs increases. Since EVs are relatively new to market and LIBs in EVs have lifespan greater than seven years, there are very few EV LIBs in the current scrap stream. The Tesla Roadster, an EV sports car

containing 6,800 18650 $LiCoO_2$ battery cells, was the first production automobile using LIB cells [16]. According to a material flow analysis (MFA) study done by Richa et al., LIBs from the first generation of EVs will start reaching their end of life around 2015 and the total volume of EOL EV batteries will quickly build up (approximately 25,000 tons in 2025 for a baseline scenario) [74]. Along with increasing market penetration of EVs, a significant amount of LIBs may be produced, used, and discarded in the near future to support growing demand for consumer electronics. Therefore, a series of forward-looking policies are needed to promote effective LIB EOL management.

If LIB manufacturers are responsible for collecting spent LIBs, they would spend about $1,120 per ton based on our previous assumption that collection costs roughly represent 40% of variable costs [83]. Then, those collected spent LIBs can either be disposed of at specified landfills, if not prohibited by legislation, or be properly recycled. If collected batteries are sent to landfills, manufacturers would pay a tipping fee, which depends on where the landfill is located. This landfill tipping fee increases every year, and can vary from $105 per ton in Massachusetts to $18 per ton in Idaho, with $45 per ton as the average number for year 2012 (see Figure 3.6). Therefore, batteries are managed via landfill disposal route, the manufacture would end up paying about $1,170, including collection costs ($1,120) and landfill tipping fee ($45), to manage one ton of spent LIBs (see Figure 3.7).

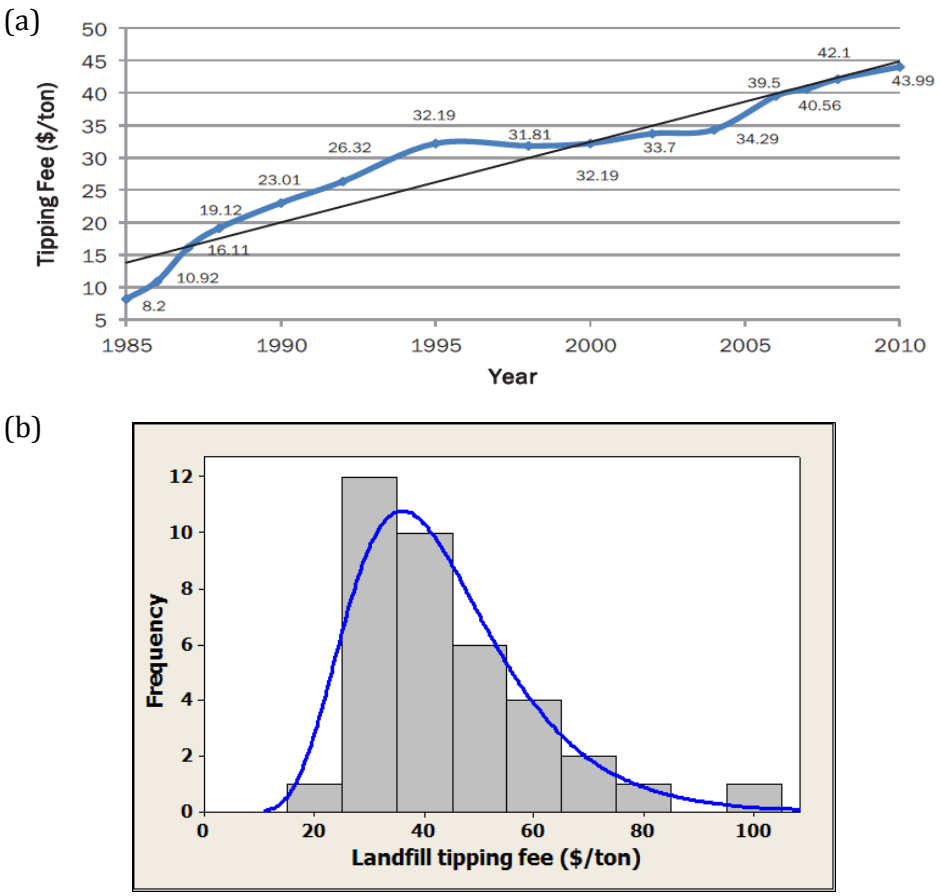

Figure 3.6 (a) MSW landfill Tipping Fees in the US, (b) the distribution of MSW landfill tipping fees for different states in the US, based on data from [6].

Although recycling costs more than landfill disposal, recovered materials can also bring revenues, which vary based on cathode chemistry as described in results presented earlier (Figure 3.5). For a co-mingled scrap stream, potential revenues can be ranked in terms of economic value from the worst case scenario (only contains $LiMn_2O_4$ cathode LIBs) to the best case scenario (only contains $LiCoO_2$ cathode LIBs). The probabilities for those scenarios follow the distribution showed in Figure 3.7, with mean equaling to $1,360. Thus, although recycling requires a cost and involves a higher-order uncertainty, recovering materials from LIBs can generate $240 per ton on average overall. Comparing

to landfill disposal, recycling requires a certain amount of investment but brings a financial gain overall.

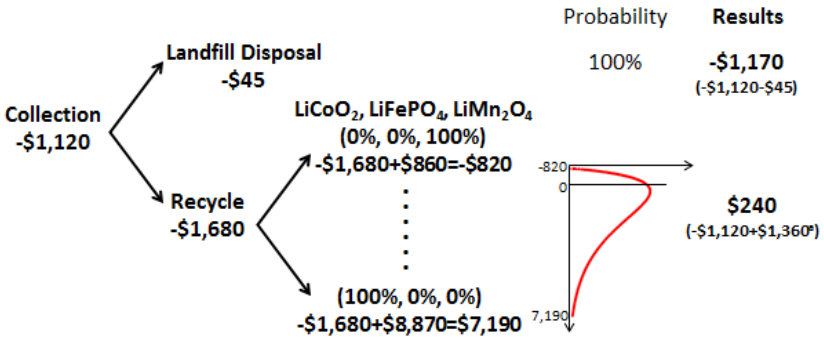

Figure 3.7 A decision tree for spent LIB management; numbers are calculated for one ton of LIBs.

Other management strategies beyond EPR may also be possible. For example, deposits at time of purchase could encourage end-users to properly dispose of EOL LIBs, which can in turn improve the collection rate [100]. Similar to the "bottle bill," a deposit-refund system requires a minimum refundable deposit which can be redeemed when the products are returned [101].

3.5 Conclusion

The rapidly growing volume of spent LIBs requires a well-functioning collection and recycling infrastructure to minimize associated environmental impacts. Although a few companies already process LIBs, current recycled LIBs in the U.S. only account for a small portion of the total number of EOL LIBs entering the waste stream every year. According to the base case in this chapter, current battery collection rates would only generate enough spent batteries to enable four recycling facilities to operate with profit in the U.S. Comprehensive analysis of LIB recycling potential and the associated uncertainties need to be performed before planning out the LIB recycling network. This

chapter has developed an optimization model to evaluate economic profitability of LIB recycling facilities for a base case and several possible co-mingled scenarios. The results show that profitability of a recycling facility depends on the relative composition of a co-mingled input LIB stream in terms of cathode chemistry type, since the potential revenue varies from $860 per ton for $LiMn_2O_4$ cathode batteries to $8,900 per ton for $LiCoO_2$ cathode batteries. As LIB technology moves towards less expensive cathode materials, incentives to recycle those batteries will diminish. Once the fraction of $LiCoO_2$ cathode batteries falls below 21% of the total scrap stream, a facility will no longer be profitable, given the fixed and variable costs assumed in the base case. In all likelihood, recycling-oriented policy, like EPR laws, will be required to augment market-based recycling initiatives.

This chapter also points out that the current collection rate of spent LIBs from consumer electronics is probably less than 10%. Improving this rate makes local recycling of LIBs possible, which can reduce the current processing cost through shortening the transportation distance. Moreover, if the price or recycling rate of valuable metals (such as cobalt and copper) or scare metals (such as lithium) increase in the future, it will bring more economic incentives to recover materials in spent LIBs. In addition, as LIB technology is widely being used in EVs, a forward-looking recycling infrastructure is required to properly manage this growing waste stream.

Chapter 4. Targeting high value metals in lithium-ion battery recycling via mechanical pre-processing

4.1 Introduction

The economic and environmental incentives as well as economies of scale for LIB recycling have been demonstrated in previous chapters. Currently, a few companies (e.g., Umicore and Toxco) process EOL LIBs; however their recycling technologies were not designed specifically for LIBs, usually processing multiple types of rechargeable batteries (e.g., nickel-metal hydride batteries) and/or non-battery scraps (e.g., metallic materials) at the same time, which results in low recycling efficiency [102, 103]. Therefore, development of a technology that can effectively recover more types of materials contained in LIBs is urgent.

A growing number of studies have been performed on EOL LIB recycling, with the focus on improving the recycling efficiency of cobalt, which is the most valuable material contained in LIBs from consumer electronics [46, 53, 75, 104]. However, results in Chapter 2 show that other materials contained in LIBs also have potentials to be recovered at a higher level, when considering both economic and environmental perspectives [11]. Copper, nickel, and lithium make a significant contribution to the potential recoverable value of EOL LIBs together, ranging from 27% for $LiCoO_2$ cathode LIBs to 74% for $LiFePO_4$ cathode LIBs. While the aluminum content is relatively low (ranging from 1% to 8% of the total mass for most LIB types), its recovery presents significant energy savings, since secondary production of aluminum saves up to 88% of the energy required during its primary production [105]. With the consideration of the

potential economic and environmental savings from recovering these contained materials, LIB recycling technology must have a broader target than cobalt recovery alone.

As LIB recycling efforts expand to target a broader spectrum of metals, the recycling technology mush also be optimized to achieve higher efficiencies and selectivities of desired metals. LIBs come in different sizes, form factors, and cathode chemistries, indicating a highly co-mingled, uncertain waste stream. A typical LIB consists of a cathode, an anode, separators and electrolyte, containing a variety of metallic materials (e.g., copper, nickel, cobalt, lithium, aluminum, etc.), plastics, carbon black, liquid, and foam. Meanwhile, a range of chemistries has been used as cathode materials. While lithium cobalt oxide battery dominates the market currently, LIB technology is transiting to low-cost cathode chemistries (e.g., $LiFePO_4$, $LiMn_2O_4$-spinel, and some mixed-metal cathodes). Segregation of materials can enrich the constituent of targeted material(s) in a certain portion, which helps to improve the efficiency of subsequent recycling processes. Since materials contained in LIBs appear in different sizes, mechanically sorting by size has been considered to apply in this chapter.

Shredding or sorting has widely been used in other products' recycling processes to increase the surface area, liberate the component materials, achieve material segregation, and improve the efficiency of subsequent recycling processes. Gaustad *et al.* reviewed a variety of physical separation technologies for removing impurities from aluminum, providing a pool of possible alternatives [106]. For LIBs specifically, while a few studies have included some type of pre-recycling steps into their proposed recycling process, the possibility of scaling these steps up is limited and usually not considered. For example, cutting battery cases is the first step of the laboratory-scale LIB recycling

process proposed in many studies [54, 107, 108]. While the authors recommended cryogenic treatment on an industrial scale according to their experimental experience (i.e., heat caused by the internal short-circuit of the cell is usually generated during the cutting), the feasibility of manually cutting every cell case and extracting the interior active materials has not been addressed for process scale-up. Nan *et al.* described that EOL LIBs were first dismantled to separate the outer steel cans from the contained materials by using a custom dismantling machine; however, specific details on the machine and the process were not clearly presented [52]. Li *et al.* used an ultrasonic washing machine to separate cathode materials from the aluminum foils and separate carbon power from the copper foil. However, this sorting process is limited by the low concentration (28% by weight) of cobalt in the targeted part of the battery. Beyond scale-up challenges, environmental impacts have yet to be fully addressed. Lee *et al.* proposed a series of two-stage thermal treatments, shredding, screening, and acid leaching process [109]. But the tradeoff between additional energy consumption to separate battery cells from the can and the additional gains from recycling yield was not quantified. Yamaji *et al.* proposed a novel method of under-water explosion to dissemble EOL LIBs [110]. While this method can successfully prevent fires during the crushing process, its associated environmental safety issues (such as the water treatment after the explosion) need to be further analyzed. These studies lay an important foundation for understanding the feasibility and potential for several pre-recycling process. However, a pre-recycling process that can be easily scaled up, requires low initial and operating cost, reduces energy and materials input, and at the same time can efficiently achieve material segregation is still missing.

The aim of this chapter is twofold: 1) to develop an automated, low-cost, and easy-to-implement pre-recycling process for EOL LIBs, 2) to demonstrate the importance of implementing battery labeling system (i.e., labeling by cathode). Currently, one of the obstacles that LIB recyclers are facing is little information on LIBs' composition due to non-disclosed cathode chemistries and cans among different battery manufacturers. The effectiveness of this proposed process is examined for current market-dominate (i.e., $LiCoO_2$ cathode LIBs) as well as three future popular cathode batteries (i.e., $LiFePO_4$, $LiMn_2O_4$, and mixed-metal cathode LIBs), from perspectives on both material distribution and economic contribution.

4.2 Materials and methodology

To evaluate the efficiency of this proposed pre-recycling process when applied to batteries of differing cathode chemistries, a mixed stream of scrap LIB cells were used in this chapter, including 64 unknown cathode battery cells removed from 10 laptop battery packs and 49 cells from 4 known cathode chemistries. The information about laptop brand and battery manufacturer for each battery pack is shown in Table 4.1 using indices to preserve confidentiality. To compare and/or identify cathode chemistries of selected battery samples, the BOM for four popular cathode chemistry types, i.e., $LiCoO_2$, $LiFePO_4$, $LiMn_2O_4$, and a mixed-metal cathode (i.e., $Li_{1.05}(Ni_{4/9}Mn_{4/9}Co_{1/9})_{0.95}O_2$), are provided in Table 4.2. All sample batteries used in this chapter are 18650 cells except for $LiMn_2O_4$ cathode batteries. Initially, to keep the methodology comparable and consistent, three batches of 18560 cells labeled as IMR[4] were purchased from three well-known manufacturers. However, the XRF results of their cathodes have shown that they actually have mixed-metal cathode materials instead of lithium manganese oxide. Since $LiMn_2O_4$

[4] IMR or IMO are abbreviations for lithium manganese spinel cathode.

cathode chemistry is currently not available in 18650 cells, we chose to use a closer form factor, i.e., 26650[5], which is also cylindrical having the same length as 18650 cells but a bit larger diameter.

Table 4.1 Information about sample battery packs.

Battery Pack #	Laptop Brand Indices	Battery OEM Indices	Cathode	Numbers of cells	Mass per cell (g)
B1	LM1	BM1	Mixed-metal (estimated)	6	41.0
B2				6	41.1
B3	LM2	BM2		6	44.5
B4		BM3	$LiCoO_2$ (estimated)	6	44.6
B5	LM3	BM4		8	45.9
B6				8	46.0
B7	LM4			6	45.2
B8				6	42.6
B9	LM5			6	45.2
B10				6	43.8
K1	NA	BM5	$LiCoO_2$	9	45.6
K2		BM6		9	46.4
K3		BM7	$LiFePO_4$	6	39.3
K4		BM8		15	45.3
K5		BM9	$LiMn_2O_4$	4	98.8
K6		BM10	Mixed-metal	6	42.2

[5] The 26650 form indicates the batter is cylindrical, having a diameter of 26 mm and length of 65 mm.

Table 4.2 Average material contents in LIBs (in wt.%).

Materials	$LiCoO_2$[a]	$LiFePO_4$[b]	$LiMn_2O_4$	Mixed-metal[c]
Aluminum	5.2	6.5	1.1	8.5
Cobalt	17.3	0	0	2.0
Copper	7.3	8.2	1.1	16.3
Lithium	2.0	1.2	1.5	2.4
Manganese	0	0	20.4	7.5
Nickel	1.2	0	0	8.0
Steel/Iron	16.5	43.2	16.5	0
Phosphorus	0	5.4	1.1	0
Graphite	23.1	13.0	33.6	20.6
Carbon black	6.0	2.3	0	2.0
LiPF6	3.7	1.2	0	14.7
EC/other	10.3	13.7	0.3	10.4
Binders	2.4	0.9	0	2.8
Plastics	4.8	4.4	20.1	4.9
Total (in g)	46.0	42.3	44.7	42.2

[a,b] the average of 2 LIB manufacturers (Table B3 in Appendix B).
[c] adopted from [111].

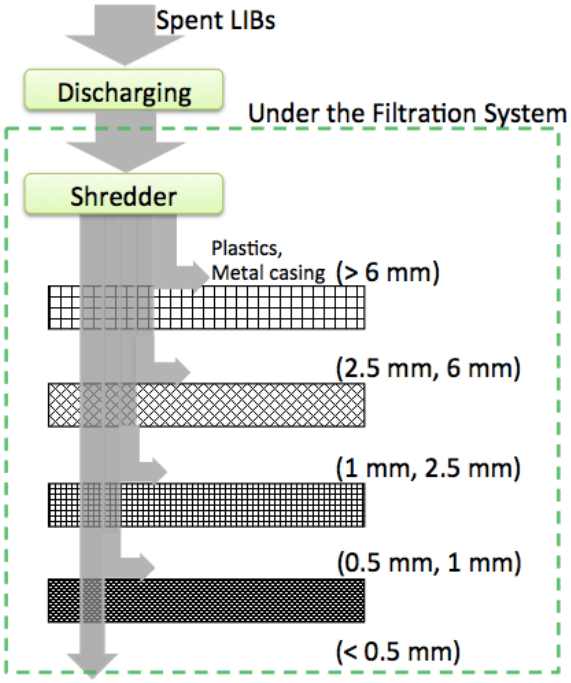

Figure 4.1 Flow sheet of EOL LIB pre-recycling process.

The flow sheet of the proposed pre-recycling process for EOL LIBs is shown in Figure 4.1. LIB packs removed from laptops were disassembled to separate the digital circuit and LIB cells. After that, LIB cells were first discharged and frozen by liquid nitrogen to reduce the risk of fire, and then mechanically shredded by a commercial granulator (i.e., EconoGrind 180/180) into small pieces (smaller than 7.5 mm). To eliminate the risk of exposure to electrolyte, the shredding process was performed under a fume hood (Figure 4.2a). Shredded LIB pieces were collected on aluminum foil and placed under the fume hood for one week to let the volatile chemicals evaporate completely. A set of custom sorting sieves was used to separate shredded LIB pieces into five size fractions: <0.5 mm, 0.5-1 mm, 1-2.5 mm, 2.5-6 mm, and >6 mm (Figure 4.2b). Size separation was performed on a Lansmont's Vibration Machine Test System (Model 7000-10) using the random vibration mode (i.e., ASTM D4169 Truck profile) for 20 minutes. Material separated into each size fraction was then analyzed for metallic composition using an Innov-X XRF analyzer (Olympus, Japan, DELTA Alloys & Metals Handheld XRF Analyzer) (Figure 4.2c). Five random samples within each size fraction were tested and averaged. XRF identifies the material content based on the specific wavelength of detected photons for each element. While lithium cannot be detected by this XRF analyzer even under the widest mode, the XRF analyzer is effective to characterize all of the other metallic materials of interest in LIBs [112].

Average primary metal prices in 2013 from USGS (Table 4.3) are used to estimate the materials' maximum theoretical recoverable value (100% recovery). Although recycling efficiencies for most of those materials are unlikely to reach 100%,

the theoretical analysis provides a starting point for material comparisons based on recoverable value alone.

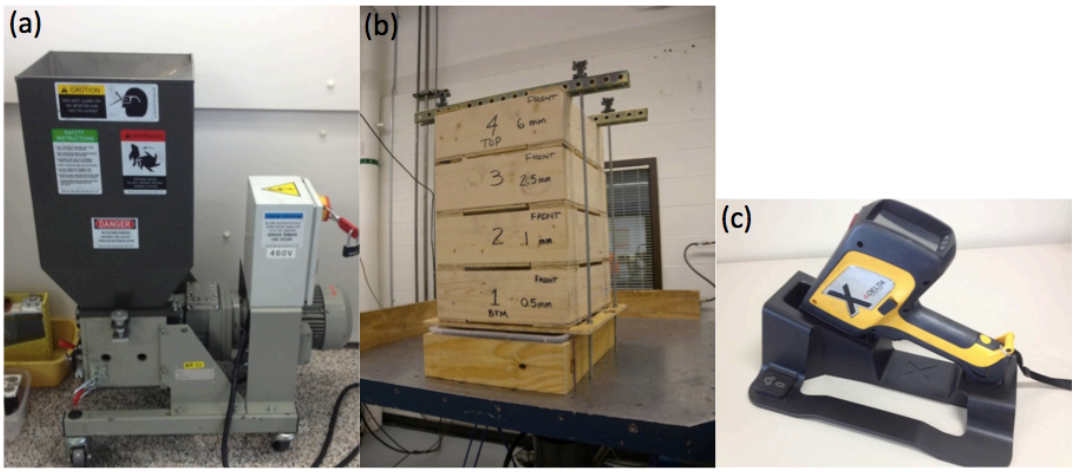

Figure 4.2 (a) the shredder in the fume hood, (b) four handmade sieves sitting on the vibration table, (c) the XRF analyzer.

Table 4.3 The price of materials [8].

Metals	Prices ($/kg)	Metals	Prices ($/kg)
Cobalt	28.44	Aluminum	2.09
Nickel	15.02	Iron	0.73
Copper	7.50	Phosphate rock	0.09
Manganese[a]	2.30	Niobium	44.00

[a] The price on the Infomine website.

4.3 Results and discussion

Demonstration of the pre-recycling process enabled comparisons of the separated size fractions on the basis of metal content, economic value of that content, and variability across multiple battery chemistries and manufacturers. The sorted fractions of shredded cells showed clear visible differentiation (Figure 4.3a-e; for battery pack #B5), particularly in the accumulation of poorly-shredded battery housing material in the largest size fraction. The larger pieces (>6 mm) are mostly battery casings and plastic

separators. Copper pieces can be visibly detected in the coarse (2.5-6 mm) and mid (1-2.5 mm) fraction. Fine black powder dominates the ultrafine (<0.5 mm) fraction.

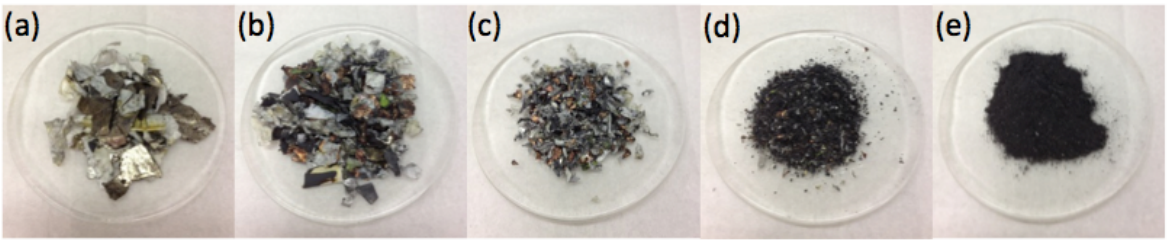

Figure 4.3 Samples of five size fractions after the pre-recycling process for battery pack #B5 (from left to right: (>6 mm), (2.5-6 mm), (1-2.5 mm), (0.5-1 mm), and (<0.5 mm)).

4.3.1 Mass of fractions

The mass distribution of sorted materials in the five fractions is similar among packs. Since the number of cells per pack varies across the ten battery packs sampled (eight packs have six cells each and the other two have eight cells each), Figure 4.4 reports mass for all five size fractions normalized on a per-18650-cell basis. Figure 4.4 also characterizes the variability among the ten packs sampled: the height of each column shows the average mass value, and the error bars on each column refer to the maximum and minimum value. The CV for these five size fractions ranges from 9% to 37% (considered to be low), as distributions with a CV<100% usually are considered low-variance. It should be noted that while the ultrafine (<0.5 mm) and fine (0.5-1 mm) fractions have roughly the same volume, the mass of the ultrafine fraction is almost twice as much as the fine fraction. The coarse (2.5-6 mm) fraction and the larger pieces (>6 mm) is the largest and smallest portion in terms of the mass (45% and 6% on average respectively).

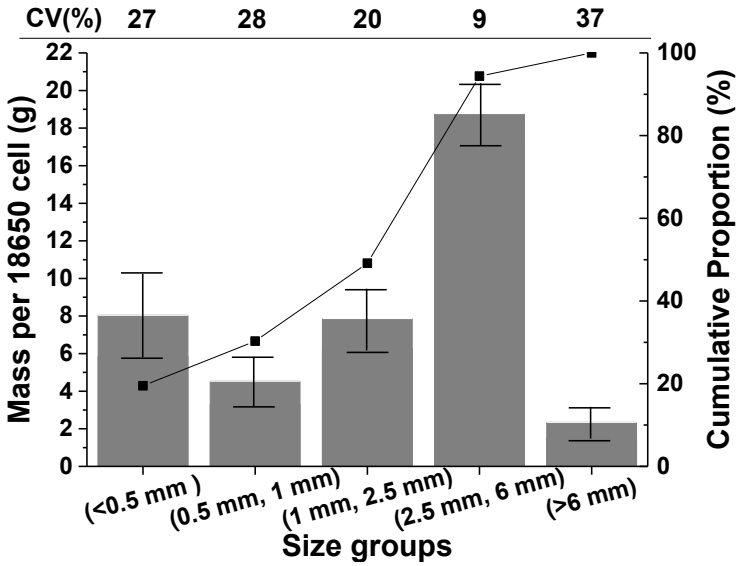

Figure 4.4 Mass of each size fraction per 18650 cell (calculated based on cells from ten unknown cathode battery packs); the figure on top of each column is CV.

4.3.2 The performance of the proposed pre-recycling process—two examples

The complete XRF results of the distribution of metals in different size fractions after the sorting process are shown in Table B4 in Appendix B. Based on the XRF results, seven out of ten unknown cathode battery packs have $LiCoO_2$ cathode batteries, and the rest have mixed-metal cathode batteries. In this section, one battery pack of each cathode type is randomly selected as a representative example (i.e., #B10 for $LiCoO_2$ and #B2 for mixed-metal; material characterization of shredded batteries is shown in Figure 4.5c and 4.6c for each battery pack respectively.

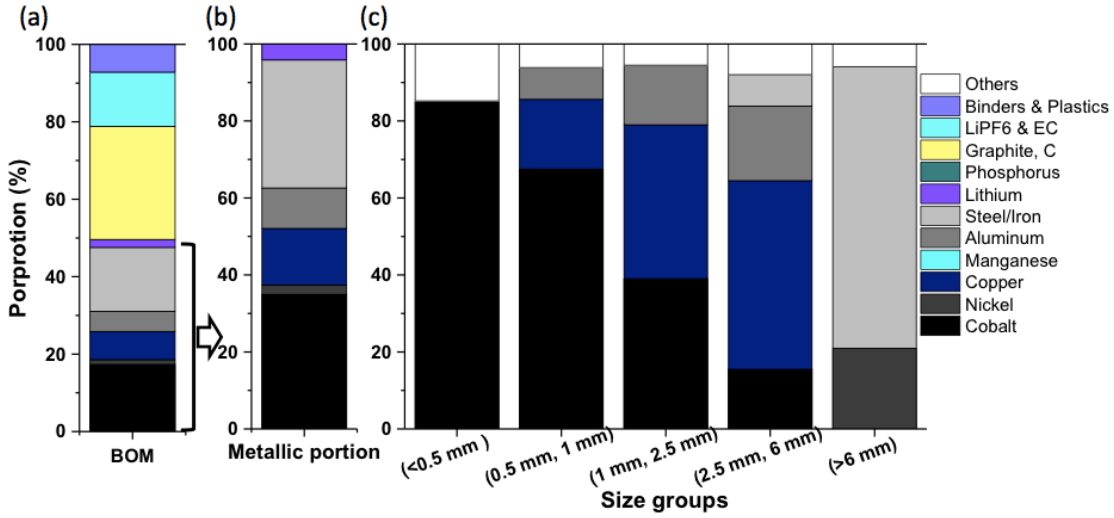

Figure 4.5 (a) The BOMs for $LiCoO_2$ cathode batteries (see Table A4.1); (b) the metallic portion in Figure 4.5(a); (c) the distribution of metallic components in each size fraction of battery pack #B10.

$LiCoO_2$ is the most commonly used cathode material in LIBs for electronic devices. The BOM for $LiCoO_2$ cathode batteries created based on two battery manufacturers is shown in Figure 4.5a (see detailed information in Table B4 in Appendix B). In total, metals make up about 50% of total battery mass (Figure 4.5a), and the metallic fraction is largely dominated by cobalt and steel (Figure 4.5b). Both metals were observed to concentrate in opposing size fractions as a result of the pre-recycling process (Figure 4.5c). In the case of cobalt, the most commonly recycled battery material, relative content was enriched from 35% by weight in the unsorted metallic portion to 67% in the fine (0.5-1 mm) fraction and then to 85% in the ultrafine (<0.5 mm) fraction. Cobalt is the only metallic component having the content 5% or higher in the ultrafine fraction. Inversely, cobalt comprised less than 1% of metallic materials in the largest fraction (>6 mm). Another valuable material, copper, showed concentration in some size fractions: from 15% of metallic materials by mass before sorting to 40% in the mid (1-2.5 mm)

fraction and to 49% in the coarse (2.5-6 mm) fraction. Beyond these high-value materials, the content of other metals have also been enriched in certain fractions by this sorting process. For example, steel only shows up in two fractions: 1) 8% of metallic materials in the coarse (2.5-6 mm) fraction, which is unlikely being targeted at recycling facilities due to its low content and low unit value; and 2) 73% in the larger pieces (>6 mm).

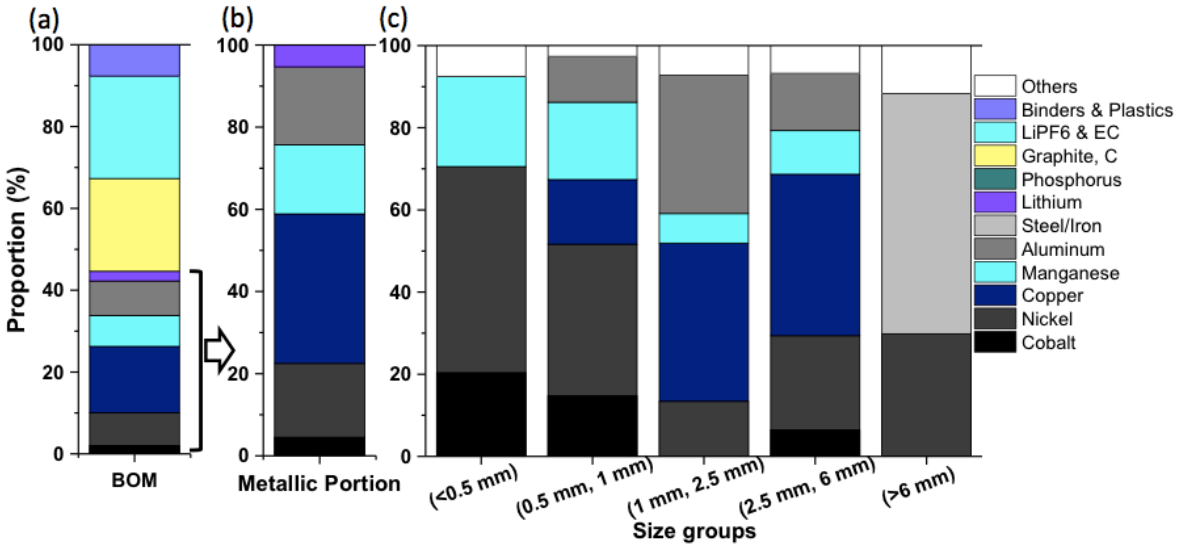

Figure 4.6 (a) The BOMs for mixed-metal cathode batteries; (b) the metallic portion in Figure 4.6(a); (c) the distribution of metallic components in each size fraction of battery pack #B2.

Besides $LiCoO_2$ cathode batteries, three out of ten selected battery packs removed from laptops were found to be mixed-metal cathode batteries, which have also become popular in EVs (such as Chevy Volt)[17]. The BOM for $Li_{1.05}(Ni_{4/9}Mn_{4/9}Co_{1/9})_{0.95}O_2$ cathode batteries made by a representative manufacturer was adopted as a reference (see Figure 4.6a and 4.6b). The XRF results show that contained battery materials were segregated by the sorting process (comparing Figure 4.6c with Figure 4.6b); but to a smaller degree than separation observed for the $LiCoO_2$ cathode batteries (comparing

Figure 4.6c with Figure 4.5c). The cobalt content was slightly enriched in the two smallest size fractions and excluded from the larger pieces (Figure 4.6c). However, it should be noted that mixed-metal cathode batteries have much lower cobalt content (35% of the metallic fraction) as compared to $LiCoO_2$ cathode batteries (cobalt is 4.5% of metallic fraction), indicating that this chemistry will be less economically favorable to recycle. For mixed-metal cathode batteries, nickel contributes significantly in both ultrafine and fine fractions, i.e., 50% and 37% of the metallic portion respectively, and has the potential to be recovered at a higher level. In addition, copper, having the highest content (40%) among metallic materials in both mid and coarse fractions, is a candidate to target in the subsequent recycling process. Common to both chemistries is the strong segregation of iron and steel, originating from the battery casing, in the largest size fraction, suggesting opportunity for automated separation and recycling of ferrous content after the pre-recycling process. Although not being considered in this chapter, iron and steel could potentially be separated via magnetic methods, which would leave nickel a rich portion in the larger pieces (>6 mm).

These examples demonstrate that the proposed pre-recycling process has the potential to effectively improve materials' concentration in certain size fractions, particularly for several high value materials, i.e., cobalt, nickel, and copper. As a clear difference in material composition can be seen between these two selected battery cathode types, sorting by cathode type before any treatment has the potential to reduce the uncertainty of input materials and improve the purity of output streams. Manufacturer labeling of LIBs to indicate chemistry would be a strong enabler for the success of this technology. However, current policies related to spent battery management either do not

have specifications regarding the labeling system or only require basic information (e.g., the crossed-out dustbin symbol, and chemical symbols for above-threshold chemicals) on the package [27, 113]. To provide a policy-directed assessment of benefits from labeling systems, the next section will compare the performances of this proposed pre-recycling process when applied to another two emerging cathode types.

4.3.3 Comparison among LIBs with alternate cathode chemistries

The average distributions of metallic materials in five fractions for $LiFePO_4$ and $LiMn_2O_4$ cathode batteries are shown in Figure 4.7a and 4.7b, respectively. The distribution of metallic materials in each size fraction varies significantly not only between two cathode types discussed in section 4.3.2 but also between two promising ones studied in this section (Figure 4.7). For example, the predominant metallic material in the ultrafine fraction is completely different, i.e., iron for $LiFePO_4$ cathode type and manganese for $LiMn_2O_4$ cathode batteries. If only cobalt is targeted for recovery, then many other materials will be missed, and at the same time, the impurities due to presence of other metals will create barriers during the cobalt-recovering process. Particularly, since a large fraction of the stream ($LiFePO_4$ and $LiMn_2O_4$ cathodes) does not contain cobalt, its concentration may become substantially diluted.

While the clear difference was observed among different cathode types, several key findings can be concluded from the sorting results. First, the dominant material in ultrafine fraction highly depends on the cathode type, largely because cathode materials, which are double side coated on the aluminum foil cathode substrate, appear to be very small particles when the battery cells were shredded. Secondly, copper, mainly from the

copper foil anode substrate (typically coated with graphite), is likely segregated into mid and coarse fraction. Finally, the battery casings make up the majority of the larger pieces.

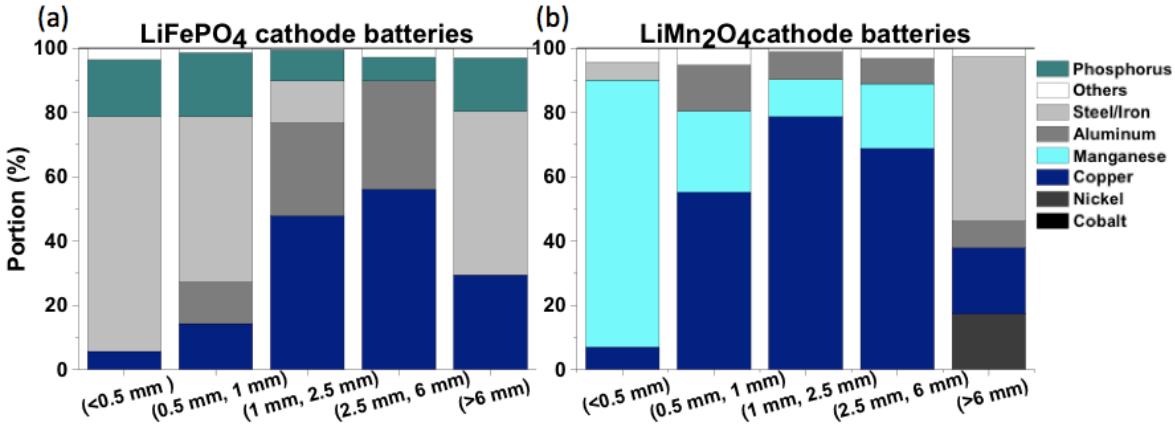

Figure 4.7 The metallic material distribution in each size fraction for (a) $LiFePO_4$, and (b) $LiMn_2O_4$ cathode batteries.

Since the potential recoverable value is the key decision factor from a recycler's standpoint, the unit economic value of each type of material needs to be taken into consideration. The contribution of each material to the total theoretical value of each size fraction for the four battery types are plotted in Figure 4.8a-d. Cobalt has the highest economic incentive for recovery from $LiCoO_2$ cathode batteries, and this value further enhanced through size separation (close to 100% for the smaller fractions, Figure 4.8a).

For mixed-metal cathode batteries, while nickel only accounts for 18% by weight in the metallic portion initially (three times more than cobalt, see Table 4.2), nickel has the highest priority to be recovered from an economic perspective. The potential recoverable value of nickel (ranging from 35% in the mid fraction to 84% in the larger pieces) exceeds the value of cobalt in all fractions (Figure 4.8b). Thus, cobalt cannot be viewed as the only economic driver for recycling, in the case of mixed-metal cathode

batteries. It must also be noted that although manganese makes a contribution on a certain level in all but the larger pieces of mixed-metal cathode batteries (Figure 4.6c), it is unlikely being targeted at recycling firms due to its low theoretical value (Figure 4.8b). In fact, recovering manganese specifically is very rare in general [8].

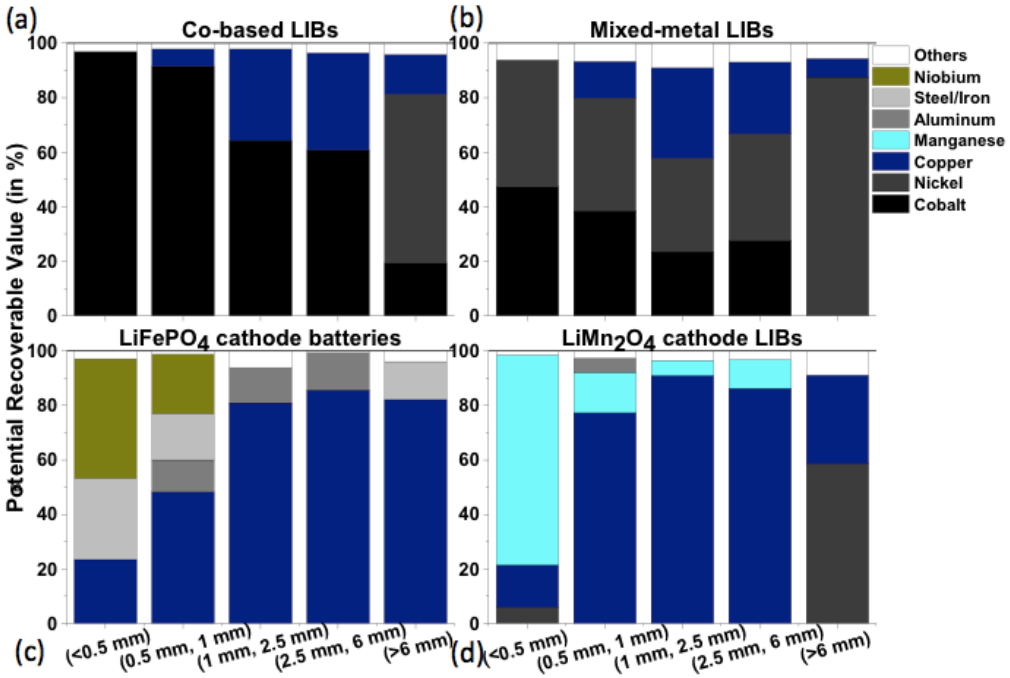

Figure 4.8 The contribution of each type of material to the total recoverable value of each size fraction for (a) $LiCoO_2$, (b) mixed-metal, (c) $LiFePO_4$, and (d) $LiMn_2O_4$ cathode types.

$LiFePO_4$ cathode batteries have become more popular recently due to low cost (25% less expensive compared to $LiCoO_2$ cathode batteries), low environmental impacts (less hazardous materials contained), and longer cycle life (up to 2000 cycles) [114, 115]. Several automotive manufacturers have already used $LiFePO_4$ cathode batteries in their EVs, such as the Coda Sedan and the Tata Nano [18, 19]. On an economic basis, copper makes major contributions in all but the ultrafine fractions due to its high unit value.

While steel is the main material in three size fractions (ultrafine, fine and larger pieces), it shows relatively low economic incentives (see Figure 4.8c). It should be noted that niobium counts about 2% by weight in both ultrafine and fine fractions. In fact, $LiFePO_4$ cathode battery samples selected in this chapter have used niobium atoms in cathode to improve the compound's electrical conductivity. While niobium has a high economic value ($47 per kg), it might not be worth the cost of recycling due to its extremely low mass content compared to other richer-contained materials, such as steel and copper. However, this sorting process successfully segregated niobium into two certain fractions, providing recyclers an opportunity to recover it.

Lithium manganese spinel is another promising LIB cathode type, having a three-dimensional spinel structure, which can improve the ion flow between the electrodes and therefore lower the internal resistance and increase loading capability [116]. They have already been successfully used in Nissan Leafs [18]. For this case, taking economic values into consideration does not change the materials' recovery priority significantly except for the larger pieces. Manganese has the highest recovery hierarchy in the ultrafine fraction in terms of both mass content and potential recoverable value; and so does copper in the fine, mid, and coarse fractions. It should be noted that selected $LiMn_2O_4$ cathode batteries are in a different form factor (i.e., 26650) from the rest of battery samples used in this chapter. LIBs labeled as "IMR" purchased from three manufacturers were found out that they were mixed-metal cathode batteries. As can be compared between Figure 4.8b and 4.8d, these two cathode types have different recovery targets due to their distinct material compositions (see Figure 4.6c and Figure 4.7b). Misinformation about battery content may present economic or safety barriers to

recycling at EOL, further supporting the need for appropriate labeling systems to include identification of battery cathode. For example, one labeling method would be to use color code casings for LIB cells, which provides an opportunity to adopt an optical sorting technologies at recycling facilities.

Subsequent recycling technologies targeting multiple types of materials (e.g., cobalt, nickel, and copper) must be developed to maximize the profit from recycling different cathode types [117]. Wang et al. (2009) proposed a hydrometallurgical process, designed to recover cobalt, manganese, nickel, and lithium from LIBs; however, before scaling up, associated environmental impacts need to be analyzed since this process requires strong acid and a significant energy input [118]. In fact, some undergoing research focusing on substituting strong acids by using organic acids to recover metallic materials from LIBs can be considered [50, 119].

4.3.4 Comparison among different battery OEMs

Previous studies pointed out that LIBs having the same cathode chemistry but made by different manufacturers are likely to show variations in their material content [11]. To understand whether this variation would bring uncertainties to this pre-recycling process, Figure 4.9a-d show the average XRF results of four size fractions of $LiCoO_2$ cathode batteries made by two battery manufacturers, i.e., #BM5 and #BM6. Material distribution in each size fraction varies slightly between these two manufacturers (Table 4.4), as determined by the range of values (mass percentages) divided by the mean value [120]. Usually if the number is less than one, it is considered low-variance; otherwise, it is considered high-variance. In this case, only three numbers are greater than one (bolded), indicating that the variation of material distribution in each size fraction

between these two manufacturers is relatively low. Similar results have been found for mixed-metal cathode batteries (Figure 4.10a–d, Table 4.4), suggesting that inter-cathode variability due to manufacturing is unlikely to be a barrier to implementing the re-recycling process. Findings from these comparisons indicate that detailed manufacturing information is likely unnecessary when enhancing the labeling systems since significant compositional difference in the same size fraction exists among different cathode types but not manufacturers.

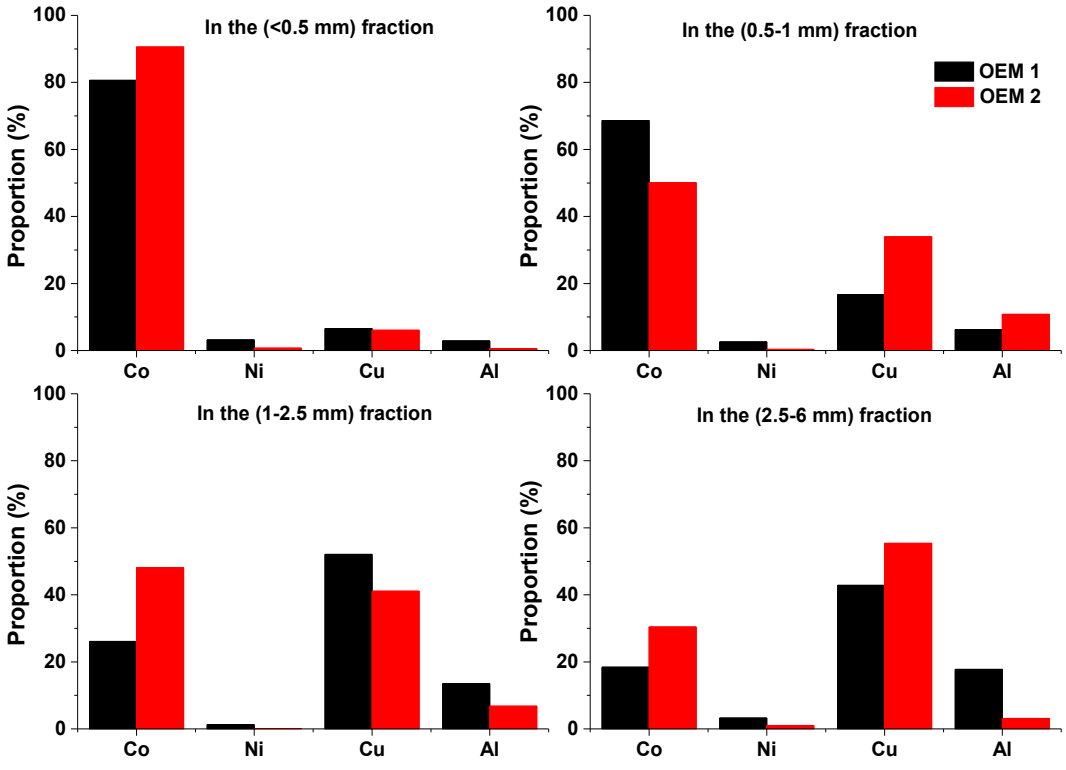

Figure 4.9 The sorting results of $LiCoO_2$ cathode batteries made by two manufacturers (a) (<0.5 mm), (b) (0.5-1 mm), (c) (1-2.5 mm), and (d) (2.5-6 mm).

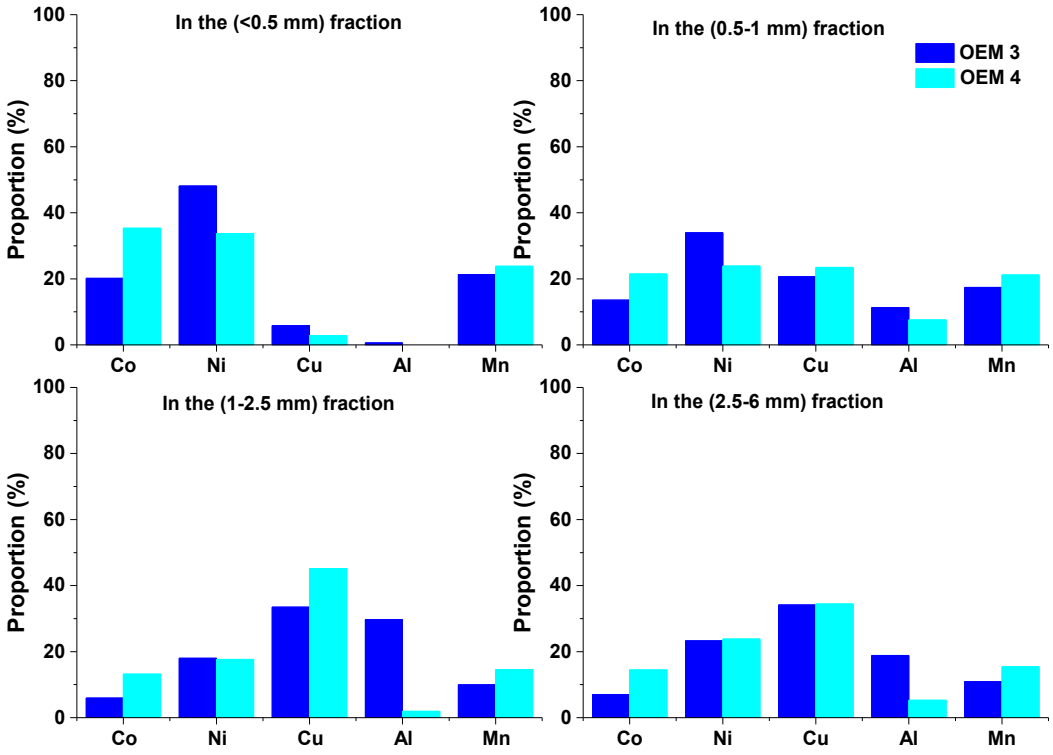

Figure 4.10 The sorting results of mixed-metal cathode batteries made by two manufacturers (a) (<0.5 mm), (b) (0.5-1 mm), (c) (1-2.5 mm), and (d) (2.5-6 mm).

Table 4.4 The measure of variability by using the range-divided-by-mean.

	$LiCoO_2$ cathode LIBs			**Mixed-metal cathode LIBs**				
Size fractions	**Co**	**Cu**	**Al**	**Co**	**Ni**	**Cu**	**Al**	**Mn**
(<0.5 mm)	0.12	0.70	Na	0.55	0.35	0.70	Na	0.11
(0.5 to 1 mm)	0.31	0.68	0.54	0.45	0.35	0.13	0.40	0.20
(1 to 2.5 mm)	0.59	0.24	0.66	0.76	0.20	0.30	**1.75**	0.38
(2.5 to 6 mm)	0.49	0.25	**1.40**	0.69	0.20	0.10	**1.12**	0.34

4.4 Conclusion

Facing a large volume of EOL LIBs entering the waste stream in the near future, it is essential that feasible, automated, low-cost recycling processes be developed. The pre-recycling process proposed in this chapter, including mechanical shredding and size-based sorting, requires only a few pieces of equipment (i.e., shredder, vibration table, and

sorting sieves) and low energy consumption, which is easy to be scaled up at recycling firms with some adjustment (e.g., a continuous inclined vibrating screening system). Our methods used liquid nitrogen to freeze batteries before processing to reduce the risk of fire that might be caused by short-circuiting or overheating during the mechanical shredding, an approach consistent with existing recycling facilities, such as Toxco [121]. When scaling up, processing materials at very low temperatures could present other challenges.

Given the results for the four most common battery cathode types, this proposed pre-recycling process can effectively enrich LIB materials into size fractions, which would enable recyclers to select recycling technologies and material recovery hierarchies that maximize mass or value to be recovered. For example, instead of processing the entire portion of EOL LIBs by using one recycling technology, combined recycling processes including several recycling methods (such as physical treatment, pyrometallurgical technology, acid leaching, electrochemical process, etc.) could be applied to different size fractions with specific recycling targets (e.g., copper for the mid and coarse fractions, and steel for the larger pieces). In particular, as battery recyclers are strongly driven by economic incentives, this chapter takes the potential recoverable value of battery materials into consideration resulting in a more clear recovery priority.

Meanwhile, the results suggest that pre-sorting by cathode type has the potential to further improve the segregation efficiency of battery waste streams. Particularly, while the lithium cobalt oxide is the most common cathode type at present, cobalt is not even contained in several projected next-generation LIBs (e.g., lithium iron phosphate, lithium manganese spinel, and lithium polymer). If LIB recycling is carried out without any pre-

sorting by cathode chemistry, a significant uncertainty would be involved and recycling yields will likely be diminished. Implementing a battery labeling system that specifies recycling-relevant information (electrode chemistry, casing materials, manufacturer, etc.) would increase the effectiveness of the pre-recycling system.

Further consideration of EOL battery management must also take into account recent trends toward use of nano-scale materials in next-generation cathode chemistries. There are considerable environmental uncertainties and concerns surrounding nanoparticles contained in products, particularly at end of life. These concerns include fate of nanoparticles in landfills [122], in waste water [123, 124], soil leaching [69], and disposal in general [125, 126]. To this end, a number of efforts are underway within the research and regulatory community to better quantify battery system impacts due to contained nanomaterials. For example, the U.S. EPA has recently launched a Lithium-ion Batteries and Nanotechnology Partnership involving industry, government and academia (including several of the authors) to conduct a LCA of LIBs used in EVs [44]. Work to quantify the risk of particulate exposure during end-of-life processing, including the pre-recycling process proposed in this chapter, is also necessary to understand the comprehensive life-cycle impacts of LIBs and will be discussed in the next chapter.

Chapter 5. Nanoparticle exposure potential during the mechanical treatment of end-of-life lithium-ion batteries

5.1 Introduction

The previous chapter has demonstrated that the proposed mechanical pre-recycling process can effectively segregate high-value metallic materials into size fractions and therefore provide opportunities for selecting subsequent recycling technologies [53, 75, 110, 127, 128]. In addition to laboratory research, some recyclers have already included mechanical treatment as a part of their battery recycling process. For example, at Toxco Inc., collected EOL LIB packs are first sent to a shredder, followed by a hammermill, to reduce the size of battery materials before the chemical recycling process [129].

Zimmer *et al.* has demonstrated that mechanical grinding will generate a substantial amount of nanoparticles through processes from within the grinding motor, and from the combustion as well as volatilization [130]. Therefore, there is a potential that nanoparticles will be formed during the mechanical treatment of EOL LIBs. In addition, nano-scale materials (e.g., carbon nanotubes (CNTs), nano-scaled $LiCoO_2$ cathode materials, and nano-sized Sn/Sb oxides anode materials) have started being utilized in LIBs to enhance the battery performance recently [131, 132]. These emerging battery technologies might lead to a significantly increased release of nanoparticles during the battery recycling process. A material flow analysis done by Espinoza et al. forecasts CNT contained LIBs in portable computers, and points out the importance of establishing new recycling processes to minimize the potential emissions of CNTs when these batteries enter the waste stream[133]. Due to the unique properties of nano-scale

particles (i.e., high surface area to volume ratio, and high particle numbers per equivalent mass), exposure to nanoparticles might cause adverse health effects [134-136]. While there are a large number of studies in the field of nanotechnology and occupational health, the majority of them focus on nanoparticle exposure assessment during the manufacturing process [137], very little attention has been given to the recycling phase. Köhler et al. indicates the potential of CNT release to the environment throughout the whole life cycle, including the recycling and disposal phase; however, their discussion only stays at the qualitative level [132]. Up to now, a significant knowledge gap exists as to the risk of nanoparticle exposure associated with the recycling process of EOL products. This chapter aims to fill this research gap by exploring the nanoparticle exposure potential during the mechanical treatment of EOL LIBs.

Several exposure metrics are available to conduct nanoparticle exposure assessments, including traditionally used metric (i.e., mass concentration) and relatively new metrics (i.e., number concentration and surface area per mass). The current occupational exposure limits (OELs) for particle exposure are based on the mass concentration [138, 139]. However, due to the unique size-dependent properties of nanomaterials (e.g., high particle counts and high surface area per unit mass), the mass concentration metric might not be able to provide an appropriate data inventory for the toxicity characterization. While there is no agreement on the best metric for nanoparticle exposure, a number of recent published studies suggested that particle number concentration and surface area might better characterize nano-scale particle exposure [140, 141]. This chapter utilizes the particle number concentration metric to measure nanoparticle exposure potential during the mechanical treatment of EOL LIBs.

The pre-recycling process, including mechanical shredding and size-based sorting process, designed for EOL LIBs introduced in the previous chapter was used here as a case study. This proposed pre-recycling process has been demonstrated to be able to reduce the impurity of LIB scrap streams through material segregation, and having the potential to improve the efficiency of subsequent recycling processes. The purpose of this chapter is threefold: (1) to measure dynamic nanoparticle number concentration and size distribution during this proposed mechanical treatment, (2) to test the effectiveness of the ventilation system (i.e., a floor mounted fume hood) in our lab in terms of perfecting workers at the breathing zoon, and (3) to compare the nanoparticle exposure potential when processing nano-enabled LIBs with those not containing specific nano-scale materials.

5.2 Methodology

5.2.1 Experimental materials and instrument description

5.2.1.1 Battery Materials

Lithium-ion 18650 batteries used in this chapter fall into two categories: 1) traditional LIBs (i.e., batteries not contain specific nano-scale materials) and 2) nano-enabled LIBs (i.e., batteries containing nano-scale materials). Battery samples in the first category were collected from a number of laptops, including multiple manufacturer brands. Each laptop had one battery pack, containing different numbers of battery cells, i.e., 6, 8, 9, or 12. The weights of these battery cells follow a normal distribution with a mean of 44.0 g and a standard deviation of 1.8 g (see Table B5 in Appendix B). Battery cells in this category were mixed with different cathode chemistry types, which is likely the case faced by today's battery recyclers. According to selected battery samples in this

chapter, cobalt-based cathode LIBs dominates this category, followed by mixed-metal cathode LIBs. However, it is unlikely that any of these selected batteries contained nano-scale materials. Battery samples in the second category are LIBs containing nano-scale $LiFePO_4$ cathode material (made by A123 System LLC). To make a fair comparison, LIBs containing the same type of cathode material (i.e., $LiFePO_4$) but at the non-nano-scale (made by Tenergy) were used in this chapter as well.

5.2.1.2 Equipment

To eliminate the risk of exposure to electrolyte, the shredding experiments were performed under a floor mounted fume hood (see Figure 4.2a). As the vibration table was unable to placed in a fume hood due to its big size, the sorting process was performed in a laboratory with the whole-building ventilation system (see Figure 4.2b).

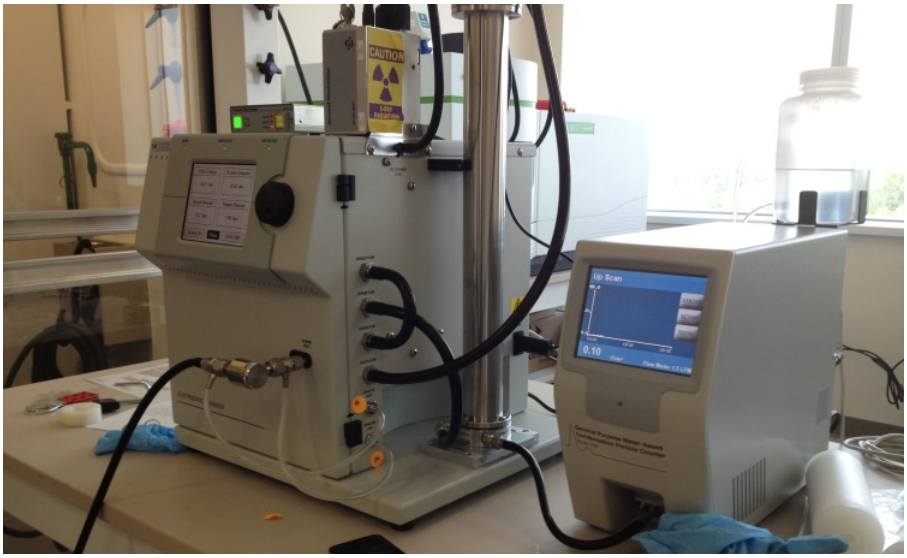

Figure 5.1 The scanning mobility particle sizer (SMPS, TSI Model 3936) spectrometer.

The instrument used to detect nanoparticles was the Scanning Mobility Particle Sizer (SMPS, TSI Model 3936) Spectrometer, including an Electrostatic Classifier (EC,

TSI Model 3080) and a Water-based Condensation Particle Counter (WCPC, TSI Model 3787) (see Figure 5.1). While the theoretical measuring size range of the SMPS is 2.5 to 1,000 nm, the actual range could be narrower depending on a set of specific parameters, e.g., the type of the Differential Mobility Analyzer (DMA, TSI), sample flow rate, sheath-to-sample flow rate ratio, scan-up time, retrace time, etc. The SMPS was located outside of the fume hood during the shredding process and was placed next to the vibration table during the sorting process. A conductive rubber tubing was used to connect the inlet of SMPS to the measuring locations.

5.2.2 Aerosol sampling

The mechanical pre-recycling process introduced in Chapter 4 has been selected in this chapter as a representative mechanical process (see Figure 4.1). Released nanoparticles during the mechanical shredding and size-based sorting processes were measured by the SMPS with different specific tasks and parameter-settings, which will be discussed in section 5.2.2.2 and 5.2.2.3.

5.2.2.1 Determination of delay time and parameters

The delay time can be critical in this study particularly for the shredding process because it only takes less than one minute for most battery cells in one batch being shredded. The delay time can break down to the following four small time-sections, including the time needed 1) for LIB cells to fall and reach the blades of the shredder (assumed as 1s), 2) for released nanoparticles to reach the inlet of the tubing (assumed as approximately 3 to 5s), 3) for nanoparticles to move from the inlet of the tubing to the inlet of the SMPS (calculated as 1.5 s), and 4) for nanoparticles to travel inside of the SMPS (5s). The sample flow rate of the SMPS was set up at the high mode, i.e., 1.5 lpm,

to minimize the particle loss. Therefore, the residence time inside the tubing (4.5 mm diameter * 230 cm long) is 1.5s, which is the time section #3. The total estimated delay time is 12 s. This estimation was proved by two sample tests using the WCPC. Battery cells were dropped in the shredder at time=0, then it took about 12s for the WCPC to detect the first obvious increase (see Figure 5.2a and b).

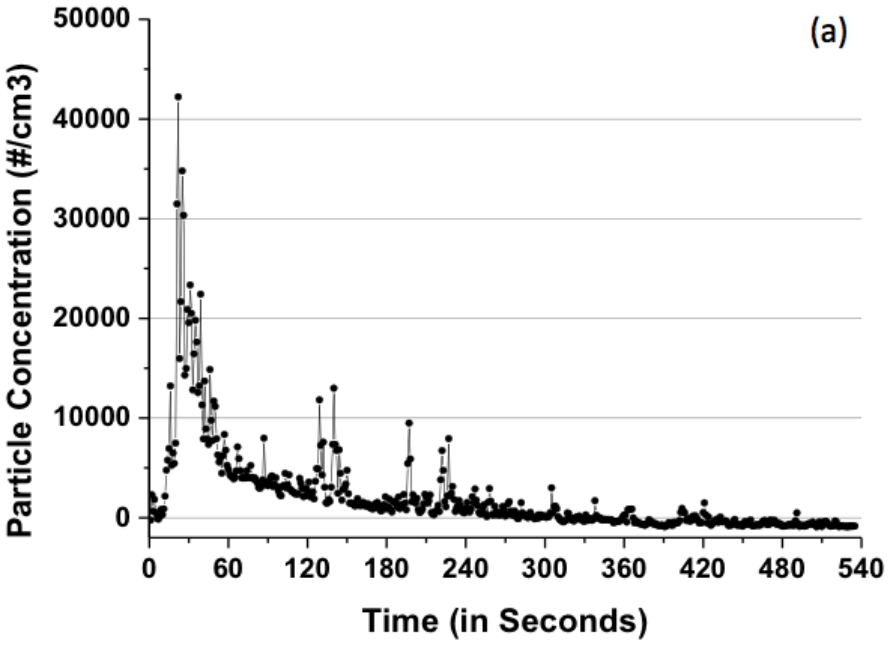

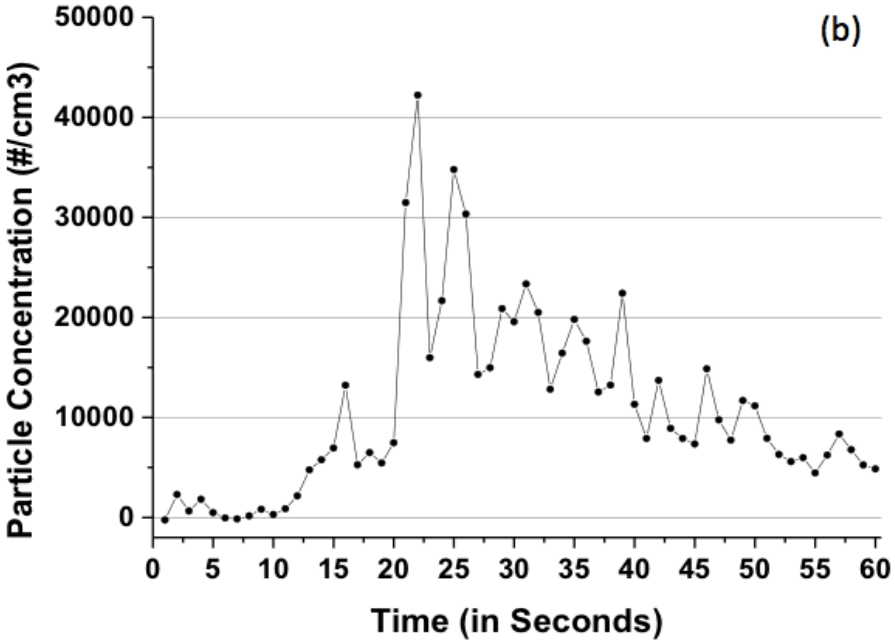

Figure 5.2 (a) The background corrected particle number concentration during the shredding process of LIB cells in battery pack #01 measured by the WCPC, (b) the magnified 1st 60 s in (a).

5.2.2.2 Exposure assessment during the shredding process

The mechanical shredding process was performed under a fume hood due to the safety concerns. To minimize the influence of the airflow in the fume hood on the movement of released nanoparticles, a box was hanged above (but not cover) the top of the shredder. The shredder used in this study has a half-open top. The tubing was placed on top of the shredder to measure the maximum nanoparticle exposure. Each time, frozen battery cells from one battery pack were dropped into the shredder, and the SMPS started to record data after 12 s.

Since the main shredding only lasts for a short period of time (less than 1 min), the recommended scan-up and retrace time for the SMPS by TSI (i.e., 120 s and 15 s, respectively) are not applicable in this case. To capture the fast-changing experimental

environment, a scan-up time of 45 s and a retrace time of 10 s were used. In total, it took 55 s for the SMPS to complete one scanning sample. For each batch, sixteen scanning samples were collected successively to capture the dynamic change of particle number concentration and size distribution over about 15-min scanning time. Selected battery packs contained different numbers of battery cells, i.e., 6, 8, 9 and 12, which were used to analyze the relationship between input mass and particle exposure potential. Table 5.1 provides the mass information for the input materials. The variation in mass among battery packs containing the same number of battery cells is very low.

Table 5.1 The mass information about the feeding battery materials.

Number of cells per pack	Battery pack # (Indices[a])	Numbers of battery packs	Average mass per pack (g)	Standard Deviation of sample packs (g)	Mass increased to 6-cell packs
6	05 –10	6	260	10	0
8	11—16	6	360	9	40%
9	17—21	5	410	4	60%
12	22—26	5	540	6	110%

[a] Refer to Table B5 in Appendix B.

In addition, the particle exposure potential at the breathing zone was also tested to identify the performance of the fume hood. Instead of on top of the shredder, the tubing was placed one meter in front of the fume hood with the sash completely down.

5.2.2.3 Exposure assessment during the sorting process

No theory or evidence supports that mechanical sorting process would form nano-scale particles. Therefore, when sorting battery pieces that shredded from LIBs without specific nano-scale materials, the nanoparticle concentration would unlikely show significant changes comparing to the background level. The focus of this section is the second battery category, i.e., batteries containing nano-scale materials; in this study, A123 nano-scale $LiFePO_4$ cathode batteries were selected as a representative.

After one-week evaporation, shredded battery pieces were ready to be sorted into different size fractions. The recommended scan up time (120 s) and retrace time (15 s) were used for the sorting process due to its stability, indicating that 135 s was required to complete one scanning sample. Ten scanning samples were collected successively for each batch, taking about 23 minutes in total. To identify how the mass difference would affect the result, battery pieces were prepared as shredded-6-cell batches and shredded-9-cell batches. The sorting experiment was performed in a laboratory with general building ventilation system available since the vibration table is too big to fit in any fume hood. The tests ran at two locations: 1) the place near the sorting sieves to measure the maximum nanoparticle exposure potential, 2) the breathing zone (one meter in front of the sorting sieves).

5.3 Results and discussion

5.3.1 Mechanical shredding—using LIBs without specific nano-scale materials

5.3.1.1 Dynamic particle concentration

As can be seen in Figure 5.2, a substantial amount of nanoparticles ranging from 5 to 1,000 nm were detected in the first few minutes by the WCPC. When shredding 6-cell batches, the number concentration of 5-1,000 nm particles can increase by as much as 46,000 particles per cm^3 after the shredding started, and slowly decrease back to the background level after about five minutes (Figure 5.2). Ultrafine particles (less than 100 nm in diameter) are the top concern from the perspective of occupational health, since those particles have a higher potential to severely harm the organ due to their specific chemical and physical properties. Therefore, the particle number concentration during the shredding process has been tested as a function of particle size in this section. Figure

5.3(a) shows the changes in particle number concentration and size distribution measured by the SMPS during the whole shredding process (including 16 scanning periods): four representative scanning periods, i.e., the 1^{st}, 2^{nd}, 5^{th}, and 16^{th}, are selected to show this dynamic trend. The background particle concentration has been subtracted from the detected numbers, so the data points in Figure 5.3(a) are background corrected particle number concentrations primarily caused by this mechanical shredding process; each curve represents the average of 6 trials. Some data points are very close or even below zero, indicating that the concentration of these particles during these specific scanning periods were very close to the background level. For example, the concentrations of particles <20 nm in Sample#16 are very close to zero, indicating that after about 14 minutes the concentration of 6-20 nm particles substantially dropped back to the background level. In addition, very limited number of 100-220 nm particles were formed from the shredding process as the concentration of those particles did not change significantly during the whole shredding process (see Figure 5.3b).

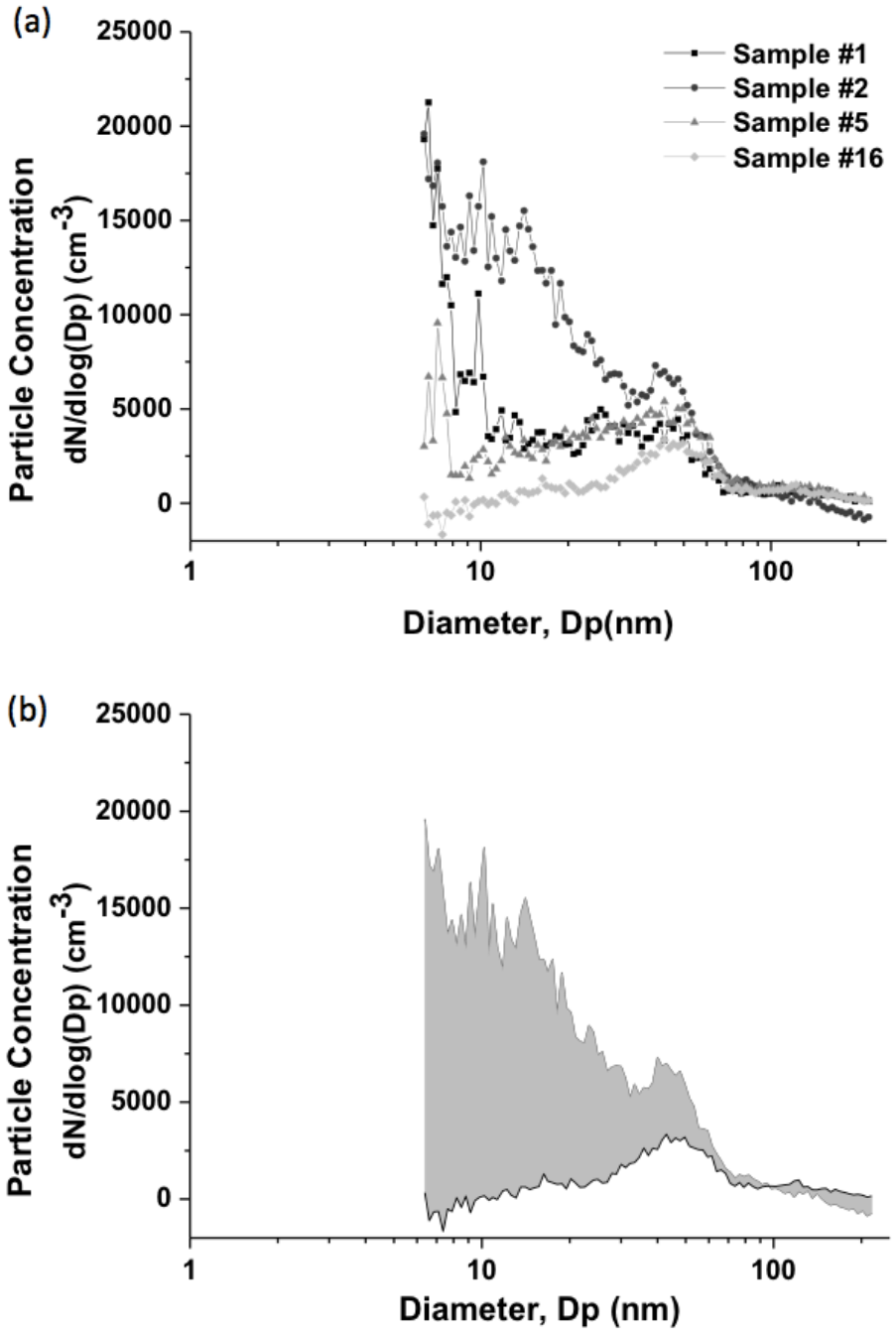

Figure 5.3 (a) The changes in particle number concentration and size distribution during representative scanning periods, (b) the range of particle concentration change during the whole 15-min shredding process.

It should be noted that the particle loss in the tubing was not considered in this study although it is theoretically possible. The tubing used in this study was over two meters long to reach maximum exposure areas. According to [142], the particle losses in a long sampling tubing can be up to 32% for particles <20 nm, but negligible for particle >20 nm. This indicates that the real nanoparticle release during the mechanical shredding of EOL LIBs can be more severe than being shown in Figure 5.3.

While a significant amount of nanoparticles released right after the shredding started, the particle concentration reaches the highest level at the 2nd scanning period, and was observed a decreasing trend afterwards. Therefore, if the batch-based shredding is installed to the industrial level, remote control or some sort of strategy to prevent workers being close to the shredder during the first few minutes might be the way to invest; if the continuous shredding is the case, the ventilation system needs to be installed at recycling facilities.

5.3.1.2 Mass vs. particle exposure potential

In the previous section, 6 LIB cells were fed into the shredder each time to keep the mass of the input consistent, thereby collecting the comparable data. In this section, batches containing different numbers of cells were shredded to analyze the relationship between the mass of shredded batteries and the particle exposure potential caused by the shredding process. The information about selected battery cells and their mass values are shown in Table 5.1. For batches containing the same number of cells (for example, 6), the average background corrected particle number concentration during the second scanning period was presented in Figure 5.4 with the label “6 cells”; the same for 8, 9, and 12 cells. Figure 5.4 shows that although the input batches were different in mass, the highest

particle number concentrations and size distributions during the shredding process did not differ significantly.

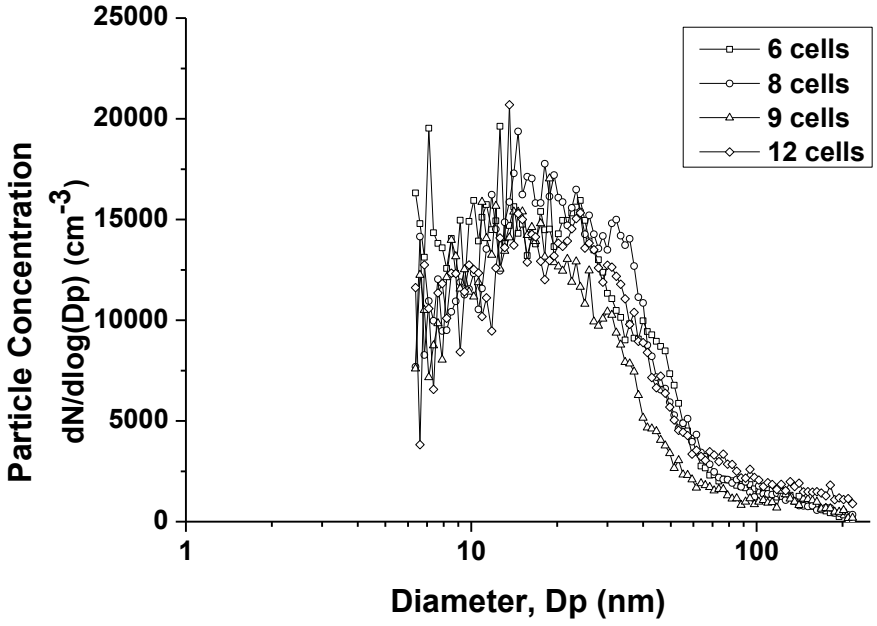

Figure 5.4 Comparison of background corrected particle number concentrations during the 2nd scanning period when processing batches having different numbers of battery cells.

There are a few possible explanations for this result. One of them is that the shredder used in this study has a half-open top (i.e., not fully open but blocked by two downward sloping plates), which might reduce the escape of nanoparticles to a certain level. However, the design of this shredder may or may not be the case at recycling facilities; therefore, additional research needs to be done by using different types of shredders in the future. Another possible reason is that the increased amount of input materials per batch is still not significant in this study. Compared to the base case (i.e., 6 cells per batch), while the input battery materials has been increased by 40%, 60% and 110% by weight, respectively, the actual increased mass was only 100 g, 150 g, and 280

g per batch. Limited available battery resources were not enough to triple the mass of input batteries in the base case and at the same time to repeat the experiment several times to get scientifically reliable data. Therefore, there is still a possibility that the nanoparticle exposure potential might increase as input LIB materials increase to a certain level.

Zimmer et al. used a variety types of substrates to demonstrate that the particle size distribution of particles generated during the grinding process tend to be bimodal (i.e., distinct ultrafine and coarse modes) [130]. Due to the specific parameters being set up in this study, only ultrafine particles can be detected by the SMPS. Since Figure 5.4 shows size-resolved particle number concentrations do not differ among batches having different numbers of cells, the average concentrations for 6-220 nm particles were calculated and then fitted with a lognormal distribution (see Figure 5.5). The complete fitting information is provided in Figure B2 and Table B6 in Appendix B. While the high adjusted R-squared value does not necessarily indicate that the model has a perfect fit, it can fully support the agreement between our results and Zimmer's study (see Table 5.2)

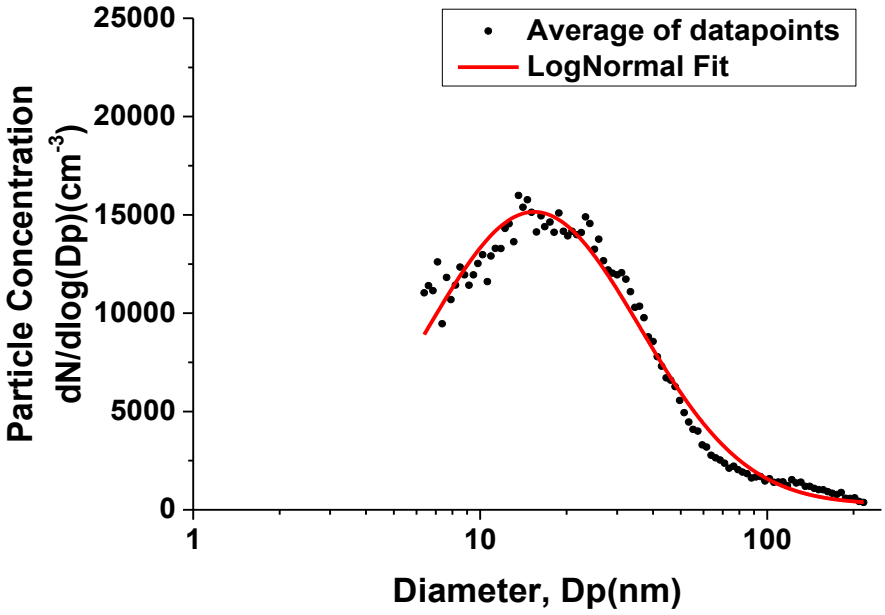

Figure 5.5 A lognormal fit of the average background corrected particle number concentration during the 2nd scanning period of the shredding process.

Table 5.2 Statistics for the lognormal fit in Fig. 5.5.

Equation	$y = y_0 + \frac{A}{\sqrt{2\pi}wx} e^{\frac{-[ln\frac{x}{xc}]^2}{2w^2}}$
Reduced Chi-Sqr	663,805
Adj. R-Squares	0.978
Parameters	Value
y_0	274
xc	32
w	0.8
A	697,124

5.3.1.3 Breathing zone test

The increase in particle number concentration was also tested at the breathing zone. Figure 5.6 shows background corrected particle number concentrations during the

second scanning period (the maximum exposure period) when shredding 6-cell batches. While the particle number concentration at the breathing zone was still slightly higher during the shredding process compared to the background level, the magnitude of particle number concentration was significantly lower outside the fume hood than inside.

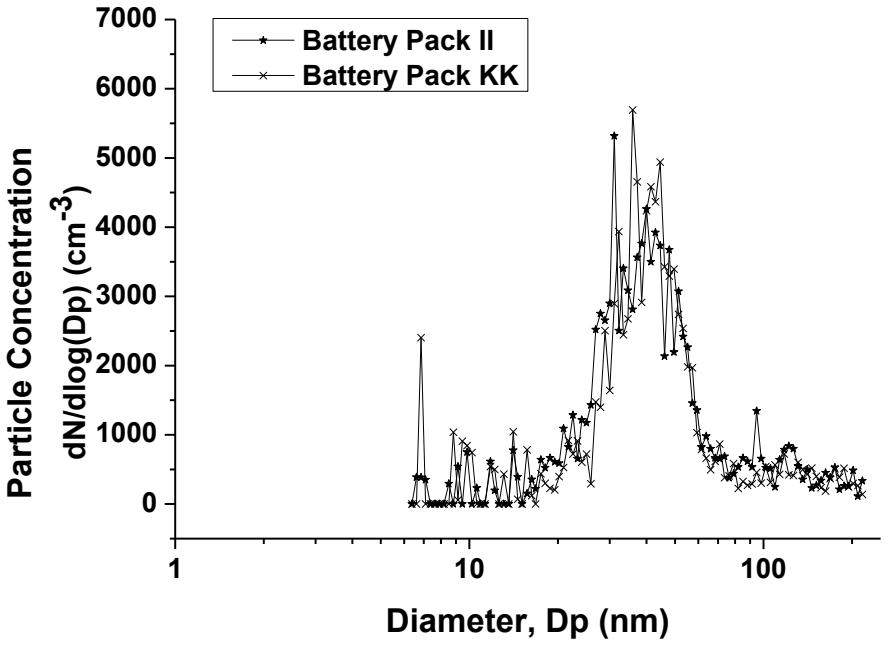

Figure 5.6 Background corrected particle number concentrations at the breathing zone during the 2nd scanning period of the shredding process.

In addition, Figure 5.6 shows that our fume hood can effectively protect workers from exposure to particles <20 nm or >70 nm during the shredding process; however, there is still a possibility for workers to be exposed to 30-60 nm size particles. The number concentration of escaped particles from the fume hood during the shredding process peaked at ~40 nm particle diameter. It should be noted that the particles ranging between 30 and 100 nm can most likely penetrate through electret filter media (the most common type of filter used in respirators on the market today) [143], which covers the

size of high-concentrated particles at the breathing zone in this study, indicating additional protection methods are required when shredding LIBs. For example, the fume hood used in this study is a traditional constant-flow fume hood; however, Tsai *et al.* demonstrated that [144] an air-curtain hood, having the vertical airflow around the doorsill, can more effectively reduce nanoparticles escaping from the hood. Therefore, a better-designed ventilation system is very important from a perspective on occupational health and safety, particularly when this shredding process scales up to the industrial level,

5.3.2 Shredding process—using A123 nano-scale $LiFePO_4$ cathode batteries

Figure 5.7 compares particle number concentrations and size distributions when shredding two different types of LIBs, i.e., traditional batteries and nano-enabled batteries (i.e., batteries containing nano-scale $LiFePO_4$ cathode material in this case). Each curve represents the average of 5 runs using 6 cells in each batch during the second scanning period. Shredding A123 LIBs led to a significantly higher level of nanoparticle exposure. This is because besides the ultrafine particles formed through abrasion and attrition during the shredding process, the contained nano-scale materials also likely released when batteries were crushed. Additionally, the particle size distribution appears different when processing two different battery categories. It should be noted that there was a certain amount of variability associated with our data, which however would need additional runs to make a conclusion. While shredding nano-enabled LIBs shows a higher potential for nanoparticle exposure, this potential might be different when processing batteries containing other types of nano-scale materials (such as CNTs).

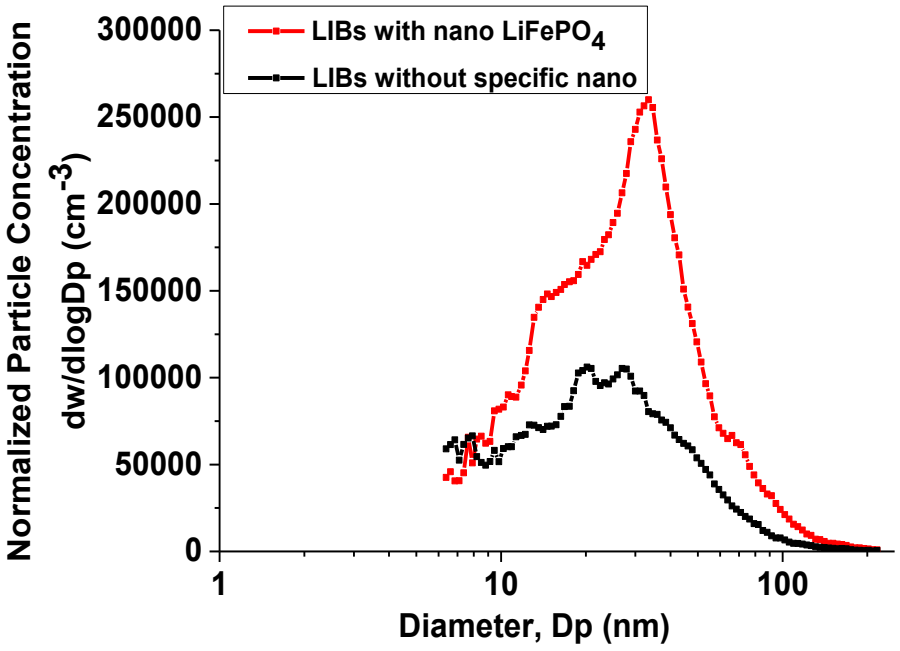

Figure 5.7 Comparison of particle number concentrations and size distributions during the 2nd scanning period when shredding different categories of LIBs: traditional vs. nano-enabled.

5.3.3 Sorting process

During the whole size-based soring process, no significant changes in particle number concentration was observed compared to the background data. Figure 5.8 provides an example: the data points are the background corrected particle number concentration (average of 3 runs) for 6-220 nm particles during the first scanning period when sorting 9-cell batches of nano-scale $LiFePO_4$ cathode battery pieces. As can be seen, the background corrected data are very close to zero. Two testing locations, i.e., the place near the sorting sieves and the breathing zone, have similar results, indicating that performing size-based sorting process on battery pieces might not cause nanoparticle release. However, LIBs containing other types of nano-scale materials should be

examined in the future. In addition, a substantial amount of black fine dusts that have bigger sizes (outside the scope of this study) were observed during the sorting process, which also requires appropriate protection strategies.

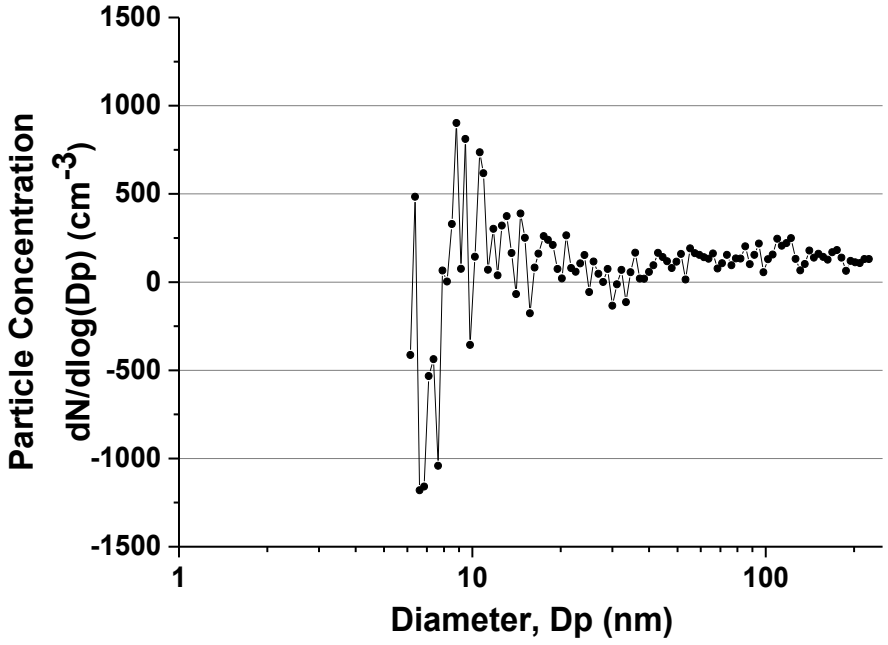

Figure 5.8 Average background corrected particle number concentration during the 1st scanning period when sorting 9-cell batches of nano-scale $LiFePO_4$ cathode battery pieces.

5.4 Conclusion

This chapter explored nanoparticle exposure potential during a representative mechanical pre-recycling process of EOL LIBs. The results show that nanoparticle exposure mainly occurred during the mechanical shredding but not size-based sorting process, and the magnitude of nanoparticle exposure might be higher when shredding LIBs containing nano-scale materials compared to when processing traditional LIBs. The nanoparticle exposure reached the highest level after about one minute after the shredding

started and slowly reduced to the background level after about fifteen minutes. Among particles ranging from 6 to 220 nm, ultrafine particles (< 100 nm) made the most contribution to the change in particle number concentration during the shredding process. With limited battery resources, the mass of input batteries for the shredding process were increased by 40%, 60% and 110% compared to the base case, i.e., 6-cell batches weighting 260 g on average; however, particle size distributions and particle number concentrations show quite similar among batches containing different numbers of cells. In addition, the result has proved that the floor-mounted fume hood used in this study can effectively reduce nanoparticle release to the breathing zone. However, additional protection methods are highly recommended to provide workers (or searchers) a safer working environment, such as a better-designed ventilation system or more efficient personal protective equipment (e.g., gloves, clothing, goggles, etc.).

Mass concentration metric alone is not able to fully capture the severity of nanoparticle exposure, as for per given mass of nanoparticles particle number concentration can be different tremendously for different size nanoparticles [145, 146]. However, most current emissions regulations rely on mass based standards. The results in this chapter show a significant release of nanoparticles during the mechanical treatment of EOL LIBs, even using small input batches. This chapter provides primary data to complement current regulations that intend to deal with the potential risks caused by nanoparticle release. In addition, as an increasing number of studies have included mechanical treatment into their design for LIB recycling, this exposure assessment proactively tested nanoparticle exposure potential associated with pre-recycling of EOL LIBs, which builds up an important foundation for conducting risk assessments.

Future research includes but not limited to the following three aspects: 1) shredders with different top designs need to be tested to explore the relationship between the mass of input battery materials and the nanoparticle exposure potential; 2) LIBs containing other types of nano-scale materials (such as CNTs) should be examined; and 3) the hazards of released nanoparticles need to be identified.

Chapter 6. Conclusion and major contributions

Dramatic increase in consumption of EVs and portable consumer electronics has raised concerns about sustainably managing the growing LIB waste streams. However, federal level regulations or policy guidance regarding disposal of LIBs is not yet in place in the U.S. Recycling of spent LIBs benefits the environment thought providing recovered materials, which requires less amount of embodied energy and has less greenhouse gas emissions compared to these virgin materials, and can also slow the depletion of raw materials. To achieve maximum sustainable performance through recycling with limited resources, a comprehensive characterization of materials contained in EOL LIBs by using both environmental and economic metrics was investigated in Chapter 2. Particularly, recyclers will highly likely face uncertain co-mingled waste streams as a variety of cathode chemistry types have been successfully used in LIBs. Given that the potential recoverable value is the main driving force to process spent LIBs from the recyclers' standpoint, Chapter 2 combines economic modeling and fundamental material characterization methods to quantify economic trade-offs for four cathode types (including the current most common type and three promising cathode chemistries) at their end of life. Results show that as chemistries transition from lithium-cobalt based cathodes to less costly chemistries, battery recovery value decreases along with the initial value of the raw materials used. A majority of the potentially recoverable value resides in the base metals contained in the cathode; this increases disassembly cost and time as this is the last portion of the battery taken apart. A great deal of compositional variability exists, even within the same cathode chemistry, due to differences between

manufacturers with coefficient of variation up to 37% for some base metals. Cathode changes over time will result in a heavily co-mingled waste stream, further complicating waste management and recycling processes.

While Chapter 2 demonstrates the economic incentives and environmental savings potential though recovering materials from EOL LIBs, the technological progress has led to a diverse mix of batteries in use that ultimately require waste management. Chapter 3 develops and applies an optimization model to analyze the profitability of recycling facilities given current estimates of LIB technologies, commodity market prices of materials expected to be recovered, and material composition for three battery types (differentiated on the basis of cathode chemistry). Sensitivity analysis shows that the profitability is highly dependent on the expected mix of cathode chemistries in the waste stream and the resultant variability in material mass and value. The potential values of waste streams comprised of different cathode chemistry types show a variability ranging from \$860 per ton for $LiMn_2O_4$ cathode batteries to \$8900 per ton for $LiCoO_2$ cathode batteries. This chapter provides a good understanding of how to maximize the economic opportunity of battery recycling while mitigating the uncertainties associated with a highly variable waste stream. In addition, the initial results and the policy case study also can help to promote EOL management and relative policymaking for spent LIBs.

To improve the battery recycling efficiency, a sustainable pre-recycling process (including mechanical shredding and size-based sorting steps) has been proposed in Chapter 4. This pre-recycling process, which can be easily scaled up to

the industrial level, aims to achieve material segregation with a focus on the metallic portion and provide clear targets for subsequent recycling processes. The results show that contained metallic materials can be segregated into different size fractions at different levels. For example, for lithium cobalt oxide batteries, cobalt content has been improved from 35% by weight in the metallic portion before this pre-recycling process to 82% in the ultrafine (<0.5 mm) fraction and to 68% in the fine (0.5-1 mm) fraction, and been excluded in the larger pieces (>6 mm). However, size fractions across multiple battery chemistries showed significant variability in material concentration. This finding indicates that sorting by cathode before pre-treatment can effectively reduce the uncertainty of input materials and therefore improve the purity of output streams. Thus, battery labeling systems will be an important step towards implementation of the pre-recycling process.

Chapter 5 proactively examines nanoparticle exposure potential during the mechanical treatment of EOL LIBs, including traditional LIBs as well as the emerging LIB technologies, i.e., nano-enabled LIBs. The proposed pre-recycling process in Chapter 4 was adopted here as a case study. The exposure assessment work in Chapter 5 takes initial steps aiming to fill the research gaps in the life-cycle inventory for LIBs with a focus on end-of-life, and builds up the foundation for risk assessment. Results show that a substantial amount of nano-scale particles are released during the mechanical shredding but not size-based sorting process. Shredding LIBs containing nano-scale $LiFePO_4$ cathode materials may have a higher potential for nanoparticle exposure. Experimental data in this chapter can inform

occupational health and safety policymaking as well as help scientists and engineers develop more efficient filtration systems.

This dissertation systematically analyzed the environmental and economic impacts of EOL LIBs and their recycling processes, providing the complete information for policymakers, recyclers, scientists, and other stakeholders to guide future policymaking regarding LIBs as well as deployment of novel recycling techniques. Future research work includes developing a complete sustainable recycling sequence (combining technologies such as physical process, thermal treatment, and/or hydrometallurgical technologies), and exploring the tradeoffs between their environmental performances and recycling efficiency. Additionally, characterizing released nanoparticles during the recycling process and conducting a full risk assessment need to be done in the future.

Appendix A. Prioritizing material recovery for end-of-life printed circuit

A.1 Introduction

Twenty to fifty million tons of electronic waste (e-waste) are generated worldwide each year; the total amount of e-waste is increasing three times faster than any other type of municipal waste [147]. This is due to a variety of factors including both increasing population and electronic product ownership and the decreasing lifespan of these products due to faster replacement by newer generations.

Even though some countries and the Basel Convention restrict e-waste trade between nations, a large amount of this waste is exported to Asia, Eastern Europe and Africa from a variety of developed countries [148]. Although there are no official statistics for illegal shipments of e-waste on a global level, estimates made by informed recycling industry sources are that about 50 to 80 percent of e-waste collected in the U.S. ends up in Asia [71, 149]. While there is some debate about the accuracy of these percentages, it is clear that a magnitude of e-waste is exported. This export of waste represents an economic loss for these countries as e-waste contains metals with significant value and embodied energy. Beyond this loss, also of concern is that these materials are often processed in the informal sector; this sector has limited capabilities for recovery, often targeting only one or two metals. Informal recycling involves workers receiving low ($3.60 per day in China [150]) or no wages to disassemble, acid-wash using aqua regia (a mixture of nitric acid and hydrochloric acid in a volume ratio of 1:3) to recover gold [149], and/or burn this waste in order to recover a small amount of material, typically copper [151, 152]. While alternatives to informal recycling vary greatly geographically, many companies have initiatives aimed at economically viable,

environmentally benign e-waste processing such as Electronic Recyclers International in the US, Umicore in the EU, and Cimelia Resource Recovery in Asia. This is also an active research and development area in academia, government, and industry with specific examples of this work cited below.

One particular target for both formal and informal recycling is the printed circuit board (PCB). While PCBs constitute only about 6% of the total weight of e-waste [153], it contains a significant portion of the value contained in e-waste. Informal recycling of PCBs can cause severe environmental pollution problems as well as human health issues. Open burning of waste PCBs to isolate copper from plastics produces hazardous byproducts such as dioxins, furans, polybrominated organic pollutants and polycyclic aromatic hydrocarbons [147]. Sludges from uncontrolled leaching processes by using aqua regia may be discharged into local rivers and streams. Lead, a widely used component of solders in PCBs, is typically improperly disposed of in the process as it has no value. Health impacts of lead have been well-characterized, particularly for children [154, 155]. Studies have found lead in air, soil, water, and local food at a much higher concentration than in non e-waste recycling areas [154].

Regardless of where these end-of-life electronic products end up, the obligation of how best to process, sort, recycle, or landfill them falls onto the waste management community. These waste management decisions are dictated by a complex set of economic and environmental trade-offs; even formal recycling of PCBs can be quite challenging due to its complexity in terms of material composition and physical structure [156]. The typical PCB consists of more than twenty different types of metals, including

precious (gold, palladium, platinum, etc.), base (copper, aluminum, etc.), and toxic (lead, cadmium, arsenic, mercury, etc.), as well as ceramics and plastics.

While it is clear that economic and environmental metrics motivate the recycling of a variety of materials within PCB's, it is challenging to target which materials should be given priority. A wide range of technologies exist at the research and development level for improving recovery of various materials in end-of-life PCBs including mechanical, pyrometallurgical, and chemical methods. Guo *et al.* used a mechanically based method to crush waste PCBs and then applied three physical separation methods (pneumatic, electrostatic and magnetic); successfully separating a fraction with more than 70% copper by weight [157]. Haiyu *et al.* investigated variables associated with copper recovery from waste PCBs by leaching in sulfuric acid, and discussed the optimum leaching condition in terms of recovery efficiency [158]. Peter *et al.* used the nitric acid-water system and the aqua regia system to leach gold from waste computer circuit board [159]. Morin *et al.* investigated the opportunities of extracting metals by applying bioleaching at industrial scale [160]. Like informal recycling, most studies focus on recovery of copper and gold even though PCBs contain other valuable metals with purity 10 times higher than that of content-rich minerals [147]. From an environmental perspective, hazardous components and heavy metals should also be recovered to avoid potential leaching in landfill disposal. A systematic evaluation of recovery priority for metals in PCBs taking into account the economic, environmental, and social drivers has not been done. Such an evaluation could help guide future research and development of PCB recycling technologies as well as inform policies and legislation pertaining to PCB design, disposal, and collection.

The priority of material recovery for end-of-life PCBs varies with the composition of PCBs, choice of ranking metrics, and weighting factors when scoring multiple metrics. The results from this work can be used as a reference by all stakeholders, including recyclers, investors, engineers, product designers, and policy-makers; the methodology can be tailored based on each unique set of resource constraints (e.g. budget, equipment, and technology).

A.2 Method

A weighted sum method (WSM), a widely-used multi-objective optimization method [161], was used to prioritize metal recovery from end-of-life PCBs considering the selected metrics. The metrics and the data used to formulate them become the basis for key factors used in the objective function of the WSM. As such, this data will be detailed first, and its incorporation into the WSM will follow.

PCBs are diverse and complex in terms of the type, amount, size and shape of materials and components; this can create challenges for collection and recycling. For example, based on the contained weight percent of precious metals (i.e. gold), PCBs can be categorized as high-grade PCBs (e.g. PCBs from laptops or cell phones) and low-grade PCBs (e.g. PCBs from TVs). In most e-waste scrap streams (including information and communication technology products, household electronic goods, toys, etc), it is unlikely that PCBs will be separated by any of the previously listed metrics (type, size, etc.); therefore a characterization of this compositional variability is important to inform recycling processes. A literature review of papers that reported PCB compositions was conducted and basic statistics were applied to this mined data in order to quantify the compositional means, ranges, and variance [153, 157, 162-179]. This compositional

information represents a co-mingled stream of low and high grade PCBs; many recyclers receive this type of mixed stream and do not have access to or choose not to apply further physical sorting technologies to separate them. Those recyclers receiving a stream of already disassembled PCBs from a single product type may have a more narrowed compositional range, however, these instances are rare.

In order to quantify the value of the materials in end-of-life PCBs, commodities metals prices were collected from a variety of sources. Commodity prices have been significantly volatile with large swings on a day to day basis. Regardless, in order to reflect current value, average spot prices for each metal in May 2011 were collected from the London Metals Exchange (LME), American Metal Market (AMM), and a scrap trading website, GlobalScrap. To provide a more averaged metric for value, annual average metal prices from the United States Geological Survey (USGS) were also collected for both 2009 and 2010. Commodity prices were selected as a key economic metric as they most accurately reflect the dynamics of supply and demand for each of the materials in PCBs. It should be noted that using metal values as an economic metric is a highly optimistic case, i.e. this would represent the maximum potential value. Additional costs for transportation and processing would decrease a recycler's profit from processing these materials. Secondary, or recycled metals prices may more accurately reflect the true value, however, these are not available for all of the metals and have considerably more uncertainty and range in their values.

In this appendix, average metal prices in 2010 from USGS are used for the base case due to the relative stability of the yearly average. Compositional data was combined with the price data to determine value in the PCB scrap stream using Equation (A1):

$$X_i = W_i * \text{Price}_i \quad \text{(A1)}$$

where, X_i is the economic value of metal i contained in one ton of PCBs, W_i represents average weight of metal i in one ton of PCBs, Price_i is the price of metal i.

A variety of environmental metrics are available to evaluate end-of-life PCB impacts such as greenhouse gas emissions, solid waste disposal, and wastewater discharge. However, comprehensive life-cycle inventory (LCI) data for PCB recycling is currently not available and the relationship between the LCI and life-cycle impacts has a high degree of uncertainty for most of these metrics. Therefore, cumulative energy demand for the elemental materials has been selected as a simplified metric representing the embodied energy for the base case. It should be noted that these energy values do not take into account the assembly and transportation of the PCBs once they have been fabricated from the supply materials. However, a considerable amount of energy is required for mining, manufacturing, and transporting primary metals. Recycling provides an opportunity to recapture some of this energy albeit with its own set of environmental impacts. Data on the difference in energy between primary and secondary production (recycling) was taken from life-cycle assessment (LCA) software database (ecoinvent v2.2 within SimaPro 7.2) and calculated according to the impact assessment methodology "cumulative energy demand v1.07"[25]. Energy savings is explored using actual energy savings (MJ/tonne PCB) metric. *Actual energy savings*, the difference between primary and secondary production energy for a recovered metal, is calculated by Equation (A2):

$$AES_i = W_i * (P_i - S_i) \quad \text{(A2)}$$

where, AES_i is actual energy savings for metal i in one ton of PCBs, W_i is the average weight of metal i in one ton of PCBs; P_i is energy demand for primary production of metal i; S_i is energy demand for secondary production of metal i.

Secondary production energy was not available for tin, tantalum, gallium, mercury, cadmium, chromium, antimony and manganese, therefore a linear regression model was applied to estimate the possible energy savings based on the primary production energy for eight of the sixteen studied metals. A regression model was used to estimate the missing secondary energy data, shown in Equation (A3):

$$ES_i = -16.2 + 0.926 * P_i \quad \text{(A3)}$$

where $ES_i, ES_i = P_i - S_i$, is energy savings for metal i. The results are summarized in Table A1, showing that the energy savings is statistically significant and positively related to the energy demand for primary production of metal i. Estimated energy savings and corresponding secondary production energy for those eight metals are shown in Table A2; estimated data points are shown in Figure A1.

Table A1 Regression results.

Predictor	SE Coefficient	't' value	Significance level
Constant	4.470	-3.63	0.011
P_i	0.008	111.76	0.000
R-sq	100%	R-sq(adj)	99.9%

Table A2 Estimated values from Equation (A3).

Metals	Estimated Energy Savings	Estimated Secondary Production Energy
Tin	281	40
Tantalum	4021	339
Gallium	2854	246
Mercury	150	29
Cadmium	0[a]	17
Chromium	518	59
Antimony	114	27
Manganese	38	21

[a] Estimated energy saving for cadmium is -0.7, which is theoretically not possible. We fixed it to zero.

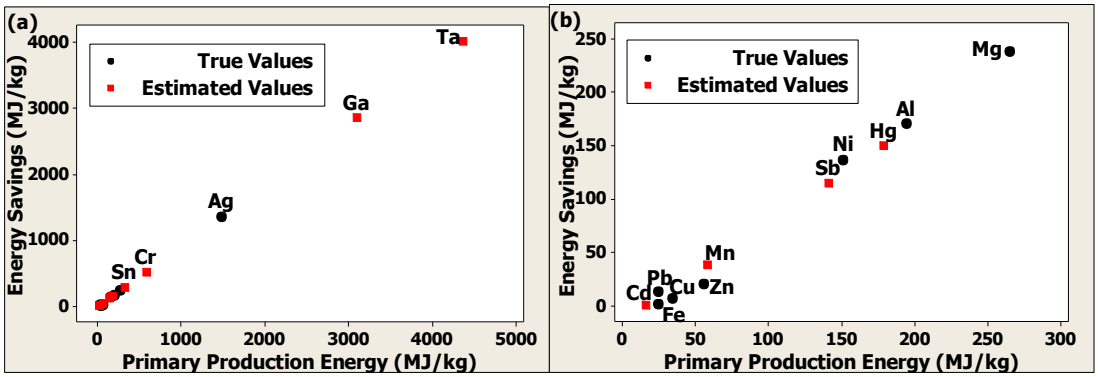

Figure A1 Primary production energy (MJ/kg) vs. energy savings (ΔMJ/kg) (a) for all metals in PCBs with a majority being clustered in the lower left corner of the graph and (b) an expanded view of metals with primary energy savings less than 250 MJ/kg.

Eco-toxicity measures the potential for pollutants (both natural and synthetic) to cause stress to ecosystems (including plants, animals, and humans); a variety of eco-toxicity metrics exist and have been widely used to identify chemical hazards[59]. One particular metric of eco-toxicity was adopted as an indicator to the potential environmental, health, and safety (EH&S) impacts for workers both in terms of the toxic potential of metals in end-of-life PCBs and their relative threat to human health. The metric used is based on the 2011 Priority List of Hazardous Substances from the Comprehensive Environmental Response, Compensation, and Liability Act (CERCLA)

[180]. CERCLA provides comprehensive information about eco-toxicity of hazardous substances, taking into account the frequency of occurrence of substances at national priorities list (NPL) hazardous waste sites and facilities, the Environmental Protection Agency's (EPA) reportable quantity ranking, EPA toxicity score, and the potential for human exposure. The CERCLA score and ranking is available in Table A3 and more detailed information on how this score is calculated is available in the CERCLA support document [181]. While this comprehensive metric is slightly complicated, it avoids a narrow view of eco-toxicity that a single indicator metric such as LC50 (the median lethal concentration) or TD50 (the median toxic dose) may provide. While CERCLA eco-toxicity points are not normalized by a mass or volume metric, a points per kilogram extrapolation was performed according to Equation (A4) in order to weight the compositional differences of materials within PCBs.

Table A3 The 2011 Priority List of Hazardous Substances.

Metals	Total Points	Rank	Metals	Total Points	Rank
Arsenic	1665	1	Palladium	705	171
Lead	1529	2	Aluminum	685	181
Mercury	1461	3	Silver	608	217
Cadmium	1319	7	Antimony	602	232
Beryllium	1033	43	Tin	488	307
Nickel	999	57	Bismuth-214	256	463
Zinc	919	75	Gallium	112	571
Chromium	898	78	Tantalum	11	680
Copper	805	125	Gold	0	699
Barium	805	126	Magnesium	0	699
Manganese	799	140	Iron	0	699

Note: data are not available for platinum; total point for platinum is assumed to be the same with palladium, 705.

$$FP_i = W_i * TP_i \quad \text{(A4)}$$

where, FP_i is the final hazardous points of metal i contained in one ton of PCBs, W_i represents average weight of metal i in one ton of PCBs, TP_i is the total points of metal i.

A weighted sum method (WSM) was used to prioritize metal recovery from end-of-life PCBs considering the economic, energy, and eco-toxicity metrics detailed above. WSM is a straight-forward method to understand how competing criteria drive decisions by integrating them into a single objective function. This makes it an excellent choice for this work given the balance of economic, environmental, and toxicity drivers to prioritizing material recovery. Both an advantage and disadvantage of WSM is the selection of weighting factors. This is a disadvantage because the choice will greatly influence the decision and is arbitrary or subjective [182]. However, as each individual firm or recycler will likely have differences in drivers for their process, it also an advantage as it provides flexibility in the approach. To overcome the subjectivity of the weighting selection, a wide range are explored in this work to better reflect variations in the system experienced by actual recyclers. In section A.3.5.1, only economic and energy metrics are considered and weighted equally in the base case; the full range of weightings from 0-1 are shown as sensitivity. Section A.3.5.2 presents an equally weighted (1/3) base case for all three metrics, again, with sensitivity on the weighting factors.

The weighted sum values for each metal can be calculated by Equation (A5). To express the data in the same unit, these two metrics have been normalized by subtracting the sample mean from each individual value and then dividing the difference by the sample standard deviation.

$$TS_i = \alpha * \left(\frac{X_i - (\sum_{i=1}^{n} X_i)/n}{\sqrt{\sum_{i=1}^{n}(X_i - \frac{\sum_{i=1}^{n} X_i}{n})^2}}\right) + \beta * \left(\frac{ESP_i - (\sum_{i=1}^{n} ESP_i)/n}{\sqrt{\sum_{i=1}^{n}(ESP_i - \frac{\sum_{i=1}^{n} ESP_i}{n})^2}}\right) + \lambda * \left(\frac{FP_i - (\sum_{i=1}^{n} FP_i)/n}{\sqrt{\sum_{i=1}^{n}(FP_i - \frac{\sum_{i=1}^{n} FP_i}{n})^2}}\right),$$

$$\alpha + \beta + \lambda = 1,\ ESP_i = AES_i \qquad \text{(A5)}$$

where TS_i is the weighted sum value for metal i, X_i is the economic value of metal i in one ton of PCBs, ESP_i is the energy saving potentials for metal i in one ton of PCBs, FP_i is the final hazardous points for metal i in one ton of PCBs, AES_i is the actual energy savings for metal i, α, β, λ are the weighting factors ($0 \le \alpha, \beta, \lambda \le 1$), and n is the number of metals in PCBs.

A.3 Results and discussion

A.3.1 Metallic material composition of printed circuit boards.

Five descriptive statistics for each metal are calculated, as shown in Figure A2, including the median, the 1st and 3rd quartiles, and the minimum and maximum values. The detailed information about the metallic material composition of waste PCBs from a variety of applications from which these statistics are calculated is provided in Table A4. Figure A2 shows most metals have high compositional variability; nickel, gold, and palladium have extreme data points marked with an asterisk. This is mainly due to PCBs from a variety of products (e.g. computers, cell phones, etc.) being comingled. These extreme values were considered outliers for calculating the mean and standard deviation. Several metals (e.g. arsenic, tantalum, barium, and gallium) appear to be less variable, however, this is mainly due to a lack of data points.

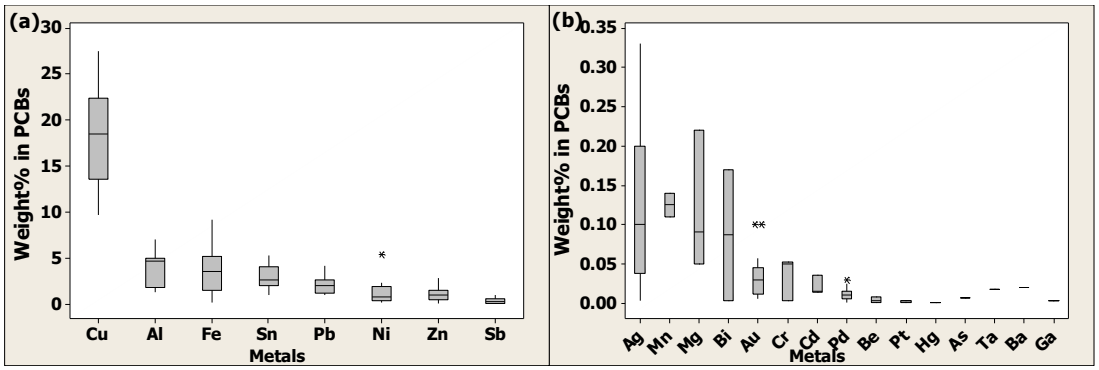

Figure A2 Compositional variation for each metal in PCBs. (a) Metals with average composition >0.30% and (b) metals with average composition <0.30%.

Table A4 Representative composition of PCB. (by wt%)

Categories	Metals	Mean W%	STDEV	CV
Base	Copper	18.6684	5.5709	0.2984
Metals	Aluminum	4.1300	2.0158	0.4881
	Iron	3.8103	2.5831	0.6779
	Tin	2.9220	1.2538	0.4291
Precious	Silver	0.1304	0.1153	0.8844
Metals	Gold	0.0359	0.0290	0.8067
	Palladium	0.0117	0.0089	0.7588
	Platinum	0.0022	0.0015	0.6870
Hazardous	Lead	2.0441	0.8713	0.4263
	Zinc	1.2213	0.7883	0.6455
	Nickel	1.2585	1.1965	0.9507
	Antimony	0.3380	0.3538	1.0467
	Manganese	0.1250	0.0212	0.1697
	Magnesium	0.1555	0.0912	0.5866
	Bismuth	0.0865	0.1181	1.3652
	Chromium	0.0350	0.0277	0.7923
	Cadmium	0.0216	0.0123	0.5704
	Barium	0.0200	Na	Na
	Arsenic	0.0070	Na	Na
	Beryllium	0.0038	0.0041	1.0858
	Mercury	0.0006	0.0005	0.7298
Rare	Gallium	0.0035	Na	Na
Metals	Tantalum	0.0172	Na	Na

Note: Summarized statistics is based on data from published papers[153, 157, 162-179].

Often, recyclers receive a mixed stream of PCBs from a large variety of products; this stream contains both high and low grade PCBs. Therefore, analyzing the direct

impact of variation of the PCB composition in the recycling system is necessary. For example, the precious metals are a target for both formal and informal recycling due to their high value. However, the coefficient of variation (CV) for these metals ranges from 68%-88% which is comparatively high. Dramatic differences in composition for precious metals could have a significant negative impact on the profitability of recyclers. Another important implication is on the potential for processing technologies. Some recyclers have access to a variety of physical sorting technologies (and the informal sector does some hand sorting); this sorting process would effectively reduce this level of compositional variability and would therefore impact the potential value of the stream.

This variation also has implications for policies regarding e-waste. Examining several of the hazardous materials shows coefficient of variation ranging from 43% (lead) to 95% (nickel). Three hazardous materials have CVs greater than 100%: beryllium (108%), antimony (105%), and bismuth (137%). Policies regarding hazardous material collection, disposal, abatement during processing, or worker exposure could create significant additional expense if these materials are at a higher level than estimated by their mean. Most processors will create estimates based on the mean composition of these scrap materials, therefore, valuable elements with skew toward lower values and hazardous materials with skew toward higher values are both very problematic. In looking at Figure 2, one can see that aluminum and chromium are two examples of elements with a majority of samples falling below the median, indicating the distribution of the sample data for these two metals are skewed. However, there are many more

elements with a skew of samples much higher than the median (e.g. magnesium and cadmium).[6]

A.3.2 Economic values

Changes in metal commodity prices as shown in Figure A3 implies a rising trend for most metals indicating increasing financial incentives for metal recovery from end-of-life PCBs.[7] Prices of some metals have increased dramatically between 2009 and 2011, such as antimony (214%), palladium (212%), silver (163%), tin (103%), and mercury (100%). Many of the other metals, while not as dramatic as those listed above, have had substantial increases in price as well. For example, platinum price increased $9,105/lb, and gold price increased $6,717/lb between 2009 and 2011. The increasing tendency for metal prices provides a strong economic incentive to collect and process these materials. Additional commodity metal price data is listed in Table A5.

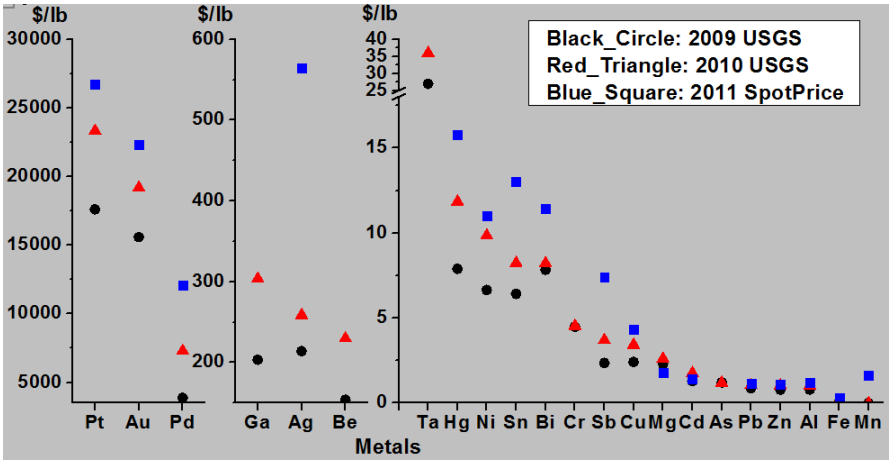

Figure A3 Annual average metal prices from United States Geological Survey (USGS) in 2009 and 2010, and the average value of May 2011 spot prices averaged from the London Metal Exchange (LME), GlobalScrap, and American Metal Market (AMM).

[6] For the economic and environmental prioritization calculation that follow, the average weight fraction for each metal in PCBs was used; sensitivity analysis exploring the extreme ranges of these compositions and their effect on the metrics examined was also applied.

[7] Barium has been excluded from our research due to no commodity information being found in either USGS publications or AMM.

Table A5 Detailed information about metal prices from USGS, LME, AMM, and GlobalScrap. ($/lb)

Metals	USGS (2009)	USGS (2010)	Change %	Notes for USGS metal prices	LME (05-27-11)	GS_US	GS_China	AMM	Most Recent Ave Spot Price
Copper	$2.41	$3.42	41.79%	Average, Domestic producer, cathode	$4.15	$4.16	$4.82	$4.22	$4.34
Iron	$0.09	$0.15	61.06%	Iron and Steel Scrap, No. 1 Heavy Melting composite price, Iron Age Average, Pittsburgh, Philadelphia, Chicago	$0.26	$0.18		$0.42	$0.29
Aluminum	$0.79	$1.02	28.09%	Ingot, average U.S. market (Spot)	$1.18	$1.18	$1.16	$1.30	$1.20
Tin	$6.42	$8.24	28.35%	Average, New York market	$12.27	$12.38	$14.44	$12.97	$13.02
Tantalum	$27.00	$36.00	33.33%	Tantalite, Ta2O2 content					
Gallium	$203.66	$303.91	49.22%	Yearend, 99.99999%-pure					
Platinum	$17,610.06	$23,333.28	32.50%			$26,115.77	$27,314.38		$26,715.08
Gold	$15,600.00	$19,200.00	23.08%			$22,366.41	$22,267.16		$22,316.79
Silver	$214.23	$258.85	20.83%			$552.27	$577.37		$564.82
Palladium	$3,874.05	$7,291.65	88.22%			$11,044.66	$13,133.26		$12,088.96
Mercury	$7.89	$11.84	50.06%	Average value, free market, dollars per flask (1 flask = 76 pounds)		$15.78			$15.78
Cadmium	$1.30	$1.77	35.89%	Metal, annual average (Average NY dealer price for 99.95% purity in 5-short-ton lots)		$1.40		$1.48	$1.44
Zinc	$0.78	$1.04	33.50%	North American	$1.02	$1.03	$1.19	$1.09	$1.08
Nickel	$6.65	$9.85	48.19%	Average annual, LME, Cash	$10.49	$10.43	$12.17	$10.90	$11.00
Chromium	$4.49	$4.54	1.05%	Ave annual import, Chromium metal (gross mass)					
Lead	$0.87	$1.06	21.98%	Average, North American Producer	$1.15	$1.14	$1.14	$1.22	$1.16
	$0.78	$0.94	20.51%	Average, LME					
Antimony	$2.36	$3.70	56.78%	NY dealer price for 99.5% to 99.6% metal		$7.65	$7.37	$7.23	$7.42
Bismuth	$7.84	$8.22	4.85%	Domestic dealer		$11.38		$11.45	$11.42
Manganese	$0.00	$0.00	21.03%	46% to 48% Mn metallurgical ore, Cost, insurance, and freight (c.i.f.), U.S. ports		$1.81	$1.43		$1.62
Magnesium	$2.30	$2.60	13.04%	Platts Metals Week, U.S. spot Western average		$1.49	$1.34	$2.58	$1.80
Arsenic	$1.21	$1.20	-0.83%	Average, Metal (China)					
Beryllium	$154.00	$230.00	49.35%	Unit value, average annual, Be-Cu master alloy, contained Be (4%)					

As shown in Figure A3, precious metals such as platinum ($23,333/lb), gold ($19,200/lb), and palladium ($7,292/lb) have the highest values. Figure A4 (a) shows the recovery priority for metals in waste PCBs from an economic perspective. It should be noted that these estimates are the highest potential value for materials recovered as they do not include the various costs for collecting, transporting, and processing the PCBs. Actual revenue will also be less due to co-mingling of the scrap materials that may degrade the quality or purity of the metals recovered. Not surprisingly, precious metals occupy four out of the top five spots due to their extremely high values. According to the USGS [183], recycling rates of precious metals in e-waste sectors are quite low due to a lack of infrastructure (detailed recycling rates are available in Table A6), however, this appendix aims to show the potential for recyclers recovering them from waste PCBs. In addition, the results promote the development of recycling technologies and also make recommendations for research priorities. Copper also emerges as an important material to recover due to a combination of value and significant weight fraction in PCBs. Existing PCB recyclers in the informal sector focus solely on recovery of gold and copper with the remainder of materials going to landfills [147]. As a consequence, a large amount of valuable metal resources are wasted from an economic perspective. Adding those precious metals to the list of targeted materials for recycling would benefit recycling facilities directly; policies aimed at incentivizing this collection and reuse would benefit from this type of methodology. Moreover, the ever-increasing consumption of electrical and electronic equipment combined with shortening lifespans means the amount of lost resources will increase over the next decade. Lack of access to sorting, upgrading, re-

melting, and fluxing technologies in the informal sector seriously constrains the recovery efficiency of PCB processing and the number of metals targeted.

Table A6 Recycling rate (RR) for metals.

Metals	RR (%)	Metals	RR (%)	Metals	RR (%)
Au	10-15[a]	Ni	57	Cr	87
Cu	43	Zn	19	Ga	<1
Pd	5-10[a]	Ag	0-5[a]	Cd	15
Al	42	Sb	57	Fe	52
Sn	75	Ta	19	Hg	62
Pb	95	Mn	53		
Pt	0-5[a]	Mg	39		

[a] End-of-life recycling rates from e-wastes.

Figure A4 (b) shows how the uncertainties in PCB composition may alter the value of recoverable materials. As stated previously, the high variability in the precious metal composition causes significant swings in economic incentive to recycle. Also of concern to recyclers is the general trend of including less and less precious metals within the PCB due to electronic product manufacturers strategically replacing them with other base metals in order to lower their production costs[184]. These results show that there is a strong economic incentive to recover palladium, however, this element is rarely recovered by recyclers. Figure 4 (b) may shed some light on this discrepancy as the extreme low values for both palladium and platinum are nearly zero; significantly lower than copper's minimum value. Recovering base metals besides copper may not have as strong an economic incentive as precious metals, however, swings in expected recoverable material value are comparatively lower. Moreover base metals (copper, aluminum, tin, etc.) are about 84% of the total metals in PCBs by weight. These results would indicate that investment in recycling technologies targeting high yield recovery of

precious metals (Au, Pd, Pt, and Ag) and base metals (Cu, Ni, and Al) could provide larger profits for recyclers.

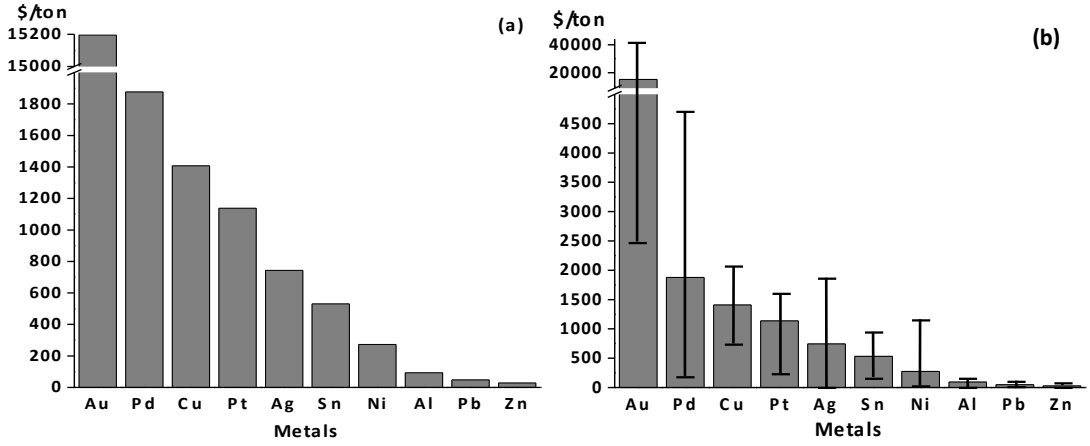

Figure A4 Top 10 valuable metals in one ton of PCBs ($/ton of PCBs) (a) average economic values, (b) with maximum and minimum economic values.

A.3.3 Embodied energy

Recovering metals from end-of-life PCBs not only has economic incentives but can also contribute to energy conservation (which in turn can provide additional economic savings). Recovering and re-melting metals results in a much lower embodied energy compared to the extraction and processing of virgin raw materials. This is particularly true for refined metals which include the precious metals and light metals like magnesium and aluminum. Based on the ecoinvent data v2.2, energy savings range from 35% for zinc to 97% for gold.

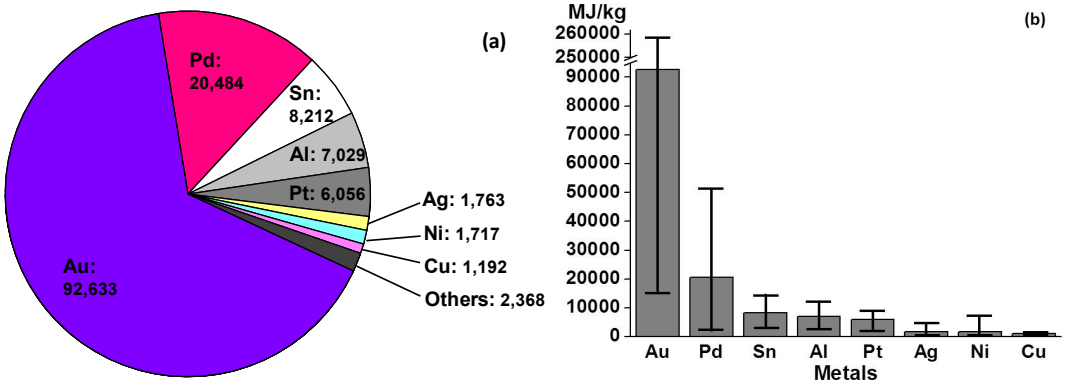

Figure A5 (a) Energy saving potentials for top 8 metals from recycling 1 ton of PCBs (ΔMJ/ton of PCBs), (b) Energy saving potentials with maximum and minimum value (ΔMJ/ton of PCBs).

Figure A5 shows energy saving potential broken down by element from recycling one ton of waste PCBs. Gold has one of the highest energy saving potentials (65% of the total energy savings), followed by palladium (14%), tin (6%), aluminum (5%), platinum (4%), silver (1%), nickel (1%), and copper (1%). Figure A5 (a) shows that all four of the precious metals remain as high priorities showing a strong environmental incentive for their recovery in conjunction with the economic incentive explored previously. Some materials move up in ranking when exploring the potential for energy savings, for example, tin, aluminum, and nickel. It should be noted that the energy required to process the secondary metals is included in the life-cycle inventory for these estimates, a difference between the economic analyses. However, the amount of transportation required for collection is highly variable and could significantly affect the projected energy savings. While it should be noticed that these numbers are calculated based on recovery process of individual metal respectively, many steps are common and therefore can be shared among all recovered metals, such as the collection, transport, shredding, and partial refining process. The compositional ranges are explored in Figure A5 (b)

illustrating less significant swings in the potential for energy savings when compared to the economic analysis. However, some of the bottom ranges for precious metals do fall below the average and top ranges for tin, aluminum, and nickel suggesting that scrap streams with significant compositional variability could alter the metal recovery priority. There is a need for researchers to explore an optimal recycling sequence for end-of-life PCBs to maximize actual energy savings and simultaneously minimize the energy consumption during secondary production.

A.3.4 Ecotoxicity

The CERCLA Priority List of Hazardous Substances was used to assess the ecotoxicity of substances contained in PCBs. Total points for 859 candidate substances are calculated by CERCLA based on three equally weighted criteria: 1) the frequency of occurrence at National Priorities List (NPL)[8] sites, 2) toxicity, and 3) the potential for human exposure[181]. The total points for metals contained in PCBs were analyzed and are shown ranked in Figure A6 (a). As the CERCLA list prioritizes substances found at more than two NPL sites, nearly all of the materials contained in PCBs appear listed with the exception of platinum and iron. A small subset of materials have zero points assigned to them, such as magnesium, gold, and iron. This indicates that conclusive data regarding their toxicity is not available, that toxicity concerns for those materials are negligible, or may indicate both. Not surprisingly, arsenic, lead, and mercury are ranked as the top three most hazardous metals as their significant eco-toxicity and human health impacts are well researched and documented, both in the medical and environmental literature.

[8] The National Priorities List (NPL) is the list of hazardous waste sites throughout the United States.

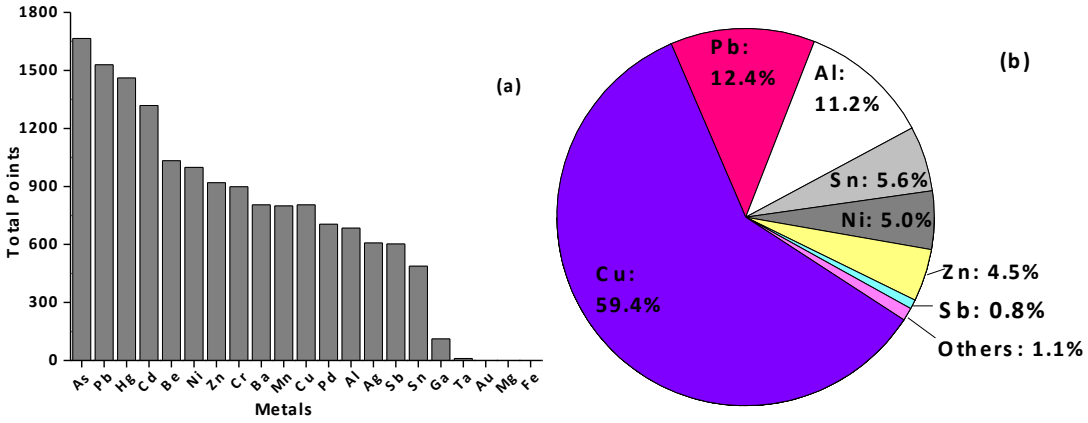

Figure A6 (a) The total points for metals in PCBs (tp), (b) The final points for metals in PCBs (fp/ton of PCBs).

While the total point for each substance provides a clear comparison for overall toxicity, it is also useful to weight those points according to the amount of hazardous material present in PCBs. As can be seen in Figure A6 (b), inclusion of the weight percent present will change the hazard priority ranking, particularly increasing that of some of the base metals. Copper, which does not have as high of a priority in regards to total toxicity potential (Figure A6a), accounts for the highest percentage of total CERCLA points per ton of PCB (59.4%) due to high content. Lead (12.4%), aluminum (11.2%), and tin (5.6%) rank second, third, and fourth respectively in total hazard. While lead ranks the second highest hazardous materials for both priority lists, the relative lead-ban legislation and lead-free solder technologies can help to reduce eco-toxicity of end-of-life PCBs caused by lead. For the highest compositionally weighted hazardous material, copper, new policies governing recovery targets or economic disincentives for design inclusion could have large impacts on the end-of-life management of PCBs. The increase in ranking of some base metals (aluminum and tin) may speak to the need of multi-criteria metrics in determining recovery targets. Aluminum has lower economic

incentive compared to the precious metals and copper, but ranks in the top for both the energy savings and eco-toxicity metrics. This material, as an example, would not be the target of recyclers for either value or a regulation, as lead would be. This loss is even more exaggerated in the informal recycling sector as at least 40% of hazardous materials are not being recovered due to sole focus on gold and copper. Given these base results, several proposed weighting systems were assessed in order to explore the trade-offs in using multi-metric analysis.

A.3.5 Weighted sum values

A.3.5.1 Economic value and actual energy savings

Combined value and energy metrics were explored using a weighted sum methodology. The energy metric has been used for this analysis is actual energy savings (ΔMJ per ton of PCBs). Figure 7A shows the combination of economic value with actual energy savings (normalized according to Equation A5) with setting $\lambda = 0$ and varying weighting factors β on the x-axis. A weighting of zero ($\beta = 0$) corresponds to only material value being considered, corresponding to the results in section A.3.2. Moving to the right on the x-axis indicates increasing importance of energy savings in the weighted sum i.e. a factor of one ($\beta = 1$) corresponds to only considering energy savings, corresponding to the results in section A.3.3. Figure A7 includes precious metals (a) as well as the base and hazardous metals (b,c,d).

There are three key trends that can be gleaned from the set of charts shown in Figure A7: relative height on the y-axis, slope, and cross-over points. The first is how high on the y-axis a particular material is, indicating its recovery priority compared to the other materials. As expected from the previous results, gold has the highest recovery

priority regardless of the weighting factors due to its high value and high embodied energy. The other key trend is the slope of the line for any particular material. A low slope or flat line would indicate relatively equal incentives for recovery from material value and energy savings metrics. A positive slope indicates a higher incentive from energy savings motivation relative to economic recovery; the reverse being true for negative slopes. Palladium (m=0.40), aluminum (m=0.28), tin (m=0.21), and tantalum (m=0.005) have the only positive slopes on this weighted sum scale indicating that their incentive in energy savings outweighs economic savings when normalized. Copper (m=-0.38), silver (m=-0.16), iron (m=-0.026), and gallium (m=-0.026) have the highest negative slopes, indicating larger economic incentive relative to environmental incentive for recovery. Slopes that are larger in magnitude (whether positive or negative) indicate the more significant this difference.

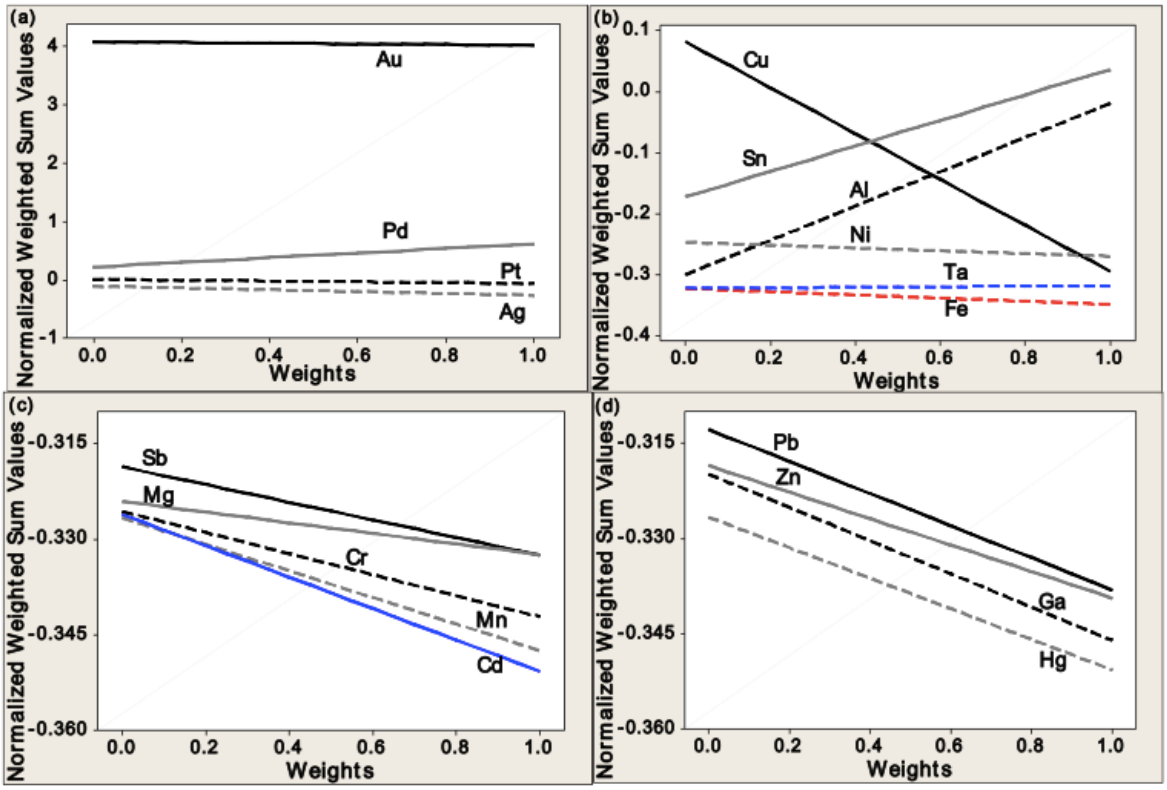

Figure A7 Normalized weighted sum values of economic value and actual energy saving for metals with different weighting factors. (a) For gold, palladium, platinum, and silver. (b) For copper, iron, aluminum, tin, tantalum, and nickel. (c) For antimony, magnesium, chromium, manganese, and cadmium. (d) For lead, zinc, gallium, and mercury.

The third important trend is the location of cross-over points which indicate the recovery priority ranking has changed due to variation in the weighting factor. As the cross-over points between all of the materials are not entirely clear in Figure A7 due to the variation in the axes, they have been outlined in detail in Table A7. Numbers indicate at what weighting two materials shift in terms of recovery priority and high or low indicates the overall trend for a one-to-one comparison of each material present in the PCBs. Of particular note is copper, this material increases in priority over not only aluminum, tin, and nickel but with platinum and silver in addition. This hybrid analysis

can help to inform policy makers whose goal is to incentivize higher recovery in order to reduce overall economic and environmental losses. The total number of cross-over points highlights the complexity in using multiple metrics to prioritize recovery.

Table A7 Weighting factors where crossovers occur (re. Figure 7) "High" means the row metal has higher recovery priority than the column metal and vice versa for "Low".

	Fe	Al	Sn	Ta	Ga	Pt	Au	Ag	Pd	Hg	Cd	Zn	Ni	Cr	Pb	Sb	Mn	Mg
Cu	High	0.58	0.43	High	High	0.25	Low	0.88	Low	High	High	High	0.93	HIgh	HIgh	HIgh	High	High
Fe		Low	Low	Low	Low	Low	Low	Low	Low	High	High	Low	Low	0.29	Low	Low	0.9	0.07
Al			Low	High	High	0.87	Low	0.43	Low	High	High	High	0.17	High	High	High	High	High
Sn				High	High	0.63	Low	0.17	Low	High	High	High	High	High	High	High	High	High
Ta					0.09	Low	Low	Low	Low	High	High	0.16	Low	High	0.33	0.22	High	High
Ga						Low	Low	Low	Low	High	High	Low	Low	0.6	Low	Low	High	0.25
Pt							Low	High	Low	High	High	High	High	High	High	High	High	High
Au								High	High	High	High	High	High	High	High	High	High	High
Ag									Low	High	High	High	High	High	High	High	High	High
Pd										High	High	High	High	High	High	High	High	High
Hg											0.83	Low	Low	Low	Low	Low	0	Low
Cd												Low	Low	Low	Low	Low	0.18	Low
Zn													Low	High	Low	0.14	HIgh	0.47
Ni														High	High	High	High	High
Cr															Low	Low	High	Low
Pb																0.51	High	0.7
Sb																	High	High
Mn																		Low

Results on economic incentives and potential energy savings could be layered with yield data in order to inform e-waste management related to recycling technologies as well. For example, while most informal e-waste recycling sectors in developing countries are focusing on recovering gold (as well as copper) from waste PCBs, they are using extremely crude methods with around 28-30% extraction efficiency[185], whereas the gold recovery efficiency in the formal sector has the potential to be as high as 99%[186]. This type of data combined with regional product flow analysis could be utilized to quantify a) incentives for collection and recycling efforts, or b) penalties for land-filling this waste category or exporting to the informal recycling sector.

A.3.5.2 Economic value, actual energy savings, and eco-toxicity

An integration of all three metrics can effectively illustrate how to balance these competing criteria in terms of prioritizing material recovery. In this section, value, energy, and eco-toxicity have been assumed equally weighted. The total score for each metal in waste PCBs has been calculated by Equation (A5), which is given in Table A8.

Table A8 The material recovery priority with equal-weighted assumption.

			Contribution (%)		
Rank	**Materials**	**Total Scores**	**Econ.**	**AES**	**Toxicity**
1	Au	2.568	48.1	47.4	4.5
2	Cu	1.250	1.9	6.8	91.3
3	Pd	0.150	17.9	50.6	31.5
4	Al	0.038	39.8	2.6	57.6
5	Sn	-0.036	72.9	15.3	11.9
6	Pb	-0.044	26.7	28.9	44.4
7	Pt	-0.149	0.6	14.5	84.9
8	Ni	-0.179	46.0	50.1	3.8
9	Zn	-0.239	44.4	47.3	8.3
10	Ag	-0.247	15.0	36.2	48.8
11	Sb	-0.326	32.6	34.0	33.3
12	Ta	-0.342	31.5	31.0	37.5
13	Mn	-0.344	31.7	33.8	34.5
14	Mg	-0.347	31.1	32.0	36.9
15	Cr	-0.348	31.2	32.8	36.0
16	Ga	-0.350	30.5	32.9	36.6
17	Cd	-0.351	31.0	33.3	35.7
18	Fe	-0.352	30.6	33.0	36.4
19	Hg	-0.354	30.8	33.0	36.2

Based on the total scores, metals have been ranked in order of recovery priority under the equal-weight assumption. In this case, gold has the highest recovery priority (TS=2.568), followed by copper (TS=1.250), palladium (TS=0.150), aluminum (TS=0.038), tin (TS=-0.036), lead (TS=-0.044), and platinum (TS=-0.149). Negative value of the total score for a certain metal does not have special meaning because it is the sum of weighted values (normalized according to Equation A5). The results have represented that given three criteria (economic, energy, and eco-toxicity) with equal

weighting factors, gold has the highest recovery priority, followed by copper, palladium, aluminum, tin, lead, platinum, nickel, zinc, and silver. Policymakers, who might consider balancing the three criteria, can make regulations or set relative policies based on the results in this section to create incentives or set up targets for end-of-life PCBs recycling. The reality is that decision-makers trying to balance economic, environmental, and social concerns in a certain region of the world might not be equally important and they might change over time; moreover, they are highly likely different from the situation for other regions. Therefore, instead of weighting these three criteria equally, policymakers should set up the weighting factors based on their actual situation. For example, economic growth is the top goal that developing countries are facing with; however, they should not sacrifice environment or human health for the economic boom. In this case, all three criteria should be considered with the same weights. For developed countries, with the solid economic foundation, protecting the environment and improving working conditions for workers should be valued more. Then, in this case, energy and eco-toxicity related metrics should be assigned higher weights. Additional sensitivity analysis associated with weighting factors is discussed in section A.3.5.3.

In Table A8, the last three columns show the relative contribution of each metric to the total score for each metal. It can be seen that gold is ranked first among nineteen metals in PCBs mainly due to the relative contribution of economic value (48.1%) and actual energy saving (47.4%). This is because according to the 2011 Priority List of Hazardous Substances from CERCLA, the conclusive data regarding toxicity of gold is not available or/and toxicity concerns for gold is negligible. Copper is ranked after gold mainly because of its high toxicity characteristic as well as the high content, which leads

copper to be the highest percentage of total CERCLA points per ton of PCBs (59.4%). This indicates that scientists could explore other materials that can replace copper in PCBs and policymakers could limit the use of copper in PCBs, a similar path that lead is now on. Of course, such substitution is a complex process requiring research and development as well as thought to system level impacts on other metals[187]. Another strategy that could significantly decrease the embodied energy is increasing copper production from secondary sources to avoid environmental impacts associated with refining from ore [188]. In addition, recyclers could ensure recovering copper occurs with sufficient health and safety oversight. In Table A8, it also can be noticed that, for the last nine ranked materials (antimony, tantalum, manganese, magnesium, chromium, gallium, cadmium, iron, and mercury), economic value, actual energy savings, and eco-toxicity make roughly the same relative contributions.

A3.5.3 Sensitivity analysis

The sensitivity analysis could be applied to a few parameters (including the material composition of PCBs, embodied energy of materials, economic value of metals, etc.), some of which have been discussed in the previous sections. In this section, sensitivity analysis has been carried out to the weighting factors in Equation A5, and the comparison among some examples has listed in Table A9.

Table A9 The material recovery priority for some case studies.

Materials	$\frac{Econ}{3}+\frac{AES}{3}+\frac{Tox}{3}$	$\frac{Econ}{2}+\frac{AES}{2}$	$\frac{AES}{2}+\frac{Tox}{2}$	$\frac{Econ}{2}+\frac{Tox}{2}$
Au	1	1	2	2
Cu	2	5	1	1
Pd	3	2	4	6
Al	4	6	3	4
Sn	5	4	6	5
Pb	6	10	5	3
Pt	7	3	9	9
Ni	8	8	7	7
Zn	9	13	8	8
Ag	10	7	10	10
Sb	11	11	11	11
Ta	12	9	12	16
Mn	13	17	13	12
Mg	14	12	15	18
Cr	15	15	14	13
Ga	16	14	17	15
Cd	17	18	16	14
Fe	18	16	18	17
Hg	19	19	19	19

Weighting factors in Equation (A5) have first been equally assigned to actual energy saving and eco-toxicity, and then to economic value and eco-toxicity; and the results of material recovery priority for both cases have been compared to the results from section A3.5.1 and A3.5.2. As can be seen in Table A9, the recovery priority for most materials change across columns (expect for mercury in this case). The results indicate that according to what aspects the estimator wants to pay attention to and how they value each aspect, the recovery priority for materials in end-of-life PCBs will not stay the same. For example, if only energy savings and eco-toxicity were in the consideration (the fourth column in Table A9), copper would have the highest recovery priority instead of gold. According to the results from this case study, the relative limit-copper or ban-copper regulations associated with PCBs should be considered by

policymakers. Again, since different stakeholders would place extra emphasis on different aspects, these three metrics might be weighted differently, which leads to inconsistent rankings.

A.4 Conclusion

The methodology presented in this appendix provides an important foundation for Chapter 2 in this dissertation. This appendix has also presented foundational findings for the first stage of ongoing research. Gold has the highest recovery priority if all three performance metrics are equally weighted; this is not surprising given the current focus solely on gold recovery. The recovery priorities for most types of metals in PCBs vary depending on the selected metrics for performance measurement as well as assigned weighting factors. The results from this work can inform all stakeholders associated with end-of-life PCB recycling. For recycling facilities, this work has quantified the increase in value possible by increasing yield and decreasing processing losses, indicated which materials may incur the highest costs if their recovery were regulated motivated by eco-toxicity, and showed possibilities for cost savings in sectors with increased energy costs. For scientists and engineers, the results have indicated which materials that currently lack recovery infrastructure should be targeted for new technology development. Depending on the concerns of different audiences, the weighted sum model created in this work can be modified with other performance metrics.

Beyond the priority ranking obtained from the set of results detailed in this work, some broader implications can be extrapolated from this data as well. One implication is the importance of weighting factors when used to create single score metrics, particularly in regards to life-cycle assessment. This has been demonstrated in the literature for other

products[189, 190] but clearly applies to PCBs as well. Aggregating multiple criteria, particularly environmental and social criteria such as eco-toxicity, cumulative energy demand, greenhouse gas emissions, etc. to a single score such as eco-points may mask some of the finer trade-offs in multi-material complex systems. Selection of particular metrics for environmental impact reduction and/or recovery targets in policy and legislation should be done carefully in order to align with the overall goals of the policy in question.

Appendix B. Supplemental information

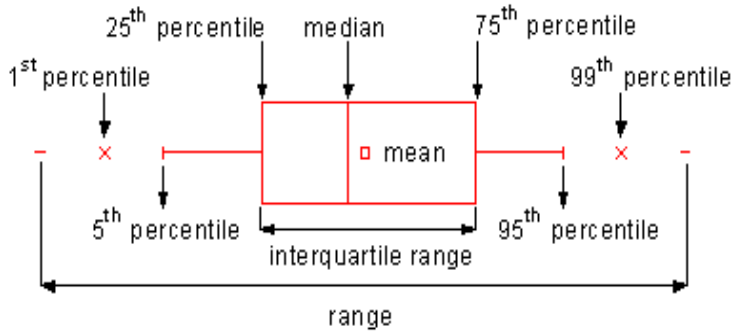

Figure B1 Key values from summary statistics represented in Figure 3(b).

Table B1 Historical and projected EV sales [191].

Year	Sales	Year	Sales	Year	Sales	Year	Sales
2008	124	2015	48,205	2022	93,179	2029	137,757
2009	97	2016	46,208	2023	96,233	2030	137,970
2010	140	2017	55,545	2024	98,675	2031	140,167
2011	15,235	2018	60,307	2025	109,713	2032	147,645
2012	27,675	2019	57,501	2026	117,108	2033	157,425
2013	37,770	2020	67,319	2027	125,847	2034	167,381
2014	41,448	2021	80,036	2028	132,470	2035	174,975

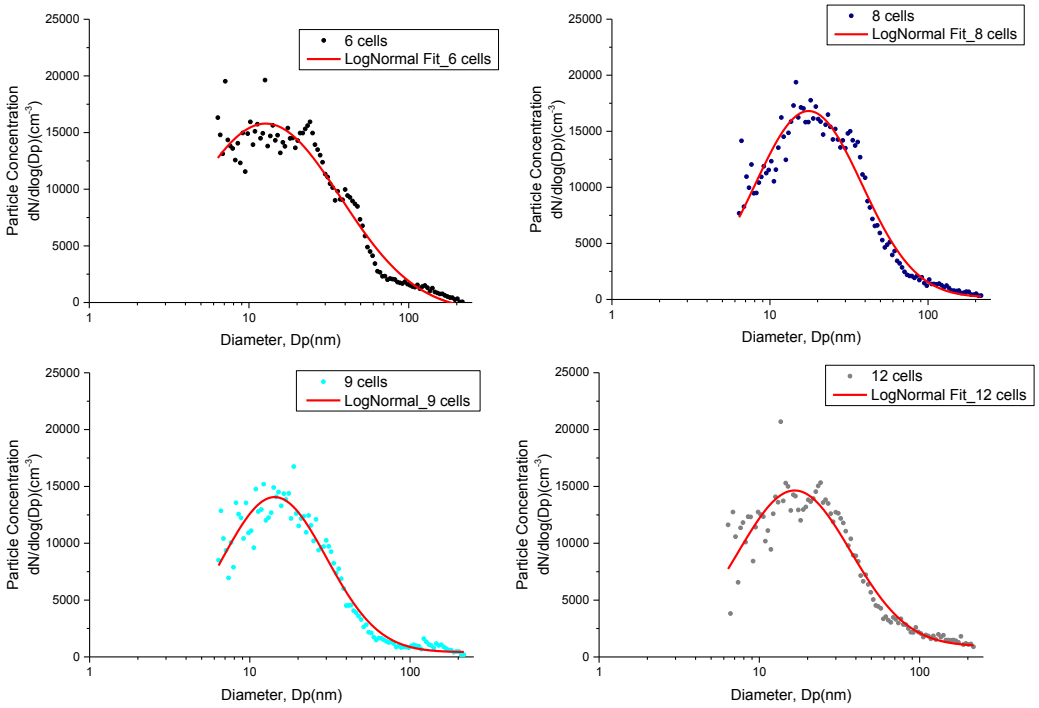

Figure B2 Lognormal fits of particle concentrations when shredding batches with different numbers of cells.

Table B2 Material compositional information for LiCoO2 cathode LIBs.

Manufacturers	Panasonic	Lishen	Sony	Moli	AT&T	Sanyo	Matsushita
Aluminum	1.83	2.98	1.90	1.90	3.00	2.00	0.80
Cobalt	9.47	6.48	8.19	7.53	6.38	6.80	3.73
Copper	3.57	3.14	5.60	5.10	6.90	3.80	2.80
Lithium	1.12	0.76	0.96	0.89	0.75	0.80	0.44
Nickel	1.12	0.00	0.00	0.00	0.00	0.00	0.00
Steel	6.08	9.11	10.40	10.10	9.70	7.80	5.60
Graphite	8.99	12.29	0.00	6.90	2.50	6.40	4.70
Carbon black	2.87	2.68	3.50	0.00	0.00	0.00	0.00
LiPF6	2.15	1.26	2.34	1.98	1.71	1.43	1.22
EC/other	0.54	0.32	2.70	4.10	5.90	4.80	2.40
Binders	1.15	1.07	1.21	1.56	1.70	1.56	0.98
Plastics	1.61	2.79	2.60	1.85	2.25	2.70	1.43
Total	45.62	46.40	39.40	41.90	40.80	38.10	24.10

Table B3 BOMs for $LiCoO_2$ and $LiFePO_4$ cathode LIBs from 2 manufacturers for each.

	$LiCoO_2$ cathode LIBs			**$LiFePO_4$ cathode LIBs**		
Components	**#1 (g)**	**#2 (g)**	**Average (%)**	**#3 (g)**	**#4 (g)**	**Average (%)**
Aluminum	1.83	2.98	5.22	2.78	2.75	6.53
Cobalt	9.47	6.48	17.33	0.00	0.00	0.00
Copper	3.57	3.14	7.29	3.56	3.35	8.16
Lithium	1.12	0.76	2.04	0.52	0.51	1.21
Nickel	1.12	0.00	1.21	0.00	0.00	0.00
Steel/iron	6.08	9.11	16.51	13.46	23.12	43.22
Phosphorus	0.00	0.00	0.00	2.30	2.26	5.39
Graphite	8.99	12.29	23.13	5.25	5.75	12.99
Carbon Black	2.87	2.68	6.04	1.97	0.00	2.33
LiPF6	2.15	1.26	3.71	0.97	0.00	1.15
EC/other	5.68	3.84	10.34	4.99	6.60	13.70
Binders	1.15	1.07	2.41	0.79	0.00	0.93
Plastics	1.61	2.79	4.78	2.72	1.00	4.39
Total	45.62	46.40	100.00	39.30	45.33	100.00

Table B4 Average metallic materials in 10 LIB pack samples (in wt.%). (Blank cells indicate that specific value is <5%).

	(<0.5)	**(0.5, 1)**	**(1, 2.5)**	**(2.5, 6)**	**(>6)**	**(<0.5)**	**(0.5, 1)**	**(1, 2.5)**	**(2.5, 6)**	**(>6)**
Components	**BB**					**VV**				
Al		11.38	25.76	23.75			11.15	33.68	13.93	
P										

Mn	20.68	15.97	12.66	11.16	6.94	21.96	18.81	7.21	10.64	
Fe					41.33					58.47
Co	19.85	12.38	7.71	7.64		20.41	14.73		6.41	
Ni	46.13	31.02	22.54	23.53	26.39	50.14	36.92	13.40	22.97	29.85
Cu	8.53	25.48	28.44	28.93	13.57		15.75	38.52	39.30	
Others	4.80	3.77	2.90	4.99	11.77	7.48	2.64	7.19	6.76	11.68
Components	**RR**					**K**				
Al		7.54		5.29			5.21	5.90	8.14	
P			6.47	5.64						5.09
Mn	23.83	21.16	14.58	15.40						
Fe					72.14					53.96
Co	35.31	21.50	13.19	14.43		89.60	61.62	29.71	35.53	7.43
Ni	33.73	23.85	17.63	23.84	22.63					20.05
Cu		23.45	45.15	34.44			25.22	55.69	44.49	9.39
Others	7.13	2.50	2.99	0.97	5.23	10.40	7.95	8.69	11.84	4.07
Components	**B**					**F**				
Al		6.60	6.98	12.34				13.93	17.86	
P					6.69				5.74	
Mn										
Fe				5.15	50.22					52.33
Co	83.88	69.31	24.38	22.54		88.73	72.98	22.10	23.74	8.41
Ni					17.38					23.03
Cu	5.46	19.21	61.20	49.06	16.70		18.05	57.75	43.26	9.48
Others	10.65	4.87	7.44	10.91	9.01	11.27	8.96	6.22	9.39	6.75
Components	**MM**					**LL**				
Al		7.57	10.18	10.21			6.11	18.46	21.03	
P				7.18						
Mn	5.01									
Fe					63.10					66.87
Co	72.56	64.99	24.69	16.09		74.36	68.43	27.36	19.46	
Ni	8.74	6.40			14.08	7.53	6.21			21.87
Cu	6.31	13.14	54.80	55.51	15.43	5.39	10.56	40.04	48.31	5.30
Others	7.38	7.90	10.33	11.01	7.39	12.72	8.70	14.13	11.21	5.97
Components	**QQ**					**S**				
Al			15.90	25.56			8.24	15.48	19.37	
P										
Mn										
Fe				17.64	61.19				8.18	73.15
Co	79.01	68.56	19.09	13.27	8.07	85.22	67.50	39.00	15.47	
Ni					16.46					20.96
Cu	12.92	20.84	58.77	35.08	11.89		18.14	40.00	49.03	
Others	8.07	10.60	6.24	8.45	2.39	14.78	6.12	5.51	7.95	5.89

Table B5 The information about traditional LIBs used in Chapter 5.

Index of battery pack used in the paper (#)	Pack Mass (g)	OEM	Cells/Pack	Tasks in the chapter
01	356	Sony	8	1) Test delay time
02	273	Dell		
03	245	Samsung	6	2) Dynamic particle size distribution; 3) Mass vs. particle exposure potential
04	246	Samsung		
05	246	Samsung		
06	272	HP		
07	251	Unknown		
08	265	Dell		3) Mass vs. particle exposure potential
09	267	Dell		
10	266	Dell		
11	357	Sony	8	
12	351	HP		
13	375	HP		
14	359	Unknown		
15	354	Sony		
16	370	HP		
17	408	Dell	9	
18	409	Dell		
19	418	Dell		
20	411	Dell		
21	411	Lenovo		
22	540	HP	12	
23	541	HP		
24	544	HP		
25	531	HP		
26	532	HP		
27	264	Dell	6	4) Test breathing zone
28	256	Lenmar		

Table B6 Statistics for lognormal fits in Figure B2.

	Adj. R-Square	Y_0	xc	w	A
Average data points	0.978	274	31.6	0.9	697124
6-cell batches	0.948	-817	41.1	1.1	1030060
8-cell batches	0.955	172	32.2	0.8	771357
9-cell batches	0.954	416	25.0	0.8	483029
12-cell batches	0.919	941	31.9	0.8	639177

Appendix C. A time series analysis on variable costs

The average variable cost used in the base case is calculated based on a number of literatures, most of which are more than 10 years old (see Table 3.3). It is difficult to find data for the most recent years since very little information on the variable cost of battery recycling is available due to confidentiality. A time series analysis is performed to address this data timeliness issue. Assuming this average variable cost (i.e., $2,800 per ton) is for the year 2001, it has likely changed over the years mainly due to changes in labor costs and input resource costs. Figure C1(a) shows unit cost indexes for both labor and input resources assuming 100 in the base year 2001. Yearly indexes for private industry workers estimated by U.S. Bureau of Labor Statistics were used to measure change over time in unit labor cost [192]. Coal was selected to represent input resources (mainly energy) since most current and past battery recycling technologies are pyrometallurgical processes. The historical coal prices were collected from Annual Energy Review[193]. While both unit labor costs and unit input resource costs increased, labor hours required and input resources needed to recycle one ton of batteries are likely to be reduced over the years as recycling technologies improved. The quantity of input labor hours and resources is assumed to follow a learning curve with 95% and 85% learning rate, respectively, as battery recycling is an energy-intensive process rather than a labor-intensive process (see Figure C1b). Taking the changes in both unit cost and quantity required into consideration, Figure C1(c) shows estimated trends for the total labor costs and input resources costs. In 2012, labor costs and input resource costs is about 12% higher and 11% lower compared to 2001, respectively. Figure C1(d) shows estimated variable costs in the past 12 years. Three possible ratios between the cost of

labor and input resources in variable costs, i.e., 20%:80%, 30%:70%, and 40%:60%, are plotted in Figure C1(d) as examples. As can be seen, for all three scenarios, variable costs swing slightly across the x axis but not too much. Particularly, estimated variable costs for the year 2012 is only about 5% lower compared to the variable costs assumed in the base case. Therefore, the calculation in the base case stays with collected data points for the variable costs for simplicity.

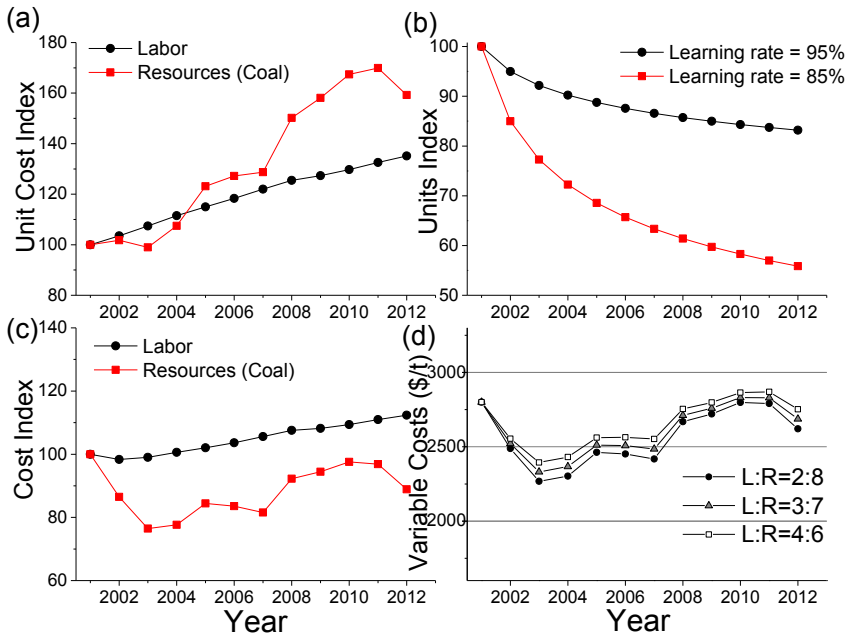

Figure C1 (a) Unit cost index for labor and coal change over the years, (b) units index based on two learning rates, (c) estimated labor and coal cost indexes, (d) estimated variable costs assuming three ratios between the cost of labor and input resources in variable costs (L:R).

References

1. Kurzweil, P. and K. Brandt, *Secondary batteries – lithium rechargeable systems | Overview*, in *Encyclopedia of Electrochemical Power Sources*, G. Editor-in-Chief: Jürgen, Editor. 2009, Elsevier: Amsterdam. p. 1-26.
2. Patil, A., et al., *Issue and challenges facing rechargeable thin film lithium batteries.* Materials Research Bulletin. 43(8-9): p. 1913-1942.
3. Ritchie, A. and W. Howard, *Recent developments and likely advances in lithium-ion batteries.* Journal of Power Sources, 2006. 162(2): p. 809-812.
4. Fergus, J.W., *Recent developments in cathode materials for lithium ion batteries.* Journal of Power Sources, 2010. 195(4): p. 939-954.
5. Thackeray, M.M., et al., *Comments on the structural complexity of lithium-rich $Li_{1+x}M_{1-x}O_2$ electrodes (M=Mn, Ni, Co) for lithium batteries.* Electrochemistry Communications, 2006. 8(9): p. 1531-1538.
6. Arsova, L., et al., *The state of garbage in America.* Biocycle, 2008. 49(12): p. 22-24.
7. Jaskula, B.W., *USGS Mineral Commodity Summaries*. 2010. p. 92-93.
8. USGS, *U.S. Geological Survey, Mineral Commodity Summaries, 2013*. 2013: U.S. Geological Survey.
9. Wilburn, D.R., *Material Use in the United States--Selected Case Studies for Cadmium, Cobalt, Lithium, and Nickel in Rechargeable Batteries.* US Geological Survey Scientific Investigations Report, 2008. 5141: p. 2008.
10. USGS, *Mineral Commodity Summaries 2012*. 2012: U.S. Geological Survey.
11. Wang, X., et al., *Economic and environmental characterization of an evolving Li-ion battery waste stream.* Journal of Environmental Management, 2014. 135(2014): p. 126-134.
12. EPA, *Electronics Waste Management in the United States through 2009*. 2011.
13. Johnson, B.A. and R.E. White, *Characterization of commercially available lithium-ion batteries.* Journal of power sources, 1998. 70(1): p. 48-54.
14. Howard, W.F. and R.M. Spotnitz, *Theoretical evaluation of high-energy lithium metal phosphate cathode materials in Li-ion batteries.* Journal of power sources, 2007. 165(2): p. 887-891.
15. BU. *Battery Statistics*. 2011 Jan 22, 2014]; Available from: http://batteryuniversity.com/learn/article/battery_statistics.
16. Berdichevsky, G., et al., *The tesla roadster battery system.* Tesla Motors, 2006. 1(5).
17. Fletcher, S., *GM's new battery chemistry? It's already in the Chevy Volt*, in *Popular Science*. 2011.
18. Hernandez, E. *EV Battery Technology differences*. 2011; Available from: http://livingleaf.info/2011/12/ev-battery-technology-differences/.
19. Lucas, P. *Tata Motors reveals lithium-ion battery supplier.* 2012; Available from: http://www.thegreencarwebsite.co.uk/blog/index.php/2012/03/02/tata-motors-reveals-lithium-ion-battery-supplier/.
20. Schneider, D., *Who's Resuscitating the Electric Car?* American Scientist, 2007. 95(4): p. 403-404.

21. Power, J., *Drive Green 2020: more hope than reality.* A Special Report by JD Power and Associates, November, 2010.
22. Deloitte, *Gaining traction: A customer view of electric vehicle mass adoption in the U.S. automotive market*. 2010.
23. Wood, L. *Research and Markets: Global Market for Lithium-Ion Batteries - Forecase, Trends & Opportunities 2013-2020*. 2013 [cited 2013 Nov 15]; Available from: http://finance.yahoo.com/news/research-markets-global-market-lithium-095300224.html.
24. Olapiriyakul, S. and R.J. Caudill. *A framework for risk management and end-of-life (EOL) analysis for nanotechnology products: A case study in lithium-ion batteries*. in *Electronics and the Environment, 2008. ISEE 2008. IEEE International Symposium on*. 2008. IEEE.
25. Hischier, R., et al., *Implementation of Life Cycle Impact Assessment Methods*. 2010, ecoinvent report.
26. CACode, *Rechargeable Battery Recycling Act of 2006*. 2006: California Code.
27. *New York State Rechargeable Battery Law*, in *18*. 2010: New York Environmental Conservation Law.
28. *Rechargeable Battery Recycling Act*, in *Public Resources*. 2006.
29. *New York State Rechargeable Battery Law*, in *Environmental Conservation Law*. 2011.
30. *Directive 2006/66/EC of the European Parliament and of the Council of 6 September 2006 on batteries and accumulators and waste batteries and accumulators and repealing Directive 91/157/EEC*, E. Union, Editor. 2006, Official Journal of the European Union. p. 14.
31. Zeng, X., J. Li, and N. Singh, *Recycling of Spent Lithium-ion Battery: A Critical Review.* Critical Reviews in Environmental Science and Technology, 2013: p. null-null.
32. Xu, J., et al., *A review of processes and technologies for the recycling of lithium-ion secondary batteries.* Journal of Power Sources, 2008. 177(2): p. 512-527.
33. Bernardes, A., D.C.R. Espinosa, and J.S. Tenório, *Recycling of batteries: a review of current processes and technologies.* Journal of Power Sources, 2004. 130(1): p. 291-298.
34. Fletcher, S. *GM's New Battery Chemistry? It's Already in the Chevy Volt*. Popular Science, 2011.
35. Schneider, D., *Who's Resuscitating the Electric Car?*, in *American Scientist*. 2007. p. 403.
36. Hernandez, E., *EV Battery Technology differences*, in *Living LEAF*. 2011.
37. Lucas, P., *Tata Motors reveals lithium-ion battery supplier*. 2012: GreenCarWebsite.
38. Dewulf, J., et al., *Recycling rechargeable lithium ion batteries: Critical analysis of natural resource savings.* Resources, Conservation and Recycling, 2010. 54(4): p. 229-234.
39. Sloop, S.E. *Recycling advanced batteries*. in *Electronics and the Environment, 2008. ISEE 2008. IEEE International Symposium on*. 2008.

40. Nan, J., et al., *Recovery of metal values from a mixture of spent lithium-ion batteries and nickel-metal hydride batteries.* Hydrometallurgy, 2006. 84(1-2): p. 75-80.
41. Nan, J., D. Han, and X. Zuo, *Recovery of metal values from spent lithium-ion batteries with chemical deposition and solvent extraction.* Journal of Power Sources, 2005. 152: p. 278-284.
42. Dunn, J., et al., *Material and energy flows in the materials production, assembly, and end-of-life stages of the automotive lithium-ion battery life cycle*. 2012, Argonne National Laboratory (ANL).
43. Espinosa, D.C.R., A.M. Bernardes, and J.A.S. Tenório, *An overview on the current processes for the recycling of batteries.* Journal of Power Sources, 2004. 135(1): p. 311-319.
44. Hart, K. and S. Amarakoon, *Lithium-ion Batteries and Nanotechnology for Electric Vehicles: A life-Cycle Assessment*. 2012.
45. Xu, J., et al., *A review of processes and technologies for the recycling of lithium-ion secondary batteries.* Journal of Power Sources, 2008. 177(2): p. 512-527.
46. Dorella, G. and M.B. Mansur, *A study of the separation of cobalt from spent Li-ion battery residues.* Journal of power sources, 2007. 170(1): p. 210-215.
47. Paulino, J.F., N.G. Busnardo, and J.C. Afonso, *Recovery of valuable elements from spent Li-batteries.* Journal of hazardous materials, 2008. 150(3): p. 843-849.
48. Mantuano, D.P., et al., *Analysis of a hydrometallurgical route to recover base metals from spent rechargeable batteries by liquid–liquid extraction with Cyanex 272.* Journal of Power Sources, 2006. 159(2): p. 1510-1518.
49. Ferreira, D.A., et al., *Hydrometallurgical separation of aluminium, cobalt, copper and lithium from spent Li-ion batteries.* Journal of Power Sources, 2009. 187(1): p. 238-246.
50. Li, L., et al., *Environmental friendly leaching reagent for cobalt and lithium recovery from spent lithium-ion batteries.* Waste Management, 2010. 30(12): p. 2615-2621.
51. Li, J.-H., et al., *Study of spent battery material leaching process.* Transactions of Nonferrous Metals Society of China, 2009. 19(3): p. 751-755.
52. Nan, J., et al., *Recovery of metal values from a mixture of spent lithium-ion batteries and nickel-metal hydride batteries.* Hydrometallurgy, 2006. 84(1): p. 75-80.
53. Shin, S.M., et al., *Development of a metal recovery process from Li-ion battery wastes.* Hydrometallurgy, 2005. 79(3-4): p. 172-181.
54. Contestabile, M., S. Panero, and B. Scrosati, *A laboratory-scale lithium-ion battery recycling process.* Journal of Power Sources, 2001. 92(1-2): p. 65-69.
55. Li, J., et al., *Preparation of LiCoO2 cathode materials from spent lithium–ion batteries.* Ionics, 2009. 15(1): p. 111-113.
56. Sullivan, J. and L. Gaines, *Status of life cycle inventories for batteries.* Energy conversion and Management, 2012. 58: p. 134-148.
57. Huijbregts, M.A., et al., *Is cumulative fossil energy demand a useful indicator for the environmental performance of products?* Environmental Science & Technology, 2006. 40(3): p. 641-648.

58. Huijbregts, M.A.J., et al., *Cumulative energy demand as predictor for the environmental burden of commodity production.* Environmental science & technology, 2010. 44(6): p. 2189-2196.
59. Bascietto, J., et al., *Ecotoxicity and ecological risk assessment. Regulatory applications at EPA. Part 1.* Environmental Science & Technology, 1990. 24(1): p. 10-15.
60. ATSDR, *CERCLA Priority List of Hazardous Substances.* Agency for Toxic Substances and Disease Registry, 2011.
61. ATSDR *Support document to the 2013 priority list of hazardous substances that will be the subject of toxicological profiles*. 2014.
62. Roell, S. *Power Forward*. 2011 Power Solutions Analyst Meeting 2011; Available from: http://www.johnsoncontrols.com/content/dam/WWW/jci/corporate/investors/2011/JCI_PS_Analyst_Day.pdf.
63. MW. *Metal World (MW)*. 2012 [cited 2014 07/07]; Available from: http://www.metalworld.com/a/0110.html.
64. Gaustad, G., P. Li, and R. Kirchain, *Modeling methods for managing raw material compositional uncertainty in alloy production.* Resources, Conservation and Recycling, 2007. 52(2): p. 180-207.
65. Olivetti, E.A., et al., *Increasing secondary and renewable material use: a chance constrained modeling approach to manage feedstock quality variation.* Environmental science & technology, 2011. 45(9): p. 4118-4126.
66. Herrmann, C., et al., *Assessment of automation potentials for the disassembly of automotive lithium ion battery systems*, in *Leveraging Technology for a Sustainable World*. 2012, Springer. p. 149-154.
67. Lain, M.J., *Recycling of lithium ion cells and batteries.* Journal of power sources, 2001. 97: p. 736-738.
68. Marano, V., et al. *Lithium-ion batteries life estimation for plug-in hybrid electric vehicles*. in *Vehicle Power and Propulsion Conference, 2009. VPPC'09. IEEE*. 2009. IEEE.
69. Lowry, G.V. and E.A. Casman, *Nanomaterial transport, transformation, and fate in the environment.* Nanomaterials: Risks and Benefits, 2009: p. 125-137.
70. Kang, H.-Y. and J.M. Schoenung, *Electronic waste recycling: A review of U.S. infrastructure and technology options.* Resources, Conservation and Recycling, 2005. 45(4): p. 368-400.
71. Kahhat, R., et al., *Exploring e-waste management systems in the United States.* Resources, Conservation and Recycling, 2008. 52(7): p. 955-964.
72. Gaines, L. *Recycling of Li-ion Batteries*. 2011. presented at Illinois Sustainable Technology Center at University of Illinois.
73. Ponce-Cueto, E., J.Á.G. Manteca, and R. Carrasco-Gallego. *Reverse logistics practices for recovering mobile phones in Spain*. in *Supply Chain Forum: an International Journal*. 2011. BEM-Bordeaux Management School.
74. Richa, K., et al., *A future perspective on lithium-ion battery waste flows from electric vehicles.* In review (companion paper) at Resources, Conservation, and Recycling., 2013.

75. Li, J., et al., *A combined recovery process of metals in spent lithium-ion batteries.* Chemosphere, 2009. 77(8): p. 1132-1136.
76. Graedel, T.E., et al., *Recycling rates of metals: A status report*. 2011: United Nations Environment Programme.
77. Zhang, P., et al., *Hydrometallurgical process for recovery of metal values from spent lithium-ion secondary batteries.* Hydrometallurgy, 1998. 47(2–3): p. 259-271.
78. Sibley, S.F., *Flow studies for recycling metal commodities in the United States*. Vol. 1196. 2004: US Dept. of the Interior, US Geological Survey.
79. Fenton, M.D. and V.A. Reston, *Iron and steel recycling in the United States in 1998*. 2001: US Department of the Interior, US Geological Survey.
80. Sibley, S.F., *Overview of Flow Studies for Recycling Metal Commodities in the United States*. 2011, US Department of the Interior, US Geological Survey: Reston, Virginia.
81. Zhao, Y., et al., *Recovery of copper from waste printed circuit boards.* Minerals and Metallurgical Processing, 2004. 21(2): p. 99-102.
82. Garrison, R.H., E.W. Noreen, and P.C. Brewer, *Managerial accounting*. 2003: Irwin/McGraw-Hill.
83. Labouze, E. and V. Monier, *Impact assessment on selected policy options for revision of the battery directive 2003*, European Commision, Directorate general environment.
84. Moura Bernardes, A., D.C.R. Espinosa, and J.A.S. Tenório, *Collection and recycling of portable batteries: a worldwide overview compared to the Brazilian situation.* Journal of power sources, 2003. 124(2): p. 586-592.
85. Shapek, R.A., *Local government household battery collection programs: costs and benefits.* Resources, conservation and recycling, 1995. 15(1): p. 1-19.
86. McMichael, F.C. and C. Henderson, *Recycling batteries.* Spectrum, IEEE, 1998. 35(2): p. 35-42.
87. O'Sullivan, A. and S.M. Sheffrin, *Economics: Principles in action*. 2007: Boston, Mass.: Pearson/Prentice Hall.
88. Krikke, H., A. van Harten, and P. Schuur, *Business case Oce: reverse logistic network re-design for copiers.* OR-Spektrum, 1999. 21(3): p. 381-409.
89. Moore, F.T., *Economies of Scale: Some statistical evidence.* The Quarterly Journal of Economics, 1959. 73(2): p. 232-245.
90. Chilton, C.H., *Six-Tenths Factor Applies to Complete Plant Costs.* Chemical Engineering, 1950. 57(4): p. l12-l14.
91. JointVenture. *Italian e-waste recycling plant to be built by Joint Venture*. 2011; Available from: http://www.waste-management-world.com/articles/2011/08/italian-e-waste-recycling-plant-to-be-built-by-joint-venture.html.
92. GarbOilPower. *The future of electronic waste*. 2010; Garb Oil & Power Corporation]. Available from: http://www.pinnacledigest.com/blog/garboilandpower/e-waste-future-electronic-waste-otcqb-garb.
93. Content, T., *Johnson Controls to launch $150 million battery recycling center*, in *Milwaukee.Wisconsin Journal Sentinel*. 2012:

http://www.jsonline.com/blogs/business/148100545.html. p. http://www.jsonline.com/blogs/business/148100545.html.
94. Mikolajczak, C., et al., *Life Cycles of Lithium-Ion Cells.* Lithium-Ion Batteries Hazard and Use Assessment, 2011: p. 71-84.
95. Enterprise, A., *Advanced Rechargeable Battery Market: Emerging Technologies and Trends Worldwide*. 2009: http://www.onlineprnews.com/news/7763-1254548054-new-report-advanced-rechargeable-battery-market-emerging-technologies-and-trends-worldwide-available-through-aarkstore-enterprise.html.
96. Kang, J., et al., *Recovery of cobalt sulfate from spent lithium ion batteries by reductive leaching and solvent extraction with Cyanex 272.* Hydrometallurgy, 2010. 100(3): p. 168-171.
97. European, C., *The Waste Electrical and Electronic Equipment Directive WEEE 02/96/EC.* Official Journal L, 2003. 37: p. 24.
98. European, C., *Directive 2002/95/EC on the restriction of the use of certain hazardous substances in electrical and electronic equipment (RoHS).* Official Journal of the European Union, L37, 2003: p. 19-23.
99. Lindhqvist, T., *Extended producer responsibility in cleaner production: Policy principle to promote environmental improvements of product systems*. 2000: International Institute for Industrial Environmental Economics (Internationella miljöinstitutet), Univ.
100. Viscusi, W.K., et al., *Discontinuous behavioral responses to recycling laws and plastic water bottle deposits*. 2009, National Bureau of Economic Research.
101. Bell, J., J. Huber, and W.K. Viscusi, *Alternative Policy Mechanisms for Generating Economic Incentives for Recycling Plastic Water Bottles.* Vanderbilt Law and Economics Research Paper, 2010(10-35).
102. Umicore. *Umicore Battery Recycling*. Available from: http://www.batteryrecycling.umicore.com/UBR/.
103. Olapiriyakul, S. and R.J. Caudill, *Thermodynamic Analysis to Assess the Environmental Impact of End-of-life Recovery Processing for Nanotechnology Products.* Environmental science & technology, 2009. 43(21): p. 8140-8146.
104. Xia, Z., et al., *Recycling cobalt from spent lithium ion battery.* Frontiers of Materials Science in China, 2008. 2(3): p. 281-285.
105. Wang, X. and G. Gaustad, *Prioritizing material recovery for end-of-life printed circuit boards.* Waste Management, 2012.
106. Gaustad, G., E. Olivetti, and R. Kirchain, *Improving aluminum recycling: A survey of sorting and impurity removal technologies.* Resources, Conservation and Recycling, 2012. 58: p. 79-87.
107. Li, L., et al., *Recovery of cobalt and lithium from spent lithium ion batteries using organic citric acid as leachant.* Journal of hazardous materials, 2010. 176(1): p. 288-293.
108. Chen, L., et al., *Process for the recovery of cobalt oxalate from spent lithium-ion batteries.* Hydrometallurgy, 2011. 108(1): p. 80-86.
109. Lee, C.K. and K.I. Rhee, *Reductive leaching of cathodic active materials from lithium ion battery wastes.* Hydrometallurgy, 2003. 68(1-3): p. 5-10.

110. Yamaji, Y., et al., *A Novel Flow Sheet for Processing of Used Lithium-ion Batteries for Recycling.* Environmental resources engineering, 2011. 58(1): p. 9-13.
111. Richa, K., et al., *A future perspective on lithium-ion battery waste flows from electric vehicles.* Resources, Conservation, and Recycling, 2014. 83(2014): p. 63-76.
112. EPA *EPA Method 6200: Field Portable X-Ray Fluorescence for the Determination of Elemental Concentrations in Soil and Sediment US Environmental Protection Agency*. 1998.
113. EU, *Directive 2006/66/EC*. 2006.
114. Gaines, L. *Reduction of Electric Vehicle Life-Cycle Impacts through Battery Recycling*. in *29th International Battery Seminar and Exhibit*. 2012. Ft. Lauderdale, FL.
115. Electropaedia. *Rechargeable Lithium Batteries*. Available from: http://www.mpoweruk.com/lithiumS.htm.
116. BU. *Types of Lithium-ion*. 2011; Available from: http://batteryuniversity.com/learn/article/types_of_lithium_ion.
117. Wang, X., et al., *Economies of scale for future lithium-ion battery recycling infrastructure.* Resources, Conservation and Recycling, 2014. 83: p. 53-62.
118. Wang, R.C., Y.C. Lin, and S.H. Wu, *A novel recovery process of metal values from the cathode active materials of the lithium-ion secondary batteries.* Hydrometallurgy, 2009. 99(3-4): p. 194-201.
119. Li, L., et al., *Recovery of metals from spent lithium-ion batteries with organic acids as leaching reagents and environmental assessment.* Journal of Power Sources, 2013. 233: p. 180-189.
120. Karpati, A., et al., *Variability and vulnerability at the ecological level: implications for understanding the social determinants of health.* American Journal of Public Health, 2002. 92(11): p. 1768-1772.
121. Thompson, S. *Kinsbursky and Toxco overview*. in *2010 US China electric vehicle and battery technology workshop*. 2011.
122. Reinhart, D.R., et al., *Emerging contaminants: nanomaterial fate in landfills.* Waste Management, 2010. 30(11): p. 2020-2021.
123. Brar, S.K., et al., *Engineered nanoparticles in wastewater and wastewater sludge–Evidence and impacts.* Waste Management, 2010. 30(3): p. 504-520.
124. Hull, M.S., et al., *Release of metal impurities from carbon nanomaterials influences aquatic toxicity.* Environmental science & technology, 2009. 43(11): p. 4169-4174.
125. Breggin, L.K. and J. Pendergrass, *Addressing Nanotechnology Waste and Product Disposal: Can the Superfund Safety Net Catch Tiny Particles?* Journal of environmental law, 2007. 19(3): p. 323-345.
126. Gao, J., et al., *Nanowastes and the environment: using mercury as an example pollutant to assess the environmental fate of chemicals adsorbed onto manufactured nanomaterials.* Environmental Toxicology and Chemistry, 2008. 27(4): p. 808-810.

127. Al-Thyabat, S., et al., *Adaptation of minerals processing operations for lithium-ion (LiBs) and nickel metal hydride (NiMH) batteries recycling: Critical review.* Minerals Engineering, 2013. 45: p. 4-17.
128. Vassura, I., et al., *Chemical characterisation of spent rechargeable batteries.* Waste management, 2009. 29(8): p. 2332-2335.
129. Gaines, L., et al., *Life-Cycle Analysis for Lithium-Ion Battery Production and Recycling.* Metal Kokkola, 2011.
130. ZIMMER, A.T. and A.D. MAYNARD, *Investigation of the aerosols produced by a high-speed, hand-held grinder using various substrates.* Annals of Occupational Hygiene, 2002. 46(8): p. 663-672.
131. Aurbach, D., *A review on new solutions, new measurements procedures and new materials for rechargeable Li batteries.* Journal of power sources, 2005. 146(1): p. 71-78.
132. Köhler, A.R., et al., *Studying the potential release of carbon nanotubes throughout the application life cycle.* Journal of Cleaner Production, 2008. 16(8): p. 927-937.
133. Espinoza, V.S., et al., *Material Flow Analysis of Carbon Nanotube Lithium-ion Batteries used in Portable Computers.* ACS Sustainable Chemistry & Engineering, 2014.
134. Oberdörster, G., *Pulmonary effects of inhaled ultrafine particles.* International archives of occupational and environmental health, 2000. 74(1): p. 1-8.
135. Oberdörster, G., et al., *Translocation of inhaled ultrafine particles to the brain.* Inhalation toxicology, 2004. 16(6-7): p. 437-445.
136. Donaldson, K., et al., *Carbon nanotubes: a review of their properties in relation to pulmonary toxicology and workplace safety.* Toxicological Sciences, 2006. 92(1): p. 5-22.
137. Dahm, M.M., et al., *Occupational exposure assessment in carbon nanotube and nanofiber primary and secondary manufacturers.* Annals of occupational hygiene, 2012. 56(5): p. 542-556.
138. NIOSH, *NIOSH Manual of Analytical Methods. (2006a) Method 5040 diesel particulate matter (as elemental carbon).* P.H.S. Department of Health and Human Services, Centers for Disease Control and Prevention, National Institute for Occupational Safety and Health. DHHS (NIOSH), Editor. 2006: NIOSH method of analytical methods 4th ed., Issue 1.
139. Norihiro, K., et al., *Risk assessment of manufactured nanomaterials: carbon nanotubes (CNTs)*, N. Junko, Editor. 2009.
140. Donaldson, K., X. Li, and W. MacNee, *Ultrafine (nanometre) particle mediated lung injury.* Journal of Aerosol Science, 1998. 29(5): p. 553-560.
141. Maynard, A.D. and E.D. Kuempel, *Airborne nanostructured particles and occupational health.* Journal of nanoparticle research, 2005. 7(6): p. 587-614.
142. Kumar, P., et al., *Treatment of losses of ultrafine aerosol particles in long sampling tubes during ambient measurements.* Atmospheric Environment, 2008. 42(38): p. 8819-8826.
143. Rengasamy, S. and B.C. Eimer, *Total inward leakage of nanoparticles through filtering facepiece respirators.* Annals of occupational hygiene, 2011. 55(3): p. 253-263.

144. Tsai, S.-J.C., R.F. Huang, and M.J. Ellenbecker, *Airborne nanoparticle exposures while using constant-flow, constant-velocity, and air-curtain-isolated fume hoods.* Annals of occupational hygiene, 2010. 54(1): p. 78-87.
145. Commission, E., *Scientific Committee on Emerging and Newly Identified Health Risks (SCENIHR).* Opinion on The appropriateness of existing methodologies to assess the potential risks associated with engineered and adventitious products of nanotechnologies, 2005.
146. Oberdörster, G., E. Oberdörster, and J. Oberdörster, *Nanotoxicology: an emerging discipline evolving from studies of ultrafine particles.* Environmental health perspectives, 2005. 113(7): p. 823.
147. Huang, K., J. Guo, and Z. Xu, *Recycling of waste printed circuit boards: A review of current technologies and treatment status in China.* Journal of Hazardous Materials, 2009. 164(2-3): p. 399-408.
148. Baker, E., *Vital waste graphics*. 2004: United Nations Pubns.
149. Coalition, S.V.T. and B.A. Network, *Exporting harm: the high-tech trashing of Asia.* The Basel Action Network, Seattle, 2002.
150. Manhart, A., *Key social impacts of electronics production and WEEE-recycling in China.* Öko-Institut, Freiburg, 2007.
151. Chi, X., et al., *Informal electronic waste recycling: A sector review with special focus on China.* Waste Management, 2010.
152. Zhang, Y., et al., *Toxic Octabromodiphenyl Ether Is Being Transported from Rich to Poor via Electronic Waste.* AMBIO: A Journal of the Human Environment, 2009. 38(2): p. 115-117.
153. Das, A., A. Vidyadhar, and S.P. Mehrotra, *A novel flowsheet for the recovery of metal values from waste printed circuit boards.* Resources, Conservation and Recycling, 2009. 53(8): p. 464-469.
154. Leung, A.O.W., et al., *Heavy metals concentrations of surface dust from e-waste recycling and its human health implications in southeast China.* Environmental science & technology, 2008. 42(7): p. 2674-2680.
155. Zheng, L., et al., *Blood lead and cadmium levels and relevant factors among children from an e-waste recycling town in China.* Environmental Research, 2008. 108(1): p. 15-20.
156. Duan, H., et al., *Examining the technology acceptance for dismantling of waste printed circuit boards in light of recycling and environmental concerns.* Journal of Environmental Management, 2010.
157. Guo, C., et al., *Liberation characteristic and physical separation of printed circuit board (PCB).* Waste Management, 2011.
158. Yang, H., J. Liu, and J. Yang, *Leaching copper from shredded particles of waste printed circuit boards.* Journal of Hazardous Materials, 2011.
159. Sheng, P.P. and T.H. Etsell, *Recovery of gold from computer circuit board scrap using aqua regia.* Waste Management & Research, 2007. 25(4): p. 380.
160. Morin, D., et al., *BioMinE-Integrated project for the development of biotechnology for metal-bearing materials in Europe.* Hydrometallurgy, 2006. 83(1-4): p. 69-76.
161. Kim, I.Y. and O. de Weck. *Adaptive weighted sum method for multiobjective optimization*. 2004. Citeseer.

162. Veit, H.M., et al., *Recovery of copper from printed circuit boards scraps by mechanical processing and electrometallurgy.* Journal of hazardous materials, 2006. 137(3): p. 1704-1709.
163. Veit, H., C. de Pereira, and A. Bernardes, *Using mechanical processing in recycling printed wiring boards.* JOM Journal of the Minerals, Metals and Materials Society, 2002. 54(6): p. 45-47.
164. Guo, J., J. Guo, and Z. Xu, *Recycling of non-metallic fractions from waste printed circuit boards: A review.* Journal of Hazardous Materials, 2009. 168(2-3): p. 567-590.
165. He, W., et al., *WEEE recovery strategies and the WEEE treatment status in China.* Journal of hazardous materials, 2006. 136(3): p. 502-512.
166. Oishi, T., et al., *Recovery of high purity copper cathode from printed circuit boards using ammoniacal sulfate or chloride solutions.* Hydrometallurgy, 2007. 89(1-2): p. 82-88.
167. Wen, X., et al. *Study on metals recovery from discarded printed circuit boards by physical methods*. 2005. IEEE.
168. Goosey, M. and R. Kellner, *Recycling technologies for the treatment of end of life printed circuit boards (PCBs)*. Circuit World, 2003. 29(3): p. 33-37.
169. Sum, E.Y.L., *Recovery of metals from electronic scrap.* JOM, 1991. 43(4): p. 53-61.
170. Theo, L. *Integrated recycling of non-ferrous metals at Boliden Ltd. Ronnskar smelter*. 2002. IEEE.
171. Zhang, S. and E. Forssberg, *Mechanical separation-oriented characterization of electronic scrap.* Resources, Conservation and Recycling, 1997. 21(4): p. 247-269.
172. Kim, B.S., et al., *A process for extracting precious metals from spent printed circuit boards and automobile catalysts.* JOM Journal of the Minerals, Metals and Materials Society, 2004. 56(12): p. 55-58.
173. Yokoyama, S. and M. Iji. *Recycling of printed wiring boards with mounted electronic parts*. 2002. IEEE.
174. Yoo, J.M., et al., *Enrichment of the metallic components from waste printed circuit boards by a mechanical separation process using a stamp mill.* Waste Management, 2009. 29(3): p. 1132-1137.
175. Vasile, C., et al., *Feedstock recycling from the printed circuit boards of used computers.* Energy & Fuels, 2008. 22(3): p. 1658-1665.
176. Park, Y.J. and D.J. Fray, *Recovery of high purity precious metals from printed circuit boards.* Journal of hazardous materials, 2009. 164(2-3): p. 1152-1158.
177. Taberman, S.O., *Environmental consequences of incineration and landfilling of waste from electr (on) ic equipment*. 1995: Nordic Council of Ministers.
178. Ogunniyi, I.O., M.K.G. Vermaak, and D.R. Groot, *Chemical composition and liberation characterization of printed circuit board comminution fines for beneficiation investigations.* Waste Management, 2009. 29(7): p. 2140-2146.
179. Shuey, S., E. Vildal, and P. Taylor. *Pyrometallurgical processing of electronic waste*. 2006.
180. ATSDR, C., *CERCLA Priority List of Hazardous Substances.* Agency for Toxic Substances and Disease Registry, 2007.

181. CERCLA. *Priority list of hazardous substances that will be the subject of toxicological profiles and support documentation*. 2007 August 10, 2010]; Available from: http://www.atsdr.cdc.gov/cercla/supportdocs/text.pdf.
182. Deb, K., *Multi-objective optimization using evolutionary algorithms*. Vol. 16. 2001: Wiley.
183. Graedel, T., et al., *Recycling Rates of Metals–A Status Report.* A Report of the Working Group on the Global Metal Flows to the International Resource Panel, United Nations Environment Programme, Paris, France, 2011.
184. Porter, J., *Computers & electronics recycling: Challenges and opportunities.* Resource Recycling, 1998. 17: p. 19-19.
185. Arora, R., et al., *Whither e-Waste in India?* E-waste: implications, regulations, and management in India and current global best practices, 2008: p. 69.
186. Lu, W., et al., *Extraction of gold (III) from hydrochloric acid solutions by CTAB/n-heptane/iso-amyl alcohol/Na2SO3 microemulsion.* Journal of hazardous materials, 2010.
187. Verhoef, E., G.P.J. Dijkema, and M.A. Reuter, *Process knowledge, system dynamics, and metal ecology.* Journal of Industrial Ecology, 2004. 8(1-2): p. 23-43.
188. Giurco, D., *Towards sustainable metal cycles: the case of copper.* 2005.
189. Finnveden, G., et al., *Recent developments in Life Cycle Assessment.* Journal of Environmental Management, 2009. 91(1): p. 1-21.
190. Guinée, J.B., et al., *Quantitative life cycle assessment of products: 2. Classification, valuation and improvement analysis.* Journal of Cleaner Production, 1993. 1(2): p. 81-91.
191. EIA, U., *Annual energy outlook 2011 with projections to 2035.* Washington DC: Energy Information Administration, United States Department of Energy, 2011.
192. BLS, *Employment Cost Index, Historical Listing*, U.S.B.o.L. Statistics, Editor. 2013: U.S. Bureau of Labor Statistics.
193. EIA, U., *Annual energy review.* Energy Information Administration, US Department of Energy: Washington, DC www. eia. doe. gov/emeu/aer, 2011.